Meta: Synthetic Immersion Kit

KTH Mechatronics Advanced Course
MF2059, HT 2020

FILIP BJÖRKLUND
JUSTUS CONRADI
NIKLAS LANDIN
JONAS LINDSTRÖM
TIANRUI LIU
QIZHEN LYU
MIKO NORE
CHRISTOPHER STRAND
JONAS XU

Meta Immersive Synthetics
Coach: José Gaspar Sánchez
December 13, 2020

Abstract

The gaming industry is soaring into new heights every year and continues to develop rapidly. The military flight simulations industry, which is in many ways closely related to the gaming industry, has fallen behind. There are realistic and graphically advanced flight simulation games, however, the problem is the lack of relatively cheap, compact and well-designed motion platforms that can deliver high levels of immersion when used together in conjunction with games. The company Meta Simulations Immersive Synthetics (Meta) are now planning on designing and building a motion platform as such. The company specialises in advanced and high fidelity physics models and visualizations of fighter jets for flight simulations. The main goal of this project is to help Meta develop a motion platform specifically designed to drastically increase the immersion factor while playing Digital Combat Simulator with in virtual reality. The main purpose of this motion platform is to give the user sensations of acceleration similar to the sensations generated by flying a real fighter jet.

During the second half of the spring term of 2020, literature studies and physical experiments on a Stewart platform were carried out to gain knowledge about the best placement of the centers of rotation, what degrees of freedom that are necessary and how large motion spans are needed and to what actuation speed. This research was then used to generate some technical design concepts for the motion platform, that were later evaluated. During the fall term of 2020, the best one of the concepts was built into a fully functioning full scale prototype. The result showed satisfactory results. The motion platform was able to give the user the sensation of acceleration while playing Digital Combat Simulator in virtual reality. However, there are various areas that can be further developed and improved to increase the immersive feeling for the user.

Acknowledgements

We would like to thank Meta Simulations Immersive Synthetics for offering this project to us and giving us valuable feedback throughout the project, as well as providing us with the necessary equipment. We appreciate the pilot Niclas Colliander for participating in the interview and testing to give us expert assessment and helping us decide on the best design decision. We would also like to thank our project supervisor, José Manuel Gaspar Sánchez, for supporting us with advice and feedback during our work. We highly appreciate the help received by employees at KTH that allowed us access to the Stewart platform and helped us to get the testing started as well, despite the ongoing COVID-19 pandemic. On this we would like to thank Björn Möller with aiding us with the access and providing equipment for tests and Gustav Sten for helping us understand how the Stewart platform worked.

We would like to thank Fabián Revilla from KTH Prototype Center for helping us manufacture countless parts for our build. Always happy and quick to reply to our inquiries and always welcoming us to the water jet room with a laugh and a big smile.

Another person indispensable for the building process was Jan Stamer, a technician working at the Industrial Production section of KTH. His endless expertise of suitable production methods along with his kind and helpful approach made it so much easier for us to produce all parts in time.

A big thank you to Seshagopalan Thorapalli Muralidharan for being the first person to try out the platform with the VR system up and running. We would also like to thank him for helping us with some last minute improvements and invaluable insights throughout the entire project.

Workshop manager at KTH, Tomas Östberg, also played a huge role in realizing the flight simulator prototype. His vast experience and knowledge in metal craftsmanship, along with all the hours of work he put in helping us build was crucial for the completion of this project. Therefore, we would like to say a big thank you to Tomas.

Contents

List of Figures

List of Tables

Abbreviations

AC Alternating Current

API Application Programming Interface

AWG American Wire Gauge

BLDC Brushless Direct Current

COG Center of Gravity

COR Center of Rotation

DC Direct Current

DCS Digital Combat Simulator

DOF Degrees of Freedom

HMD Head Mounted Display

IMU Inertial Measurement Unit

KTH Kungliga Tekniska högskolan / Royal Institute of Technology

MCU Microcontroller Unit

MOSFET Metal–Oxide–Semiconductor Field-Effect Transistor

MP Motion Platform

OLED Organic Light-Emitting Diode

ORB Object Request Broker

PC Personal Computer

PCB Printed Circuit Board

PID Proportional–Integral–Derivative

PWM Pulse-Width Modulation

TCP Transmission Control Protocol

UART Universal Asynchronous Receiver/Transmitter

UDP User Datagram Protocol

VIMS Visually Induced Motion Sickness

VR Virtual Reality

Chapter 1

Introduction

This chapter explains the background and the details of the project, relevant interviews and requirements that were set.

1.1 Background

Military simulations have fallen behind on flight simulation technology and the solutions available today are built on legacy technology and non-scalable architectures. Comparing the emulation fidelity as well as the immersion factor, the military simulation products are over 10 years behind the gaming industry. This is due to the outdated graphics, poor user interfaces and the slow development and scalability. This project aims to change these factors and make a flight simulator that can maximize end user experience while still being affordable so that it can be scaled to a larger number of pilots. This will be done by leveraging state-of-the-art consumer gaming graphics in VR together with a motion platform.

1.2 Stakeholders

The stakeholders of this project is the company Meta Simulations Immersive Synthetics (Meta), located in Stockholm, Sweden. The company is part of the Meta Aerospace Group. The contact persons from the company involved in this project are Daniel Malmquist (CEO), Niclas Colliander (Military Aviation Specialist and former fighter jet pilot) and Markus Sällman Almén (Head of AI Development).

The company specialises in advanced and high fidelity physics models and visualizations of fighter jets for flight simulations. Their main focus as of today is on military aviation training simulations, but were previously involved in the gaming industry. The vision of the company is to drastically improve and revitalise the professional military simulations market, since it has not kept up with the recent development of the closely related gaming industry. Meta combines expertise from artificial intelligence, gaming and aerospace striving towards their vision. The ability to scale their work to reach many customers is very important.

One of the next step in the development of their products is a motion platform, for the purpose of giving the user sensations of realistic accelerations that complements the VR experience of flying a fighter jet. Although there already exists lots of motion platforms for gaming and simulations, none of them suits the purpose of the desired motion platform for this project. The

main flaws of existing motion platforms are generally the price which is too high as well as poor design solutions and insufficient performance. Limited motion range and poor material choices are also common problems.

1.3 Project Description

The goal of this project is to research and develop a flight simulator motion platform for use in pilot training. The project is held in the courses MF2058/MF2059 Mechatronics, Advanced Course at KTH, in conjunction with Meta Simulations Aerospace group, during the spring and autumn terms of 2020.

The project is split into two parts. First research of the state-of-the-art motion platforms, flight simulation, VR, actuation, and control. This part will also contain tests on an existing platform, to gain an understanding of what the requirements of a new platform should be. Design concepts for the fall term will also be generated during the spring. The second part will focus on delivering a working prototype of a new motion platform, that will meet the requirements specified in the first part.

1.3.1 Project Organisation

During the spring term the team was divided into smaller subgroups with three pairs and one group of three. These groups were used in the beginning of the project when searching for information was the most important task. The groups can be seen below, were group 1 was in charge of writing about existing work, other implementation, control theory specifications and simulations on the platform. Group 2 worked on what degrees of freedom are needed, motion span, how to avoid ghost forces, actuation and faking the sensation of acceleration. Group 3 were digging into VR and VR sickness, how the center of rotation affects immersion and also how important the location of the center of rotation is. Lastly, group 4 worked with middleware, platform physics, cost investigation, off the shelf products and DCS specifications. For the spring term, a GANTT chart was established early during the process. The work mainly followed this plan, but due to various reasons, the "Development of chosen concept" activity was not fulfilled. The GANTT chart for the spring term can be seen in appendix A.1.

- Group 1 - Qizhen and Tianrui
- Group 2 - Justus and Jonas X
- Group 3 - Niklas and Filip
- Group 4 - Miko, Christopher and Jonas L

For the fall, the project was focused on development and construction. In order for this to work smoothly and to make sure everyone knew their responsibilities, the team was divided into three different subgroups. These groups had the responsibility for their own subject, with some minor rotation happening between the groups during the project. The group allocations and responsibilities can be seen below. The GANTT chart for the fall term can be seen in appendix A.2.

- Mechanics – Justus, Niklas and Jonas L
- Control – Tianrui, Qizhen and Jonas X
- Electronics & Software – Miko, Filip and Christopher

The project used an agile approach to project management, especially during the fall. The reason for this was to focus on the highest priorities, finish important parts of the project in time, making sure everyone understood what everyone was working on and easily getting help from other team members when needed. To implement this management system, the team used the applications Trello [1] and Slack [2] as project management tools. A Scrum inspired board was created in Trello in order to organize the different tasks in a structured and agile way. The board contained the columns *to-do*, *to-do this week*, *doing*, *stuck* and *done*. Based upon stakeholder and technical requirements, tasks were placed on the board in the to-do column. From this column the different subgroups could drag these cards in the other columns depending on the priority of each task. During each weekly meeting, the group went through the items placed in the stuck-column in order to solve the different problems together. The goal of this was that no one or no group would at any point have too many tasks being worked on at the same time and also involving everyone in the entire project. These methods therefore worked similar to the Scrum sprints and daily scrums.

Slack was used as a project communication tool. Slack allowed communication in the different subgroups via different channels in Slack which further allowed for the entire team to know what was going on while not being overwhelmed by all of the different topics being discussed at the same time. Due to the pandemic, these digital tools were extra important for the project management system in order to have a successful project. The conference tool Zoom [3] was also extensively used to have digital meetings with the team.

1.4 Scope

The motion platform is intended to create the feeling of maneuvering an airplane for flight training. However, the simulation has limits. The intended motion platform has to be of a certain size, therefore, only motion platforms using gravity to simulate acceleration will be investigated, limiting the acceleration magnitude to 1G.

1.5 Interviews

During the research phase of the project, several interviews were held to gain insight in what sensations of acceleration that are important during advanced maneuvers such as in-flight refueling and formation flying.

1.5.1 Interview with pilot Niclas Colliander

In this section, the relevant insights from the interviews with Niclas Colliander are presented.

Colliander explained that the longitudinal acceleration is crucial to feel, since it is difficult for a human to visually estimate speed and acceleration in the longitudinal direction. The speed

matching with the other aircraft during formation flying or with a fuel hose during refueling is easier if the pilot can feel the longitudinal acceleration. In real life flying, the longitudinal acceleration is produced by the thrust of the engines.

The sensation of the introduction to a roll maneuver is important as well. Colliander explained that you only feel the beginning, or introduction, to the movement, so this sensation should be supported by the motion platform.

About gaining and losing altitude, the pilot is not dependent on sensations of acceleration to accomplish these maneuvers. Thus, it is not necessary for the motion platform.

When driving a car and turning in corners, the lateral accelerations and forces are crucial feedback for the driver, as they play an important role for making decisions about speed and steering angles. However, this is not the case when flying. Ideally the pilot should not feel any lateral forces at all. If the pilot feels these kind of forces, it would be an indication that the flying is not optimal. Colliander therefore advised that it could be a valuable feature to include in the motion platform.

Colliander also mentioned that some *indications* could be valuable features for the motion platform. With *indications* he meant small sensations of forces that indicate a special event, such as when the aircraft touches the ground during landing. This indication could for example be made by shaking or vibrating the seat under the pilot.

1.5.2 Other interviews

Besides from the interviews with Colliander, two more interviews were held over telephone to gain more diversified information and opinions. For these telephone interviews, a set of predefined questions were used. The questions were as follows:

- When a fighter jet pilot is in training/flying school, what forces/accelerations do you think are most important for her/him to feel?
- What forces/accelerations do you think are most important to feel when you are an experienced pilot?
- What forces/accelerations do you think are most important in maneuvers like mid-air refueling or formation flying?
- Do you have any experiences with flight simulators? What worked well and what did not?
- How would you say that the perfect flying simulator would look like/function?

Jonas from Swesim

The first person to answer these questions was Jonas, with an unknown last name, from the association called Swesim located in Årsta outside Stockholm. Swesim is an association driven by volunteer work by its members. They build flying simulators that people can pay to use as entertainment [4].

Jonas is not a professional pilot, but an enthusiastic hobbyist with some experience from building and flying simulators. His opinion was that six degrees-of-freedom is important for helicopter

simulators, though three degrees-of-freedom; pitch, roll and heave, would be enough for airplane simulators. He stressed the importance of a rumbling seat, as flying in a simulator without it felt *flat* and non-immersive in his experience. On the mechanical side, he emphasized that hydraulics is not a good choice for a flight simulator since it would be too complex, too dangerous and too expensive in comparison with strong electric motors. The important aspects for the motion platform from the flying school's point of view are that the simulators are cheap and fulfill the requirements from the government as well as easy maintenance. Immersion would therefore not be a priority according to Jonas. On the other hand, he was sure that a realistic and immersive motion platform would sell well among enthusiasts and hobbyists.

Program leader from Swedish Airforce

The first interview with Jonas led to the second interview with the program leader of the first and second division of the flying school in the Swedish Air force, whose name will not be mentioned here due to secrecy. The program leader explained that the simulators they use in their school does not have motion and that he did not know of any good fighter jet simulator with motion. He was not sure if motion would add any value to their simulators. As Jonas mentioned, he said that helicopter simulators often have full motion because it is crucial to feel the forces when flying a helicopter. As Colliander mentioned, he believed that feeling the acceleration forwards and backwards would be the most important ones to include in a motion platform. He thought it would be valuable to simulate the G-forces as well, though it would be tricky to implement in a motion platform.

1.6 Requirements

By close communication with the stakeholders, the background research and the answers from the interviews, the following stakeholder requirements and technical requirements were derived.

1.6.1 Stakeholder requirements

- The motion platform (MP) shall contribute to an immersive and good training experience for pilots in training.
- The MP should be small and compact, so that it should be possible to have several of these in a room similar to a computer room in a school.
- The MP shall be safe to use.
- The MP shall give the user feelings of acceleration in different directions that are important for maneuvering the aircraft.
- The MP shall be robust.
- The MP shall have a high quality design.
- The MP shall be able to be produced in large quantities.
- The MP shall be able to be shipped worldwide.
- The MP shall be compatible to use with several different aircraft models.

- The MP shall be relatively low-cost in terms of production and thereby in purchase for the customer.
- The MP should ensure that the risk of VR sickness is minimized ensuring that longer periods of usage is possible.
- The MP shall be fast and easy to install and implement together with the software.

1.6.2 Technical requirements

Below are all the technical requirements for the motion platform listed. The technical requirements were made from the results of this report and linked to the stakeholder requirements.

Weight and dimensions

- The MP shall have the maximum dimensions of $180 \times 180 \times 180$ cm.
- The MP should not weigh more than 150 kg.

Features and components

- The system shall provide a joystick, that does not prevent the user from accessing the seat.
- The system shall provide a throttle, that does not prevent the user from accessing the seat.
- The system shall provide foot pedals.
- The system shall include a seat with adjustable back rest angle, from 90 degrees to 130 degrees.
- The seat assembly shall provide mounting for seat, joystick, pedals and throttle.
- The seat assembly shall have adjustable distance from the back rest to the pedals, from 60 cm to 90 cm.
- The seat shall be adjustable in height to fit a person that is between 160 cm to 195 cm tall and to adjust the COR for the pitch motion accordingly.
- The visual feedback from the simulator shall be a VR headset.

Software, electronics and simulation

- The MP shall make use of a simulation of the forces and accelerations up to 1G a pilot would be exposed to while flying.
- The system shall accept input in real-time from the exports of the video game Digital Combat Simulator (DCS).
- The simulation shall be based upon the calculations of the real-time exports of DCS.

- The actuators of the system shall be electronic.
- The MP shall have an embedded system to control the actuators.

Kinetic characteristics

- The MP shall at least provide a maximal velocity of 30 deg/s in the pitch direction.
- The MP shall at least provide a maximal velocity of 30 deg/s in the roll direction.
- The MP shall at least provide a maximal motion range of 45 deg in the pitch direction.
- The MP shall at least provide a maximal motion range of 15 deg in the roll direction.

Real-time, immersion and control characteristics

- The delay from user input to motion output shall not exceed 50 ms.
- The delay from user input to visual output shall not exceed 20 ms.
- The MP shall not do any movements that is not needed for the simulation within an error span of 1 deg.
- The MP shall provide the same movements as the calculated reference values provide within an error span of 1 deg.

Other characteristics

- The MP shall have at least one DOF, pitch.
- The COR of the pitch motion should be maximum 5 cm above/below the center of the user's ear.
- The COR of the roll motion should be minimum 5 cm under the seat.
- The MP shall be capable of supporting a user weighing under 100 kg in all possible working positions.
- The system shall provide input to DCS for controlling the simulation.
- The system shall provide two emergency stop buttons; one for the user and one for the technician, that stop the MP movement completely within 10 ms.
- The cost of the MP shall be no more than around 10,000 Euro.

1.7 Reader's Guide

The report is divided into 8 chapters and follows the pattern:

Chapter 2 describes the theory and includes a short literature study and state of the art on selected subjects found relevant for the project.

Chapter 3 presents the methodology of the project and discusses why key decisions were made, the methods, tools and techniques used to solve the problems in the project and how the design concept was developed.

Chapter 4 describes how the project was implemented. The hardware construction as well as the software and electronic implementation.

Chapter 5 displays the tests that were performed during the project in order to verify and validate the desired functionality.

Chapter 6 examines the final results of the project and how well the requirements were met.

Chapter 7 reflects upon the results and contains a discussion on the projects results. The achievements are highlighted and critically reviewed as to how well they match the requirements and what we should have done differently in hindsight.

Chapter 8 presents possible future improvements on the project.

Last appear appendices with extra information for the very keen reader.

Chapter 2

Literature Review and State Of The Art

This section is dedicated for the theory and state of the art flight simulators and motion platforms.

2.1 Physiological systems

In this section, the biological systems that allow people to perceive acceleration will be presented. This needs to be known in order to convince the person that they are experiencing accelerations, when in reality they are seated in a simulator.

2.1.1 Acceleration sensing

Humans have an innate sense of balance. In order for the human bipedal design to be efficient, the brain always needs to know if the body is about to fall over. This sense of balance is provided by the *vestibular* system. This system is located in the ear, and is comprised by three semicircular, liquid filled, canals connected to two liquid filled sacs, called the saccule and utricle. The saccule, utricle and canals contain nerve protrusions, small sensory hairs, that when moved send a signal to the brain.

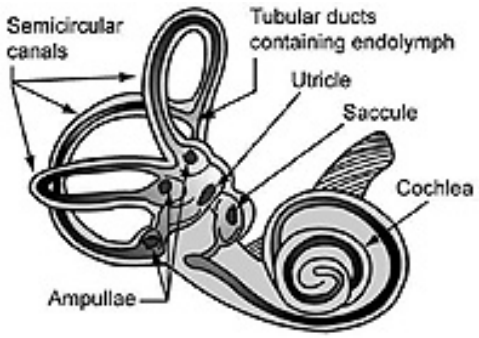

Figure 2.1: Diagram of the inner ear.[5]

When the human body is experiencing an angular acceleration, the liquid in the semicircular canals moves, in turn moving the sensory hairs. The brain then interprets this signal as an angular acceleration. Since the semicircular canals are at right angles to each other each of the

3 degrees of rotation is accounted for, see figure 2.1. In a similar way, the saccule and utricle can sense linear acceleration. In figure 2.1, the layout of the inner ear can be viewed.

The inner ear can primarily sense the direction of acceleration, not the magnitude [6]. Therefore it is sufficient to tilt the head, or in most cases the whole body, to produce a sensation of a moving acceleration vector.

2.1.2 Force sensing

Another important sense to detect acceleration, especially while seated, is the sense of touch. The sense of touch is responsible for the sensation of force. According to Newton's second law, acceleration and force are related, since there must be a force for an acceleration to occur.

For example, a pilot is sitting on the runway in a fighter aircraft waiting to take off. While stationary, the pilot is only experiencing the reaction force from the seat cushion, see figure 2.2a. When the pilot opens the throttle, the aircraft accelerates. This acceleration causes a force from the chair to the pilots back. The force from the seat cushion is still present, and the sum of forces is according to 2.2b. In accordance to Newton's second law, the acceleration vector has the same direction as the resulting force vector.

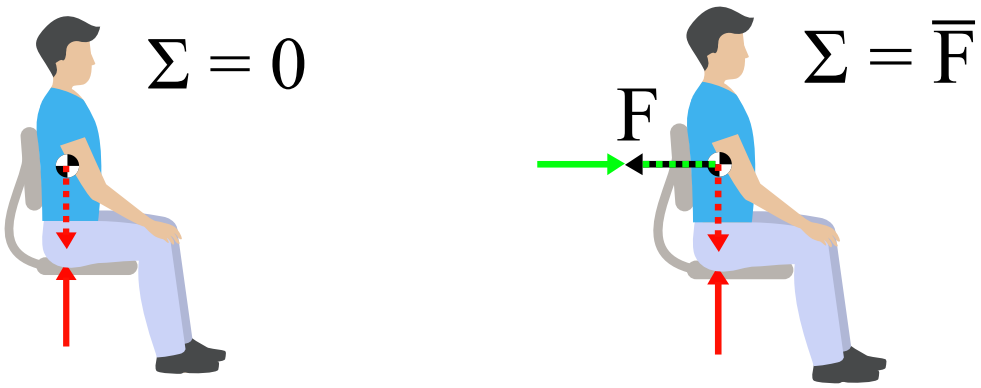

(a) Forces on a stationary pilot.

(b) Forces on an accelerating pilot.

Figure 2.2: Comparison of forces acting on a pilot. Made in Affinity Designer, using assets from Freepik.com. 03/2020

This result is not limited to only linear acceleration, but also angular acceleration. The acceleration vector direction is a sum of all forces acting on the body, including torquess. To trick a person to believe that an acceleration is occurring, the force on their body has to be replicated.

This can be done in a number of ways, and is covered in section **??**, and further in section **??**.

2.1.3 Visual acceleration

When judging speed and acceleration, people heavily rely on their vision. When limited to the two-dimensional plane, such as on a monitor, people can judge the size of objects from past experience. The relative speed to the object can then be determined by evaluating the changes in size of the object. [7] To then determine the acceleration relative to the object, the change in

speed is used. However, when given no depth data, only relying on relationship between objects, and past experiences, the brain can jump to incorrect conclusions, as seen in figure 2.3.

Figure 2.3: Illusion of a man standing on a bottle. [8]

In reality, people use *binocular vision*. Due to their distance apart, each eye sees a slightly different view of the world. By using the angles of the eyes, and the difference in perspective, the brain can determine the distance to an object. Figure 2.4 shows how this works.

Figure 2.4: Stereoscopic image of two Passiflora caerulea. The 3D effect can be seen by crossing your eyes! [9]

Prolonged travel at a constant speed causes the neurons in the visual system to adapt. The acclimatisation to a constant speed happens gradually, and the neurons in the visual system reduce the frequency they fire. The sensitivity to relative speed and acceleration is however preserved.[10]

2.1.4 VR sickness

Virtual Reality (VR) is most commonly referred to technology that allows a user to experience some kind of simulated world with a visual sensation of being immersed into that world. There are two primary methods within VR, namely: stereoscopic head-mounted displays (HMD) and larger projection based systems. The first method use some kind of display that is physically mounted on the head of the user, while the other method uses an external projection system that

could be as large as a room. Head-mounted displays can be divided into three different ocularity types: monocular, biocular and binocular. A stereoscopic view can be achieved using a binocular system. Most fully immersive head-mounted displays are of the binocular configuration [11].

A big percentage of the users of virtual reality experience discomfort during the usage. When using a stereoscopic head-mounted display (HMD), around 80-95% of individuals experience some combinations of symptoms such as nausea, eye strain, disorientation or similar. Around 5-50% of these individuals experience these symptoms to be so severe that they end their participation [11]. It is therefore clear that this needs to be considered when developing a VR system.

This is called VR sickness, or by some called visually induced motion sickness (VIMS). Other names for the phenomenon is simulator sickness, cyber sickness and RGB yawn. Dizziness and nausea are the most common symptoms but the user can also experience salivation, drowsiness, disorientation, headaches, difficulty focusing, blurred vision and in some cases vomiting. The symptoms can start within minutes of using the system and may also continue for some time after the participation has ended [11].

The phenomenon occurs due to a combination of the precision and balance of the perceptual system, technical shortcomings especially in the HMD and also age and gender. It is not fully understood what causes this sickness but the most common theory is the sensory conflict theory. This theory states that the physiological side effects are a result from conflicts between sensory inputs. For example, VR sickness could occur if the visual system would see that the body should move at the moment but this is not followed by an input from the vestibular system. Or in other words, if one would drive a car in a VR simulation and see that the car moves, but does not feel the acceleration, then the user would likely get some symptom of VR sickness. Also, VR sickness according to this theory could occur if the sensory inputs are in conflict with that one would expect from previous personal experience.

According to Steve Aukstakalnis in Practical Augmented Reality, the key technology factors in VIMS are the following:

- Latency
- Incorrect interpupillary distance settings
- Display field of view
- Optical distortion of scene geometry
- Frame rate
- Persistence

Most of the above factors are mainly related to the technology within the actual VR system, the HMD. A wider VR system, with a physical platform that interacts with the VR system, could be effected by the latency. The latency is the lag between a movement of the user and the resulting output from the VR system, i.e. the time from when the user make or experience a movement to the corresponding visual movement is shown on the display. For modern VR HMDs, the base latency between a user movement and the output on the display is around 18 ms [11]. A wider system might have to consider this in the implementation since the system makes a movement that the user feels.

A study from 2019 showed that with an end-to-end latency of 63 ms, users reported significant cybersickness symptoms [12]. This study also showed that in order to minimize the effects of

VR sickness, developers should ensure that the end-to-end latency is far below 58 ms. A latency over 69 ms reduced the user performance and the sense of body ownership started to be reduced at 101 ms.

In order to minimize the risk of VR sickness, a motion platform therefore should both consider the end-to-end latency and also minimize sensory conflicts via a well working control of the platform. The model of the simulation should also be as good as possible in order to give a high feeling of immersion.

2.1.5 Center of rotation

When investigating the impact of the center of rotation (COR) for the motion platform, several different COR needs to be kept in mind, as they play different roles especially for this application. For any airplane, the COR will be at its center of gravity (COG). Figure 2.5 illustrates this in the case of a plane making a pitch motion [13].

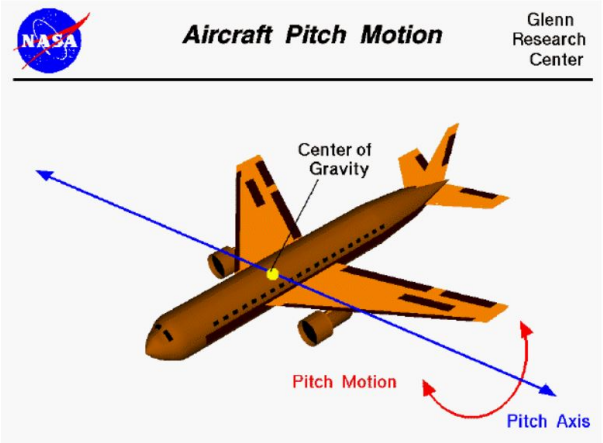

Figure 2.5: The pitch axis and therefore the COR goes through an airplane's COG [13].

At the rear end of the fuselage of a fighter jet, there are stabilators. These control how much force are applied at the rear end of the fuselage, which makes the pitch motion. See figure 2.6. Here the COG/COR is located behind the pilot in a fighter jet [14].

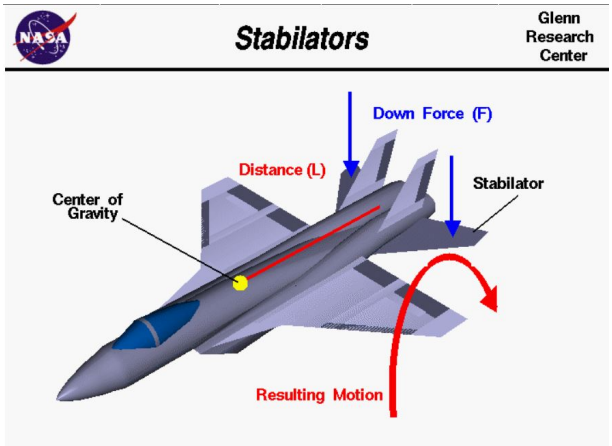

Figure 2.6: COG/COR of a fighter jet making a pitch motion [14].

Also, the roll motion of any airplane has its COR in the COG [15]. Thus, it is clear that for a fighter jet, the COR is behind the pilot. However this does not mean that the COR should be placed behind the user in the motion platform.

The idea of the motion platform is to tilt the user so that they experience the gravity force, or gravity acceleration, in a specific direction on their body, corresponding to the acceleration vector acting on the pilot in the airplane in the video game. In order to tilt the user to a desired position, without getting unwanted forces on the way there, it is probably best to have the COR as close to the user's ears as possible, as seen in section 2.1.1. This is because the user's sense of acceleration is located in that area. For instance, if the user on the motion platform wants to experience a force pulling them to the right, the motion platform has to tilt to the right so that the gravity force pulls the user to their right. If the COR is located under the seat of the user, they will experience a jerk of the head to the left, which is the opposite direction. This is an unwanted, or parasitic force [16].

Another problem with having the COR under the user on a motion platform is that centrifugal forces will act on the user's head during a rotation around that COR. This is because the COG of the head is located at a distance from the COR. However, if the COR is instead at the head, the distance from COR to COG for the head is zero, which means that there will be no centrifugal force acting on the head. Figure 2.7 illustrates these two scenarios.

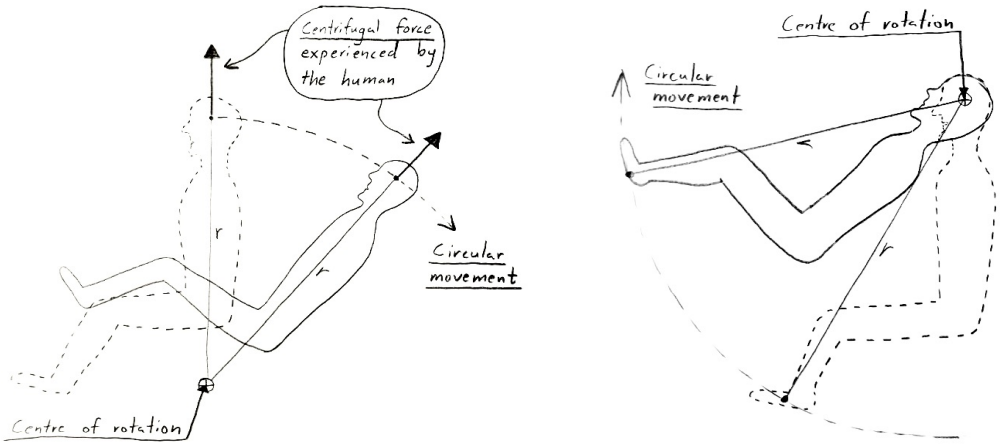

(a) COR under the user. (b) COR at the head of the user.

Figure 2.7: COR under the user vs. COR at the head of the user.

However, one thing to be aware of, is that the largest centrifugal force is instead moved to the COG of the feet, which are now the furthest away from the COR of the motion. Depending on the desired feeling of the motion, the COR should be placed carefully with this in mind. Possibly, a compromise with the COR at the user's chest would be a reasonable compromise. By using a chair with adjustable height, it is possible to make smaller adjustments of the location of the COR, relative to the user. This in turn means that the height of the user will have a smaller significance as if a chair with a fixed seat height.

2.1.6 Degrees of freedom

It is possible to move in six different degrees of freedom (DOF) in three dimensional space, and an aircraft is able to move in all of these degrees of freedom. A motion platform can be made to

produce a number of DOF, although not all six of them are necessary for flight simulation. The paper "Motion Simulation Capabilities of Three-Degree-of-Freedom Flight Simulators" written by Nicolas A. Pouliot et al. investigated this topic [17]. it focused on comparing six-degrees-of-freedom with two different three-degree-of-freedom platforms. Three rotational DOFs in addition to heave, pitch and roll DOFs. Analysing the motion cues when simulating three characteristic maneuvers (take-off, turn-entry and throttle-impulse maneuvers), revealed that a three-degree-of-freedom simulator was capable of producing motion simulation quality comparable to six-degree-of-freedom in most cases. The motion sensations, produced by a vestibular model, showed nearly the same results. The rotational DOFs located at the center of gravity (of the aircraft) performed the best in all three maneuvers [17].

Another research paper "Design and Analysis for a Three-Rotational-DOF Flight Simulator of Fighter-Aircraft" by Chang-Chun Zhou and Yue-Fa Fang also discussed this subject [18]. Here it mentions that for flight simulators, the translational movements are nearly inoperative in six-degrees-of-freedom motion platforms [18]. This raises the question of the importance of linear DOFs, which is further investigated in Chapter 3 as well as different combinations of DOFs.

2.2 Platform simulations

To reproduce the acceleration felt by a pilot to the user in a motion platform, different solutions have been made. In this section, some existing motion platforms and designs will be presented.

2.2.1 Cockpit scale simulation

A way of making the pilot believe that they are in a real aircraft, is to take the cockpit, straight out of the aircraft, put it on a motion platform, and simulate the movement. The benefits of such a setup is that the pilot gets very familiar with the actual cockpit of the aircraft in 3D space. However, full-cockpit simulators usually use projectors to project the flying space in front of the cockpit, leading to a 2D representation, possibly causing depth issues as in section 2.1.3. The mass of the simulator is also large, therefore powerful actuators are needed to achieve satisfactory performance. Cockpit scale simulators are often extremely expensive. An example of a simulator as such is shown in figure 2.8.

(a) Inside a cockpit scale flight simulator.

(b) Outside a cockpit scale flight simulator.

Figure 2.8: Cockpit scale flight simulators, inside and outside views. [19]

2.2.2 Virtual reality simulators

Since the advent of consumer virtual reality (VR) headsets for gaming, VR flight simulation have become viable for consumers and small businesses. Instead of having a full cockpit with projected display, the cockpit, and everything else around the aircraft is shown on a head mounted display. Each eye is shown a separate image, as in section 2.1.3. The head mounted display is also tracked in space, allowing the pilot to look around. Some VR systems incorporates hand tracking, for further interactivity with the environment. The motion platform can be made light, since only the pilot and the most necessary controls need to be attached. The rest is virtualised by a computer, and sent to the VR system. A VR headset can be seen in 2.9.

Figure 2.9: HTC vive VR headset. [20]

2.3 Platform actuation

In this section, ways of moving a motion platform are introduced. Today there are many platforms available on the market over a large price range. The platforms differ in functionality and performance. Features that may vary are DOF and the way the platform is actuated. Most commonly used are two, three or six DOF. In general, the more DOF the platform has, the more expensive it is. Platforms can be bought complete, however there are also guides online for building platforms on your own.

2.3.1 Industrial Robots

In some existing projects, industrial robots are used to actuate cockpit scale simulation platforms, especially ones for helicopters. As shown in figure 2.10, the industrial robot imitates the function of a human arm. It consists of a waist rotation axis perpendicular to the ground, a shoulder rotation axis equivalent to the rotation of the arm, an elbow rotation axis that rotates the arm, and a wrist at the front end of the arm. The motor arranged in each joint drives each joint to rotate through a speed reducer, so that various postures in three-dimensional space can be freely realized, thus various complex trajectories can be generated.

With additional linear movement implemented on the base, the six DOF system can achieve high dexterity, larger motion envelopes, sustained centrifugal accelerations, and the possibility to place pilots in extreme orientations. Most of the characteristics can be neglected when simulating fixed wing aircraft. The size and cost are high.

Figure 2.10: Industrial robot actuator [21].

2.3.2 Linear Actuators

Different solutions can be used to move the simulation platform. One way is to use electrical linear motion actuators, see figure 2.11.

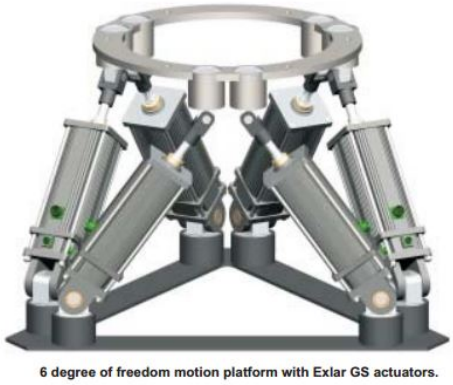

Figure 2.11: Platform utilizing linear actuators [22].

Linear actuators converts a rotary motion of a Direct Current (DC) or Alternating Current (AC) motor into a linear motion. The key parts of a linear actuator can be seen in figure 2.12. Depending on what direction the motor is rotating the shaft can either have a push or pull movement [23]. The gear between the motor and the lead screw allows the actuator to output higher torque, at the cost of speed.

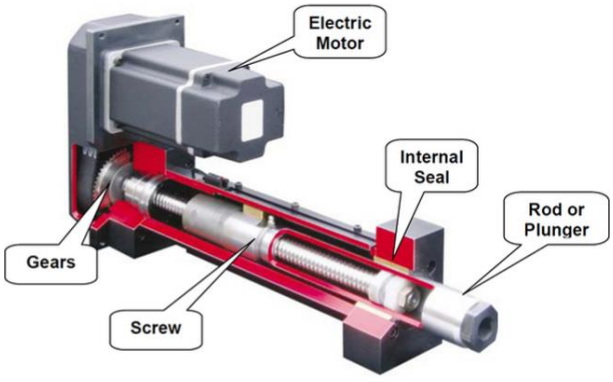

Figure 2.12: Key parts of a linear actuator [24].

Apart from electrical linear actuators there are also pneumatic actuators that utilize air pressure and hydraulic actuators that use liquids. Pneumatic actuators usually use an air compressor to force air through a hose connected to a cylinder that is controlled by valves. Air is by nature compressible, so pneumatic actuators can withstand shock. Pneumatic actuators suffer from air leakage which decreases efficiency and requires maintenance [25]. Hydraulic actuators works in a similar fashion, but instead of using air and an air compressor, a incompressible liquid and pump is used. Hydraulic actuators can produce very large forces and due to the liquid being incompressible, hydraulic actuators hold their position well [23]. Hydraulic actuators also suffer from leakage, but in the case of liquids it is possibly more costly as it may damage its surroundings. Overall, electrical linear actuators require less maintenance, are generally easier to control and are more quiet while running [26].

2.3.3 DC motor with rod

dAnother technique is that a DC motor rotates and changes the position and angle of a rod connected to the motor and the platform, as shown in figure 2.13. This way of moving the platform can be further improved by adding a wheel in the middle, see figure 2.14. This improves the force and motion of range, but at the cost of speed and space.

Figure 2.13: Platform using DC motor and rods to move its position [27].

Figure 2.14: Improved version with a gear attached between the motor and the rod [28].

2.3.4 Omni wheels

Pitch, roll and yaw can be accomplished by utilizing the friction of rotating omni wheels against a half sphere. Omni wheels have small rollers around the wheel itself, see figure 2.15. Three motors are used, one connected to each wheel. By controlling each wheel's speed separately the three rotational movements can be achieved. An example of how it works in a simulator can be seen in figure 2.16.

Figure 2.15: Omni wheel and its possible movement [29].

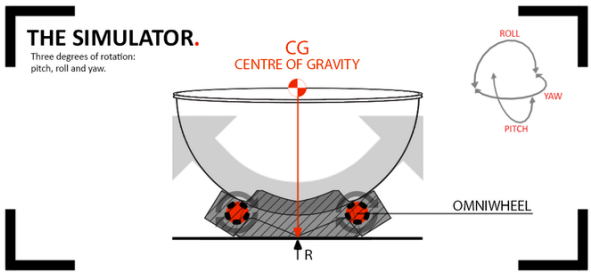

Figure 2.16: The omni wheels rotate against a half sphere that contains the user [30].

2.4 Existing work

A full flight simulator consists of a force motion system as well as a visual system. The force motion system needs to have either three or six DOF and the visual system needs to provide a view out of the flight deck, to be classified as a full flight simulator [31]. Moreover, full flight simulators are divided into four levels, between A and D. Level A and B include three axis of motion where level B includes ground handling simulation. Level C and D consists of six axis of motion where the highest level D consists of night, dusk and day visuals, dynamic control loading and the highest fidelity [31].

The level A and B flight simulators are not common. There exists only around a dozen of each level. Level C and D are much more common, with roughly 230 level C flight simulators being used in the US today. Lastly, level D simulators are the most common with around 400 to 450 existing at the moment [32].

The flight simulators in level D are so realistic, that pilots can obtain their license with it, without any real flight training. For high level flight simulators, Stewart motion platform are often used. However, to achieve even greater accelerations centrifuge simulators are used [33].

2.4.1 Commercially available motion platforms

When the DOF is limited to two, it is most common to use pitch and roll. Pitch and roll are used for simulating turning and forward acceleration. In figure 2.17 below, two off the shelf products with different price categories can be seen.

(a) Seat mover MS2 (2 Axis), $749.

(b) Professional P2 (2 Axis), $1949.

Figure 2.17: Two DOF motion platforms [27].

Three DOF motion platforms offer a motion capability in vertical axis to simulate vertical accelerations in addition to what two DOF motion platforms can do. These platforms are mostly used in driving simulators. When three DOF are used there are different solutions on which three degrees to use, e.g. pitch, roll and yaw. Another option is pitch, roll and heave. Pitch and roll are generally used in all cases. In figure 2.18, two off the shelf examples using pitch, roll and yaw can be seen.

(a) Consumer H3 (3 Axis), $1949

(b) Professional P3 (3 Axis), $2699

Figure 2.18: Three DOF motion platforms [27].

Furthermore, off the shelf simulators using pitch, roll and heave are also available. This is mostly used for helicopter simulators, although figure 2.19 shows an airplane simulator.

Figure 2.19: Generic Airplane Simulator (pitch, roll and heave), $21 369 [34].

Six DOF motion platforms, called Stewart platforms, are mostly used in professional simulators like flight training simulators. Six DOF motion platforms are able to carry high payloads. In figure 2.20, two off the shelf flight simulators can be seen.

(a) Consumer H6 (6 Axis), $3799.

(b) Professional P6 (6 Axis), $5299.

Figure 2.20: Six DOF motion platforms [27].

2.5 Digital Combat Simulator

Digital Combat Simulator World (DCS World) is a free-to-play digital battlefield game that supports VR. It consists of realistic simulation of military aircraft, tanks, ground vehicles, navy ships, world war two vehicles, trains and ships. DSC have multiple planes available for the user, including JF-17 Thunder, F-16C Viper, F-14 Tomcat and more [35]. The high level of realism in the game, makes it an excellent base for a simulation, with realistic graphics, accurate details in the cockpit as well as fully working and interactive buttons and instruments.

From the DCS base game it is possible to export a certain amount of parameters from the aircraft simulation, however the possible outputs are limited. From the base game, only the linear accelerations of the centre of mass of the aircraft can be exported. The simulation outputs data through a LUA script after each frame has been rendered. [36] The simulated aircraft provided by the stakeholders can be programmed to output more data, possibly enabling the motion simulation to be of higher fidelity. To access this data, there are a number of approaches.

Log file: The variables specified can be continuously appended to a log file. The data can then be read by another program or controller.

TCP output: TCP is a protocol for transferring data over a network. It uses sockets to determine the destination of the data. This network can also be local to a single computer. TCP has many features guaranteeing correct and error-free data transfer, making it robust [37].

UDP output: Similarly to TCP, UDP is a protocol for network transfer of data. However, it ignores error-checking, hand shaking and other robustness features, making the overhead much smaller, therefore making the UDP protocol superior in speed [38].

Chapter 3

Methodology

This chapter goes through the development of the final concept design choice, and the design of subsystems realising this concept.

3.1 Centre of rotation placement

During the development and research process, many design concepts were generated, discussed and sketched. The most important aspect for the decision of the design was considered to be the placement of the centre of rotation (COR).

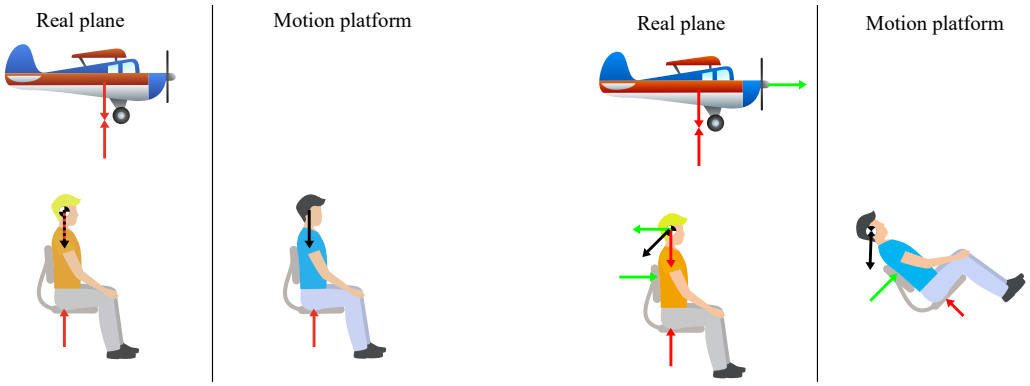

(a) Aircraft sitting on the runway.

(b) Aircraft accelerating on the runway.

Figure 3.1: Using gravitational acceleration to simulate an acceleration on the vestibular system.

The most sensitive organ for determining the direction of acceleration is the vestibular system. In order to simulate a linear acceleration, one can tilt the head, so that the constant gravitational acceleration is in the same direction as the resulting acceleration vector from the simulator. For an intuitive explanation, in figure 3.1 the resulting acceleration vector direction is the same for both real and simulated cases, from the pilot's point of view. This result was extended to include other degrees of freedom (DOF). From chapter 2, a main design idea was developed and shared between all concepts. This result however only allows the simulation of linear acceleration. Since a pilot also exhibits angular acceleration, a proposal for having a different COR for simulating angular acceleration was discussed. It is proposed that this COR would be close to the COR of the real aircraft.

3.2 Immersion test on Stewart platform

The immersion test on the Stewart platform with the pilot confirmed that it is sufficient for the platform to only have two DOF. One for pitch and another for roll. However the placement of COR matters as it affects the immersion.

As it was difficult to vary the COR on the Stewart platform it was not possible to conclude a concrete placement of COR from just the tests. The main uncertainty is regarding the COR for pitch as this affects the feeling of linear acceleration, which is essential for the immersion. But from the test concluded, state of the art and feedback from the pilot, the following conclusions have been reached:

- For roll it is sufficient to place the COR under the chair.
- For pitch the theoretical placement of COR should be in the head. But this might make the user experience a swing like effect, especially in the feet when simulating smaller accelerations, such as in precision flying scenario.
- A viable option is to have two separate COR for pitch. One at the head and the other below the seat. In this case one COR would mainly handle linear acceleration and the other would handle angular acceleration. The synergy between the COR would need to be tested and tuned.
- Having an adjustable chair, where the height can be changed would enable the COR to be placed at different heights. One compromise would be to have it between the seat and the head, around the chest area.

Regarding the motion span and actuation speed it was concluded that the output from the Stewart platform was satisfactory. With all this in mind the preference of the group is the second design concept, that allows for separate COR for pitch and roll. The second design concept is a collection of three different solutions. The following allocations of COR are possible at the moment:

1. COR in head for both pitch and roll.
2. COR in head for pitch and below chair for roll.
3. COR in head & below chair for pitch and below the chair for roll.
4. COR in head & below chair for both pitch and roll.

Table 3.1 illustrates how the real movements of the airplane will be simulated by the motion platform depending on the location of COR. The numbers represent different COR placement alternatives in the list above.

3.3 Platform Design

To come to a final design for the MP an iterative approach was used. Concepts were developed, compared and evaluated in stages. Concepts were eliminated during this process until one final design was decided upon.

Table 3.1: Impulse (step) response of pitch with varying mass.

Aircraft	Motion platform	1	2	3	4
Longitudinal acceleration	Pitch (gravity)	Head	Head	Head	Head
Pitch	Pitch	Head	Head	Below seat	Below seat
Lateral acceleration	Roll (gravity)	Head	Below seat	Below seat	Head
Roll initiation	Roll jerk	Head	Below seat	Below seat	Below seat

3.3.1 Inital concepts

To begin the iterative process, a meeting was held with the stakeholders, where results from the SOTA were presented. The group presented two fundamentally different ways of designing the platform. One concept was similar to that of the Yaw-VR described in chapter 2.3.4, and the other was an original design, based on having curved rails. After presenting these design ideas, the stakeholders took some time to discuss what concept to move forward with.

Due to the originality and simplicity of the design, the stakeholders decided to move forward with the curved rails concept idea. Furthermore, another argument for going with this design was that it would add something new instead of building another version of the omni-wheel concept which is already available to buy. An early sketch of this design is shown in figure 3.2.

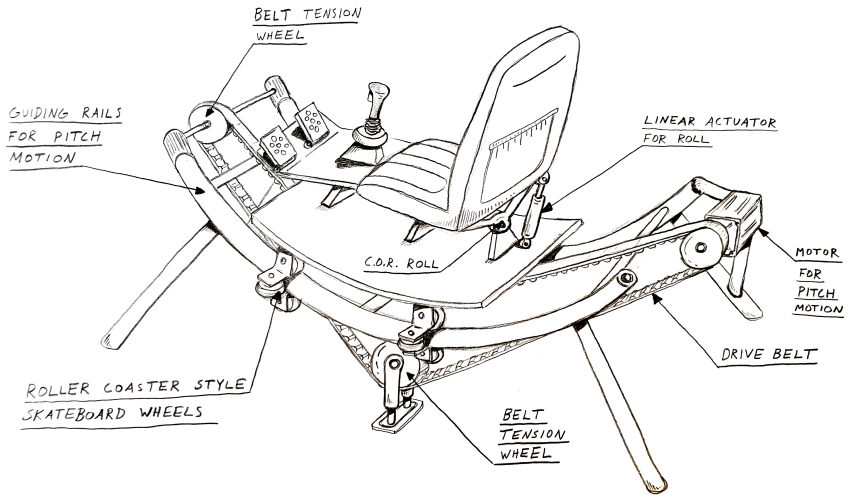

Figure 3.2: Early sketch of the curved rails concept. Adjustments made with Affinity Designer.

In figure 3.2 the method for actuating the pitch motion is shown as a belt drive connected to drive wheels. This was a suggestion at the time, and other methods of actuation were developed.

Another concept that was discussed early was a swing concept. The idea with this concept was having the platform attached to a swing and the platform hanging in the air. Motors were suppose to drive the swing at the joints. It has the ability to adjust the COR to be located at the head as well. Although, this concept was neglected due to the risks of having the platform hanging in the air, and also because the motors needed to handle extreme torque loads.

The swing idea sprung from the concept of making the curved rails smaller and smaller, and at

the same time move them higher and higher to still maintain the same location of the COR. This is due to the fact that the center point of the circle which the curved rails are a section of makes up the COR for the pitch motion.

First, direct drive was discussed, meaning that an electrical motor drives the motion platform by direct contact. At first a rubber friction wheel was discussed. Simply a tire, pushed up against a curved platform moving the platform. Due to fears of slip, this idea was dismissed. Instead, an idea resembling cog wheels was evaluated. The underside of the platform would be part of a very large cog wheel, and the motor would drive this cog through gears. This idea was also dismissed due to the complex production and possibly rough actuation. An illustration depicting direct drive is shown in figure 3.3.

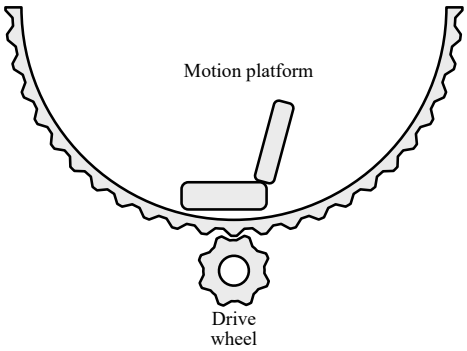

Figure 3.3: Direct drive. Made with Affinity Designer.

After these actuation methods were dismissed, a "pulling" actuation was discussed. Having a motor using a chain, belt or wire rope to pull the cart along the tracks. To compare these suggestions, they were evaluated according to their performance regarding fault risk, smoothness and maintenance. Using a chain was eliminated due to the fact that it is less smooth than a belt or wire rope, and requires lubrication. Chains are also generally more noisy. A wire rope has the risk of slipping on the rollers, or getting tangled. Therefore the belt was chosen as the preferred actuation method.

To gain a better understanding of the scale of the MP, simple sketch-like 3D-CAD models were developed. At first the sketch in figure 3.2 was modeled in 3D. The user sits on a cart on top of the rails. This 3D model is shown in figure 3.4.

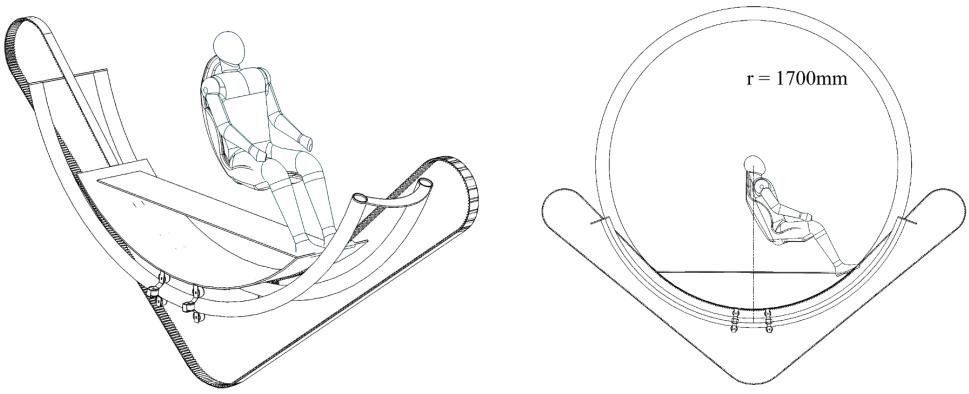

Figure 3.4: First CAD model. Made with Solid Edge 2020 and Affinity Designer.

With the pitch COR located at the head of the user, and an upright seating position, this design was obviously too large. From the beginning of the project, the stakeholders (SH) have stressed the importance of *compactness*. One suggestion from the SH was a configuration where there is a single rail between the user's legs. The problem with having a single rail between the user's legs is that the design would still have to be relatively large, due to the fact that the person has to be sitting on top of the rail. After discussing this concept more it became clear that some structure on the outside of the person was needed to allow the person to be placed between the rails, making the design more compact. Also, having the roll COR lower at the hips, for example, is not possible with one rail without tilting the legs into the rail, and therefore this concept was neglected. The single rail idea was also developed in 3D and is shown in figure 3.5.

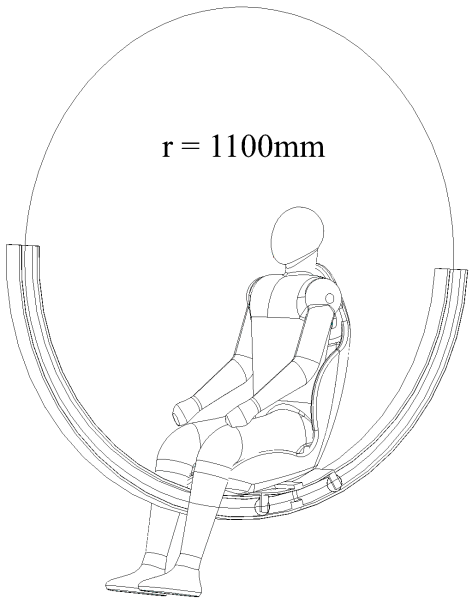

Figure 3.5: CAD model showing the rails between the legs. Made with Solid Edge 2020 and Affinity Designer.

To achieve the same rail radius as in figure 3.5 the rails could also be positioned on either side of the user, as shown in figure 3.6.

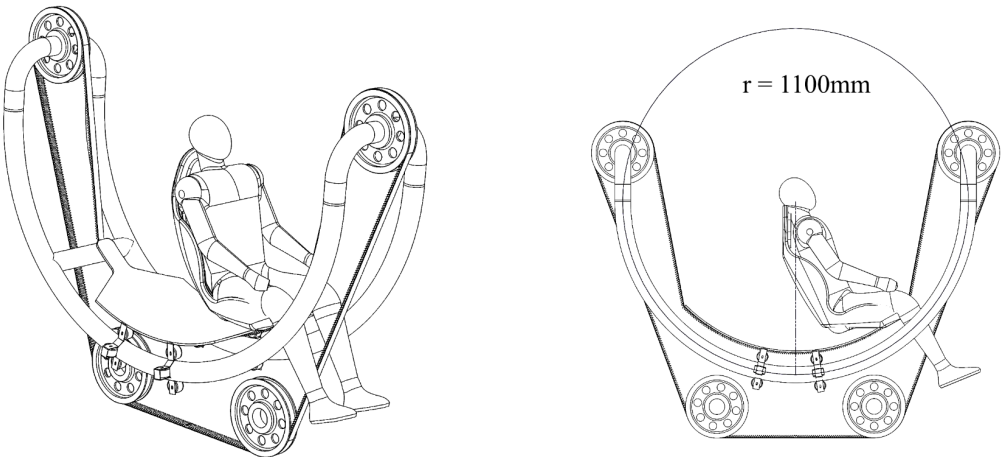

Figure 3.6: CAD model showing the rails on either side of the legs. Made with Solid Edge 2020 and Affinity Designer.

Since the user is between the rails, the radius can be made even smaller as mentioned earlier. The radius was chosen to intersect with the user around the thighs, because that is approximately the location of the COR of the roll motion. The roll axis was now approximately tangential to the rails, minimising possible interference between the two axes. This iteration is shown in figure 3.7.

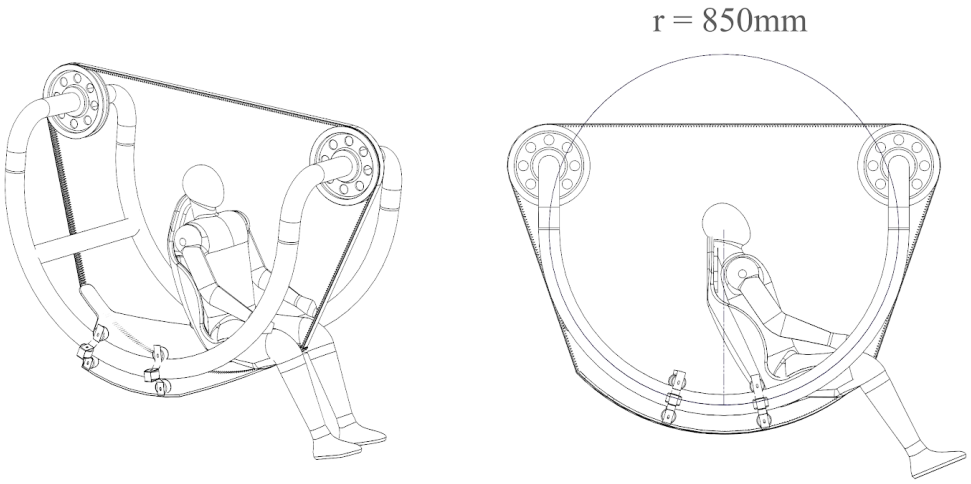

Figure 3.7: CAD model showing the rails around the thighs. Made with Solid Edge 2020 and Affinity Designer.

This design was presented to the SH, who offered some criticism. The main points from the feedback are summarised below:

- No mechanism above the user because that gives an impression of a much larger platform.
- Strive for a more compact design.
- The centre of rotation can be compromised if it makes the MP more compact.
- A tall MP has the impression of being larger than a wide one.
- Pitch is much more important than roll. The rolling action of the MP can be neglected if it proves difficult, time consuming or otherwise deducts from the performance of pitch action.

Another realisation was that the tension of the belt depends on the position of the cart. This is due to the fact that the geometry of the belt path changes depending on the position of the cart. When the cart is at the bottom point the belt path is the longest, and when the cart is at either one of the end positions the path is the shortest. In an effort to minimize this problem, a curved belt guide was designed at the underside of the cart to make the belt follow a circular path as much as possible. However, this could only be done to some extent, otherwise the belt guide would be very long and stick out of the construction at the end positions of the cart. Because of this tension problem, there needs to be belt tensioners in order to keep the belt tight at all positions. This set in motion a redesign to meet these new requirements. The SH were interested in a concept similar to the one shown in figure 3.6, but it needed to be much more compact, and follow all the points listed above. A frame to support the MP was also designed. A more detailed cart, and mounts for the driving wheels and tension wheels were implemented. The user has been put in a seating position with more bend in the knees, making the radius

of the rotating human smaller, further increasing compactness. This iteration of the concept is shown in figure 3.8.

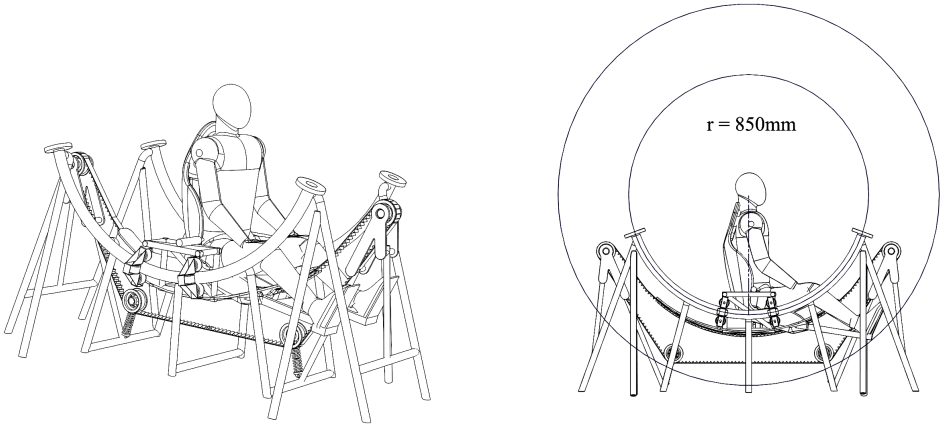

Figure 3.8: CAD model showing the more compacted design. Made with Solid Edge 2020 and Affinity Designer.

As with the other concepts, this was presented to the SH, and they again stressed that the MP was not compact enough. The only way to reach the compactness required was to move the COR downwards from the user's head. Instead of having the COR at the ear, it was moved to around the chest. This has the effect of making the radius of the rails smaller, and making the radius swept by the feet smaller, and possibly introducing some ghost forces according to the logic presented in chapter 2.1.5. The effects of these ghost forces were determined by the SH to be negligible. To support the smaller rails, the frame can also be shrunk. By advice from a production specialist, the profiles of the frame were changed from round pipe to square profile, facilitating production. A model of the floor, where the MP is to be mounted was also made, and fasteners were made to connect the frame to the floor. Possibility to adjust the side wheels were implemented, as well as a more detailed construction for the tension wheel suspension were made. All these changes can be seen in figure 3.9.

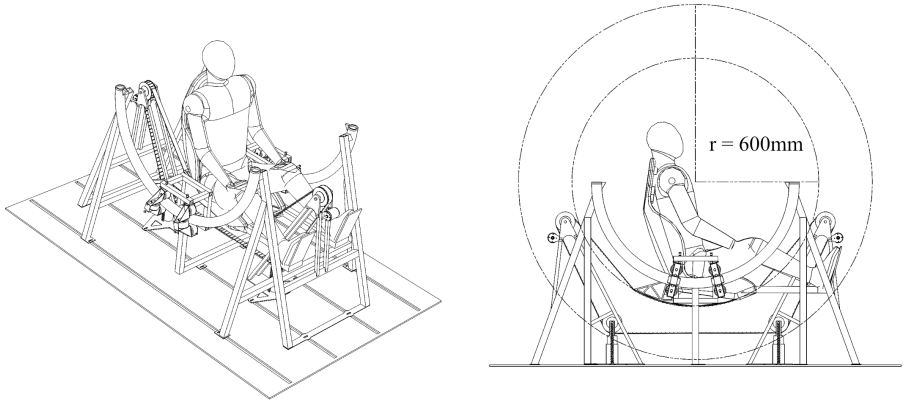

Figure 3.9: CAD model showing the changed COR. Made with Solid Edge 2020 and Affinity Designer.

3.3.2 Main frame and curved rails

With the final radius of the curved rails in place, the design of the main frame and curved rails could be finalised. The core of the design is the curved rails, and the frame just needs to support them and provide stability. The frame was designed in multiple pieces, that would be joined with screws during production. This is to facilitate construction, assembly, disassembly, as well as moving. An illustration of the frame and rails is shown in figure 3.10.

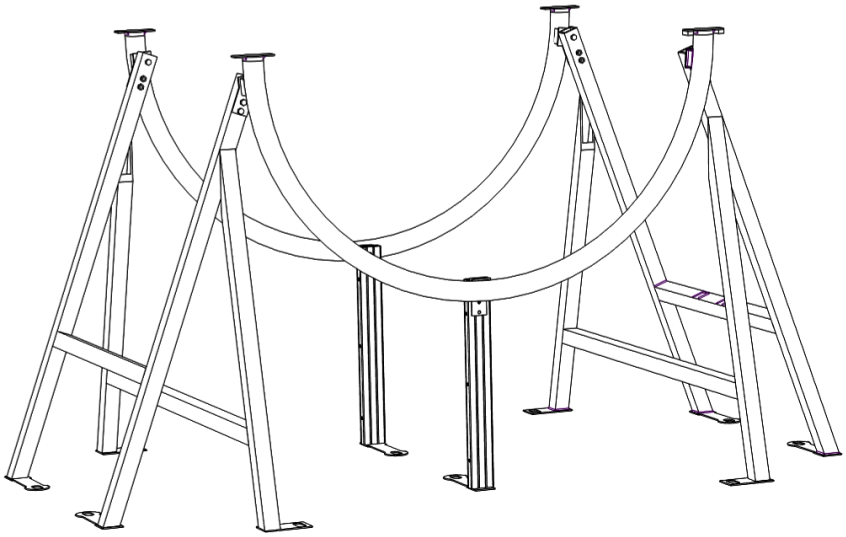

Figure 3.10: CAD model showing the frame. Made with Solid Edge 2020 and Affinity Designer.

3.3.3 Drivetrain and pulley frame

Due to a miss-calculation it was believed that the motor torque alone was enough to drive the MP. After some more detailed analysis, it was however clear that gearing would be necessary. Since the gearboxes will need to withstand the loads of moving the MP they need to be quite large. Details on how the gearbox was chosen can be read in chapter 3.7.2. The result of this caused the motor-gearbox assembly to become large and cumbersome. In figure 3.9 the motors are mounted next to the pulleys, and this was no longer possible. The powertrain was moved down, to be mounted on the floor, and extra belts and pulleys were added to transmit the torque up to the pulleys. While using belt drive, the belts need to be under tension to properly transmit torque. There were a number of proposed designs to achieve tension. First, a design was proposed that would move the entire powertrain vertically. This was however complex, and may be difficult to set after assembly. A simpler solution was to mount an adjustable tension wheel on the frame, always pushing the belt to maintain proper tension. The powertrain can be seen in figure 3.11.

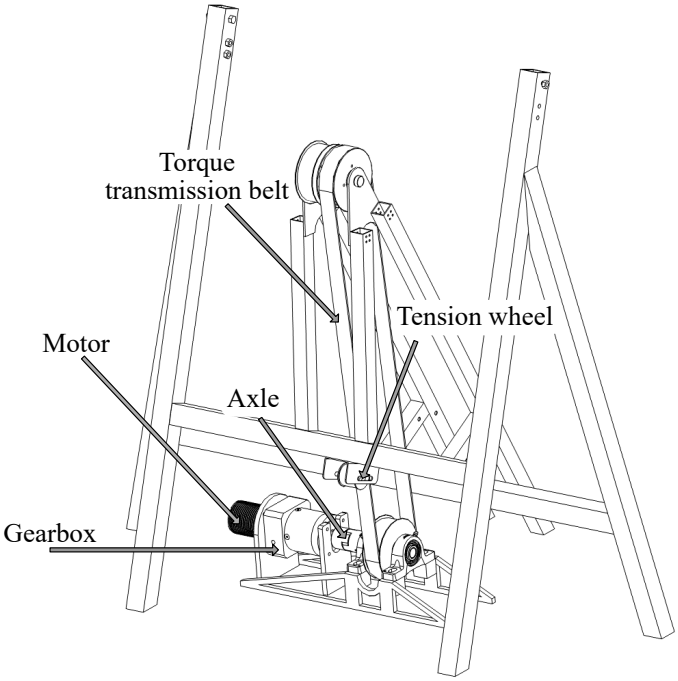

Figure 3.11: A CAD model showing the powertrain. The rest of the frame has been hidden. Made with Solid Edge 2020, and Affinity Designer.

In figure 3.12 there is a more detailed view of the mount where the motor and encoder are mounted. The encoder is embedded into the mount, because it was too wide to be fitted on top of the mount, interfering with the shaft key and keyway of the motor's shaft. The encoder was used to get a better resolution of the motor's position.

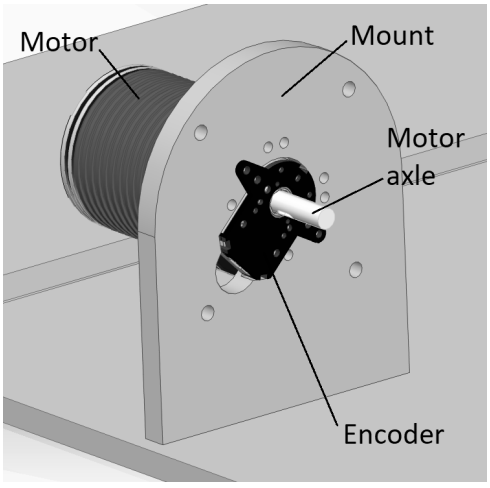

Figure 3.12: The motor and encoder mount. Made with Solid Edge 2020 and Paint

Two powertrains are responsible for the pitch movement of the cart along the rails. One is located on the floor at the front and one on the floor at the back of the main frame.

As there will be large radial forces acting on the pulley connected to the gearbox, the axle holding the pulley is mounted in two bearing houses. In this way, the bearing houses, that are attached to the floor via steel profiles, take up these radial forces instead of the output shaft

of the gearbox. The output shaft of the gearbox is only rated for a certain amount of radial force, why it is necessary to offset these forces to other components. A schematic view of the components comprising the powertrain can be seen in figure 3.13. The mount these components are attached to, is visible in figure 3.11.

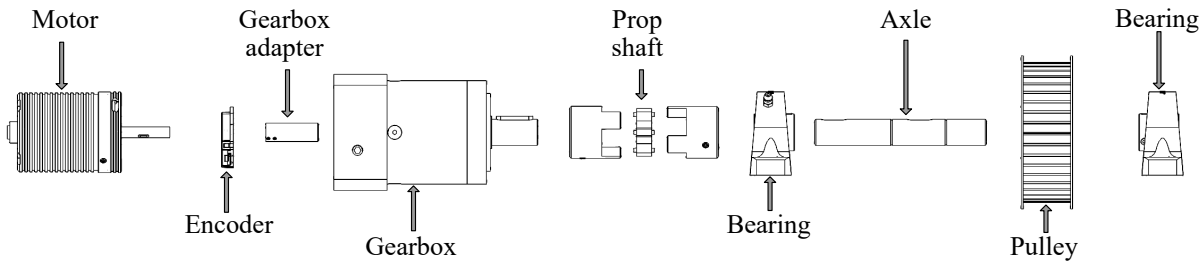

Figure 3.13: CAD model of the gearbox and motor assembly. Made with Solid Edge 2020, and Affinity Designer.

The main belt tensioners also underwent some changes. It was clear that two tensioners were unnecessary, therefore, one was replaced by a static wheel. The remaining tensioner was also placed at an angle, normal to the belt, to be more effective. The changes in wheel tensioner design are presented in figure 3.14.

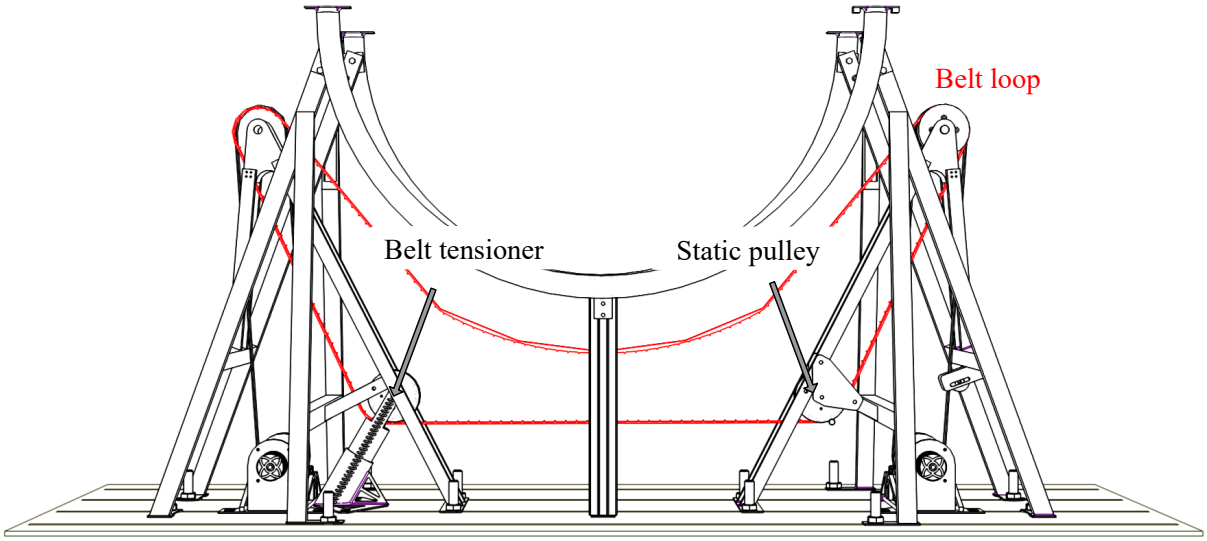

Figure 3.14: The belt tensioner. Made with Solid Edge 2020 and Affinity Designer.

The belt tensioner is mainly comprised of two concentric pipes, a belt pulley and two springs. The inner pipe can move inside the outer pipe like a piston in a cylinder, and is under tension by the two springs. The springs are easily accessible and easily changed to other springs with different spring constants to fine-tune the force. Also, gravity helps to pull the pulley downwards to keep the belt tensioned at all times. This feature was necessary because the geometry of the belt loop is a function of the position of the cart. And in order for a belt to function correctly, it has to be tense at all points.

3.3.4 Cart

At this stage, the main parts of the frame and pulley system where designed and ready for production, so focus was placed on the cart. The main design idea for the cart is having a chassis supporting the wheel holders, and having a mount for the chair and footrests. Since the chair shall support a rolling motion, it needs to be mounted on an axle. Having the feet stationary while the upper body moves would create an unsatisfactory sensation, therefore the foot rests should be mounted to the chair, and not the cart.

The cart is designed to allow parts of the user and chair to be positioned under the rails to allow for a more compact design overall. The challenge with designing the cart was to make it take up as little space as possible to allow for a compact design while still making it strong enough to support the weight of the user. The cart should also be as lightweight as possible to lower the mass that the motors have to pull.

The chassis for the cart is a simple design using square profile. Underneath there is a base plate for mounting both the hinges for the chair roll mount. This plate also provides mounting holes for attaching the belt and belt guide. This assembly is illustrated in figure 3.15.

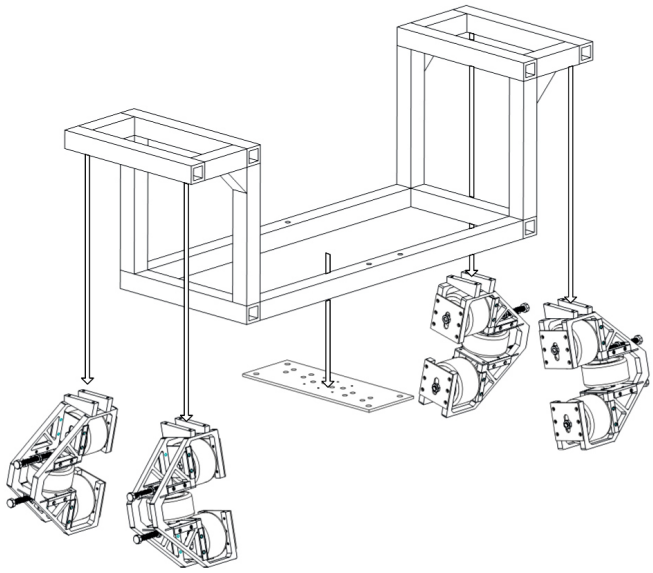

Figure 3.15: CAD model showing the cart chassis, wheel holders and mounting plate. Made with Solid Edge 2020 and Affinity Designer.

3.3.5 Wheel holder units

Each of the wheel holder units holds three wheels. The upper wheel prevents the cart from falling down, the side wheel locks the cart sideways and the lower wheel prevents the cart from lifting from the rails in case of the belt pulling the cart when it is at one of the end positions. The design does not have any suspension except from the softness of the wheels and the padding of the chair. In an ideal world, suspension should not be needed in this kind of design because it is just a cart moving along a perfectly smooth rail. But in reality there will be some roughness on the rail and other parts which makes some suspension desirable.

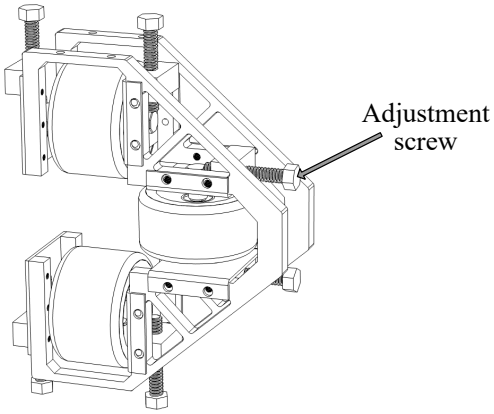

Figure 3.16: CAD model showing the wheel holder unit. Made with Solid Edge 2020 and Affinity Designer.

All three wheels are manually adjustable using screws so that they will fit the rail tightly. A possible problem with this design is if the rails do not have the same thickness along their length, and/or if the two curved rails are not perfectly parallel to each other when mounted to the frame. A solution to this would be to have moving wheels in the holder, and put them under tension by the help of springs that push the wheels against the rails. However, this design would be quite complex and was discarded due to the time limitations. The wheel holder is illustrated in figure 3.16.

3.3.6 Chair mount and roll mechanism

A model of the chair was needed to design parts that interact with it. A 3D scan was made of the chair using photogrammetry, a technique using multiple photographs taken from different angles to automatically generate a 3D geometry. The program is called Autodesk Recap. This was done to speed up the modeling of the chair, which would have been complex to do manually. Form-critical parts of the chair, such as the mounts underneath, were measured and modeled by hand, as they need to be exact to connect to other parts. The resulting chair is shown in figure 3.18.

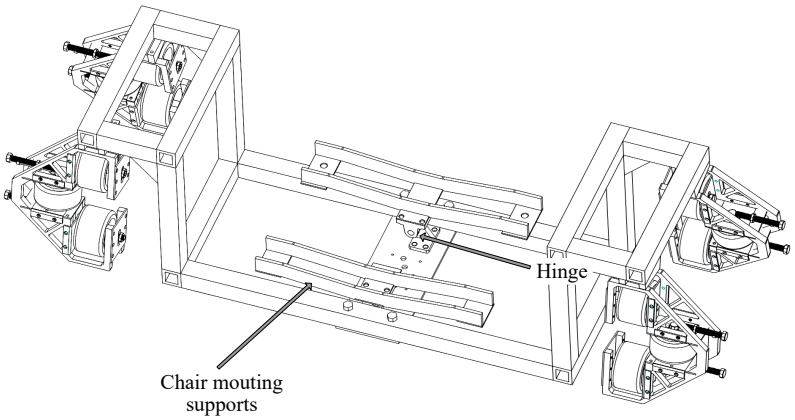

Figure 3.17: CAD model showing the hinges and chair support. Made with Solid Edge 2020 and Affinity Designer.

To mount the chair on the cart, hinges were used. The hinges connect to the base plate on the underside and to the chair supports above. The chair support structure was designed to be as low-profile as possible, while still maintaining structural rigidity. This is to keep the user low in the chair, having the head closer to the COR. The chair support structure was designed using FEM analysis in order to ensure a robust result. A challenge with designing these was to make them stiff enough to make the chair sit firmly on the axles without displacing too much resulting in unwanted movements of the chair. Under the chair there is limited space, why the beams could not be made too wide. The chair supports and hinges can be seen in figure 3.17. A design that allows user adjustment in height was at this stage disregarded. It was not possible to design a working solution within the time frame.

The feet should be securely held in place, since if they would slip off the foot rests, the legs could collide with the frame. Due to time constraints, the foot rests were designed to be static. The base of the foot rests were designed to use the same material as the cart chassis, and to have a sheet metal top to hold the feet in place. Holes for Velcro foot straps were also designed to implement secure holding of the feet.

To mitigate changes in geometry of the belt loop, as the cart travels, a belt guide was designed. It comprises a circle sector, and has the same radius and center point as the circle as the COR shown in figure 3.9. This design is an effort to make the geometry of the belt as constant as possible during the movement of the cart, to make the belt tense during the whole movement and also to make the control of the motion as simple and close to linear as possible. An image of the foot rest and belt guide is illustrated in figure 3.18.

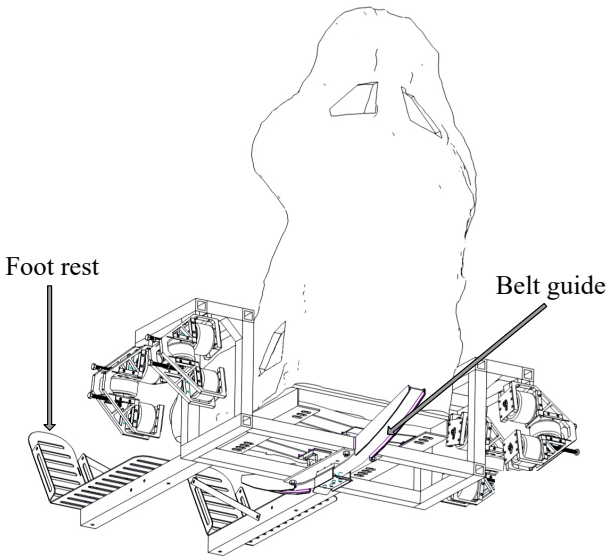

Figure 3.18: CAD model showing foot rests, and the semicircular belt guide. Made with Solid Edge 2020 and Affinity Designer.

A requirement from the SH was that the joystick must not intrude on the user, or inhibit the user from accessing the MP. The joystick mount was therefore designed to be as small as possible. Different placements of the joystick were discussed. The SH expressed a desire to have the joystick mounted to the side. Because of the compact size of the MP, the cart moves very closely to the rails, there is therefore no space to mount a joystick there. The joystick could be on the side, if mounted on the cart chassis. This is however undesirable, as the joystick would be stationary while the user rolls. The joystick was therefore placed in the traditional position, between the legs. A mount was designed with sheet metal in mind. It was designed to

fit between the seat cushions, and mount with bolts to the underside of the chair. The joystick mount is shown in figure 3.19.

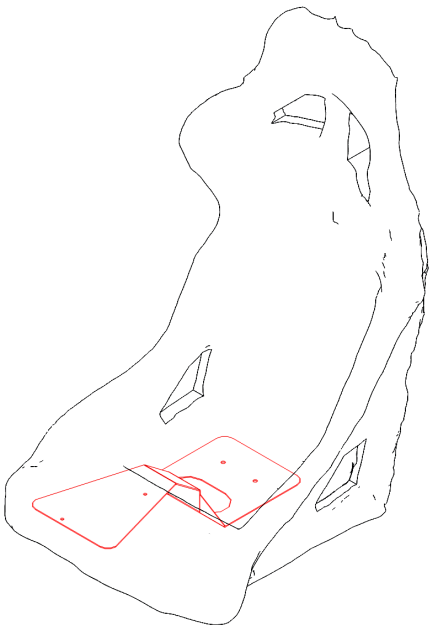

Figure 3.19: CAD model showing the joystick mount. Made with Solid Edge 2020 and Affinity Designer.

3.3.7 Belt mounting assembly

On the underside of the cart, the two belt ends meet and should be fastened tightly to the cart. Figure 3.21 shows the belt mounting assembly design. The upper belt is connected to the cart and loops around to the motors. The fixing belt is a piece of the same belt turned upside down. When they are clamped together using screws they deform and join tightly.

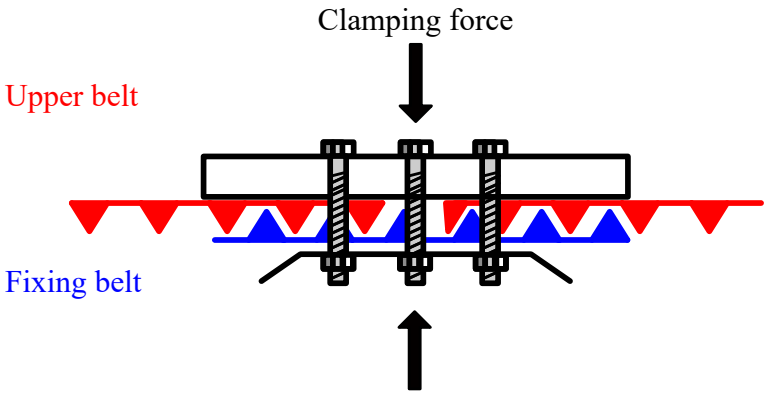

Figure 3.20: The belt mounting assembly.

There are large forces pulling on the belt that is fastened with the aforementioned mounting assembly. Therefore it would not be durable to just drill holes in the belt and mount it with bolts, as the bolts with time would rip the belt apart. In the design mentioned above, the pulling

force is more evenly distributed over a larger surface and distance of the belt ends, making them last longer. A 3D design of this concept is shown in figure 3.21.

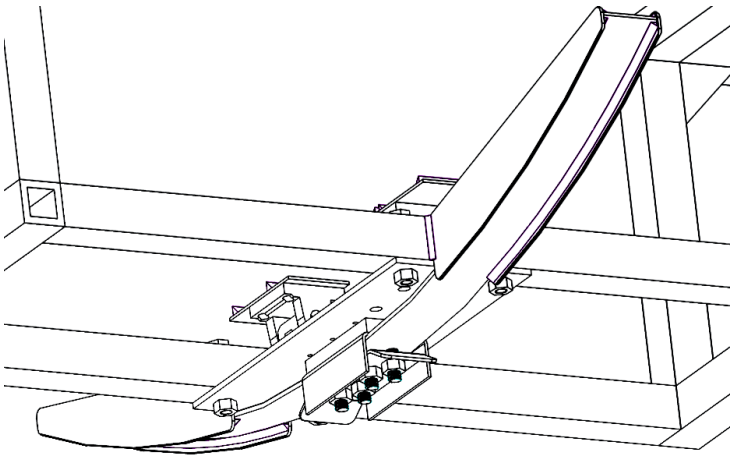

Figure 3.21: CAD model of the belt mounting assembly.

3.4 Simulation Model

A model of the system was made in Simulink. This was done in order to study the overall behavior of the MP. It also enabled the initial development of the controller without access to the finished hardware.

3.4.1 Simplifications

Since the cart moves in a circular motion, the model is non-linear. But after discussion with an expert within control theory it was determined that linear control should be sufficient enough for the intended task.

There were some difficulties when it came to the modelling of the chosen concept. Most of these difficulties were due to uncertainties regarding the belt that is used to actuate the cart. The belt will deform as the cart moves along the rails. When the belt changes shape the contact area between the belt and the pulley will also change. This change of contact might affect the torque transfer from the motor to the cart. Since the belt system is complex and the deformation of the belt is hard to anticipate it was simplified to be represented as a changing belt force vector. The pulleys were also simplified to be represented by two points, neglecting the contact change between the belt and the pulley. The simplified model can be seen in figure 3.22.

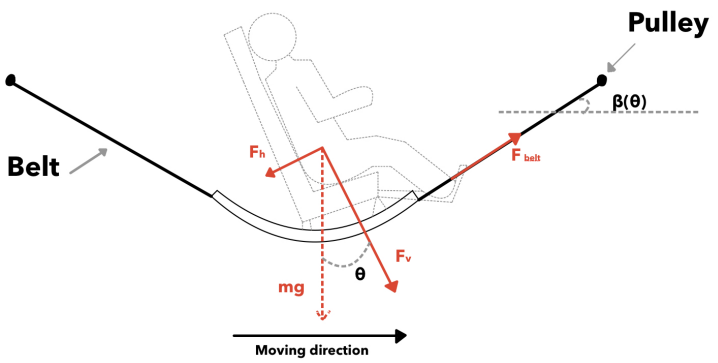

Figure 3.22: The simplified model. θ is the angle of the user and β is the attachment angle between the belt and the simplified motor. β is dependent on θ and changes as the user moves on the platform.

The final concept uses two motors to actuate the platform but the simplified model only takes one of the two motors into account, depending on the moving direction. If the cart moves towards the right, see figure 3.22, the right motor pulls the belt and the cart, while the left motor just assists with feeding the belt forward. The uncertainty regarding how the belt would deform, made it unclear how much difference the supporting motor would actually do. As the cart moves back and forth the geometry of the belt changes, resulting in the active length of the belt changing, see figure 3.23. This change in active belt length results in varying tension for the belt loop. It should also be noted that since the belt is only mounted in the middle of the belt guide, see figure 3.21, the belt will start separating from the belt guide as θ increases, this is also illustrated in figure 3.23. When this behaviour becomes evident, the system is more non-linear. The model assumes the belt is in full contact with the belt guide at all times, meaning it is not accurate when θ exceeds a certain value.

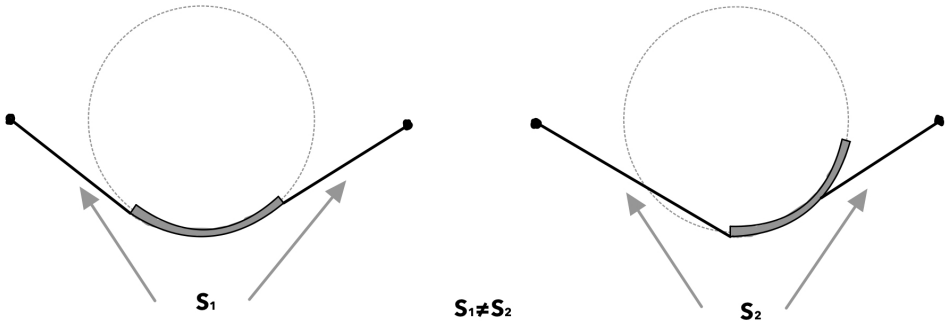

Figure 3.23: Illustration of how the active belt length (S_1 and S_2) can change depending on the position of the cart. In reality the belt is attached to pulleys and creates a continues loop, see figure 3.14. As θ increases the belt starts to separate from the belt guide.

As previously mentioned the mechanical design has taken this into account by adding a curved belt guide and a belt tensioner. However it is unclear how effective the belt tensioner will be. If the varying tension is still a problem even with the belt tensioner, then the other motor will have to counteract it, by feeding the belt less. The uncertainty regarding the support motor will first be answered when the hardware is finished. It was therefore considered to be acceptable to just model the system with one motor.

Due to the drivetrain, see figure 3.11 and 3.14 there is a relationship between the motor angle

θ_m and the cart angle θ. The relationship between the two is assumed to be linear according to:

$$\theta = \frac{\theta_m r_p}{nr} \tag{3.1}$$

Where n represents the gearing ratio of the gearbox, r_p is the radius of the pulley and r is the radius of the MP.

3.4.2 Model

The angle between the pulley and the belt attachment point, β, is dependent on angle of the cart, θ, see figure 3.24.

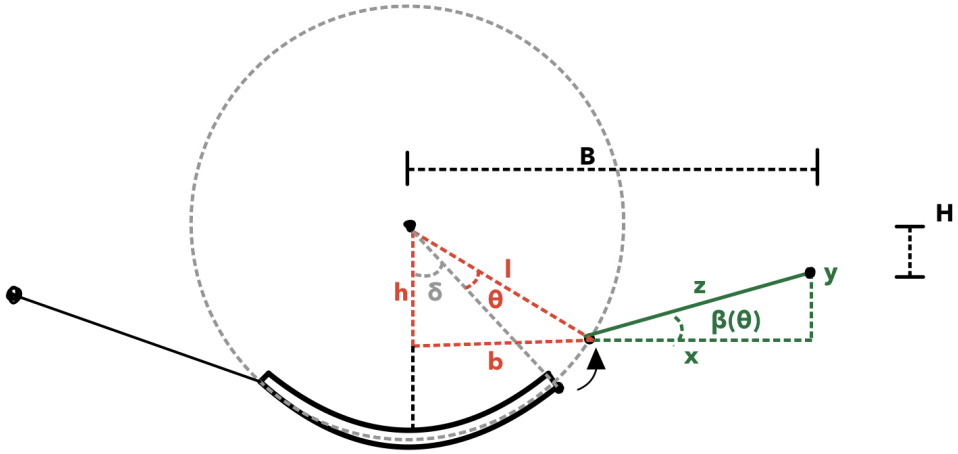

Figure 3.24: Dimensions used to calculate the angle between the pulley and an arbitrary belt attachment point (β). The black dimensions represents the distance between the motor and COR. δ represents the starting angle when the cart is in the starting position (θ=0). The red dimensions are needed in order to calculate the green dimensions and vary with θ . The green dimensions are used to calculate β. z represents the active belt length on the pulling motor side.

β can be calculated as follows:

$$h = l \cdot \cos(\delta + \theta) \tag{3.2}$$

$$b = l \cdot \sin(\delta + \theta) \tag{3.3}$$

$$x = B - b \tag{3.4}$$

$$y = h - H \tag{3.5}$$

$$\beta(\theta) = \arctan(\frac{y}{x}) \tag{3.6}$$

Since F_h is dependent on θ and F_{belt} is dependent on β, it is necessary to project F_h onto F_{belt} in figure 3.22, resulting in F_{h_belt}. The final relation between the two force vectors can be seen in figure 3.25. Depending on the the relationship between β and θ the resulting normal vector will have different directions.

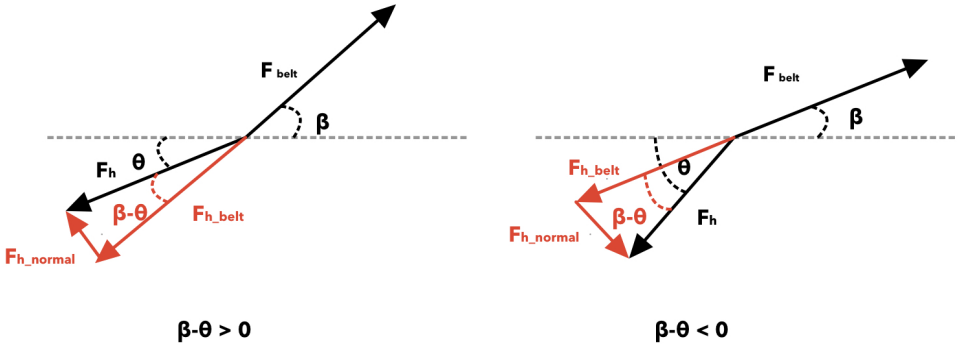

Figure 3.25: How the load, F_h, is projected onto the belt vector F_{belt}. If β is larger than θ the resulting normal force will contribute to the normal force of the load, F_v. If the opposite is true the resulting normal force will counter the normal force of the load.

F_{h_belt} can be calculated as follows, where the first factor is F_h in figure 3.22:

$$F_{h\_belt} = mgsin(\theta) \cdot cos(\beta - \theta) \tag{3.7}$$

Using F_{h_belt} the dynamic equations of the cart can be calculated:

$$F_{belt} - F_{h\_belt} + F_c = mr\ddot{\theta} \tag{3.8}$$

$$(T_m - J_m\ddot{\theta}_m)n - J_p\frac{\ddot{\theta}_m}{n} = F_{belt} \cdot r_p \tag{3.9}$$

F_c represents the friction acting on the cart wheels, $\ddot{\theta}$ is the angular acceleration of the cart, $\ddot{\theta}_m$ is the angular acceleration of the motor, J_m is the inertia of the motor, J_p is the inertia of the pulley.

By combining equation 3.1, 3.7, 3.8 and 3.9 the following equation is derived:

$$\ddot{\theta} = \frac{T_m n - r_p mgsin(\frac{\theta_m r_p}{nr})cos(\beta - \theta) + F_c r_p}{\frac{mr_p^2}{n} + J_m n + \frac{J_p}{n}} \tag{3.10}$$

The brushless DC motor is modelled in equation 3.16 and the torque of the motor is calculated in equation 3.12.

$$\frac{di}{dt} = \frac{1}{L}(U_i - Ri - K_{emf}\dot{\theta}_m) \tag{3.11}$$

$$T_m = K_t i \tag{3.12}$$

Where K_t is the motor constant. Using equation 3.10, 3.11 and 3.12 the system was modelled in Simulink together with the motor controller, see section 3.6.2. The final Simulink model can be seen in figure 3.26.

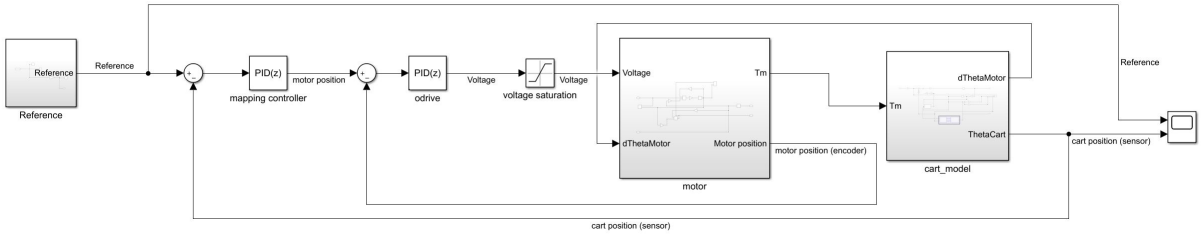

Figure 3.26: Subsystems of the Simulink model. The motor controller (Odrive), see section 3.6.2, is modelled with a tuned PID-controller.

3.5 Electrical design

The electrical design was made based on the most important components, described in this section.

3.5.1 DC motor and motor driver

A motor that satisfies the required torque to drive the weight of the cart and the user was the main focus for choosing the electronic components. Since it was important that the motor was electronic, a brushless DC motor (BLDC motor) was chosen. A BLDC motor is a synchronous motor that behaves like a shunt DC motor. It is a high performance motor that provides large torque, is powerful, reliable, smooth and efficient when controlling the speed and torque while also being compact and cheap compared to motors that provides the same power. [39]

To choose a sufficient motor, some calculations had to be made considering the worst case scenario. This would be where the motor had to pull the combined weight of a person together with the cart straight upwards with a certain acceleration. The known parameters were the radius of the pulley and the required angular acceleration. To convert angular acceleration to linear acceleration with the equation 3.13

$$a_{req} = a_{angular} r_{rail} \tag{3.13}$$

where $a_{angular}$ is 200 deg/s^2 and r_{rail} is 0.6 m and thus the a_{req} is calculated to be 2.44 m/s^2. The required force can then be calculated with the equation 3.14

$$F_{req} = m \cdot a_{req} + mg \tag{3.14}$$

where m is the mass of the person together with the cart, assumed to be 150 kg and g is the gravitational acceleration. The required force, F_{req} was calculated to 1839.52 N. The torque needed from the motor M_{req} can be calculated with the equation 3.15

$$M_{req} = F_{req} r_{pulley} \tag{3.15}$$

where r_{pulley} is the radius of the pulley, 0.05 m. The required torque M_{req} was calculated to 91.98 Nm. A motor with sufficient power could be chosen with the eqation 3.16

$$P_{req} = M_{req} \cdot \pi n_{rps} \tag{3.16}$$

where n_{rps} is the revolutions per second of the pulley, set to be 1.36 to reach the maximum position in 1 second, and P_{req} is the power needed, that was calculated to 786.59 W.

To accurately control the motor using a microcontroller, a motor driver is needed. Depending upon the type of motor and type of control required, the type of motor drivers will also change. A motor driver essentially controls the direction of the motor based on the commands it receives from the controller and thus supplies the motor with the appropriate voltage. Contrarily, only using a microcontroller without a motor driver will not be able to give enough power to drive a motor as they are sensitive to high voltage.

It is crucial that the movements from the motor is precise, therefore it was necessary to use an encoder that monitor the position of the motor. With the help of the encoder, the exact position of the motor or the apparatus which is moved by motor is measured.

3.5.2 Linear actuator

A linear actuator is an electric motor that generates motion in a straight line, so that the motion is linear rather than rotary. This motion is used to move the chair in a roll motion around the roll axis. The linear motor was needed to be strong enough to move both the weight of the chair and the user sitting on the chair. The basis of of a linear actuator can be seen in section 2.3.2. Since the DC motor inside controls the movement of the actuator, the ratio between the strength and speed of the actuator is fixed for a given motor. The translation between the rotational movement and the linear is also reducing the linear speed. Therefore it is challenging to find a linear actuator that is both fast and strong at the same time.

When making the design of the roll movement with the aid of a linear actuator, some mechanical limitations had to be considered. The roll movement of the chair can only tilt with a relative small angle since the chair hits the bottom of the cart plate at a certain degree.

Using the CAD model, this maximal angle was found to be 7°. This angle determines the torque required to tilt the chair which in turn determines the force needed from the actuator. Linear actuators has a smaller dynamical force capability, when loaded statically the structure of the actuator holds the load at place with a higher maximal possible static force. The design of the actuator therefore took the dynamical load into account. The basis of this calculation can be seen in figure 3.27.

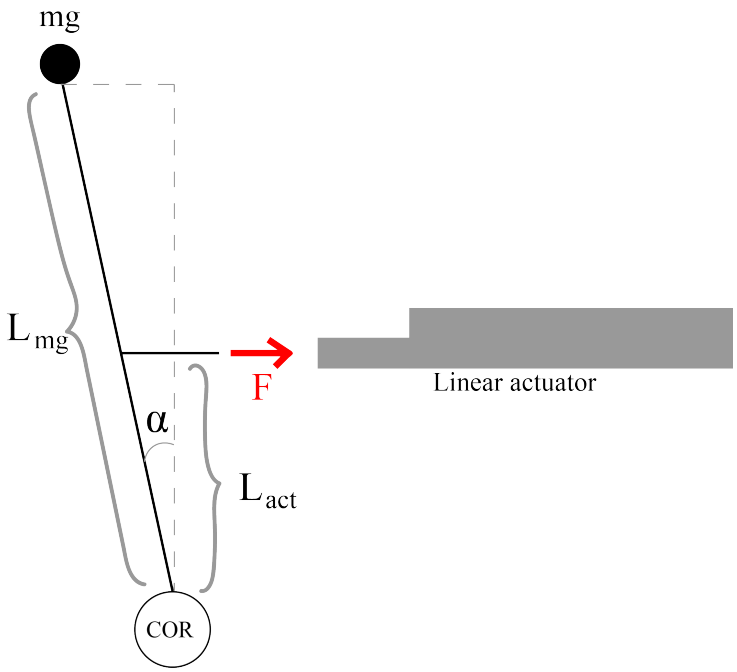

Figure 3.27: The force involved in the roll actuation. Created with Adobe Illustrator.

From this it could be found that the force required to start a motion from one end position of the roll is given by equation 3.17,

$$F_{req} = \frac{\sin \alpha L_{mg} mg}{L_{act}} \tag{3.17}$$

With $\alpha = 7$, $m = 100$ and lengths given from the CAD model, the required force was calculated to be $195N$.

The technical requirement of a speed of 30 deg/s was used as basis for how fast the linear actuator should be. The speed of linear actuators are specified in mm/s so a conversion between these two gave that this correspond to around 200 mm/s, which is unreasonably high for normal linear actuators. As a reference instead, the decision was made to follow a speed value of 7 deg/sec since this means it would reach the max position in 1 sec. This in turn corresponded to around 50 mm/s.

3.5.3 Sensors and switches

Temperature sensors measure the temperature on the outside of the motor. When the motor reaches a certain temperature, it will trigger the fans in order to cool down the motors. Limit switches were placed on the rails to trigger an emergency stop if the cart reaches a position that is too close to the end of the rails for safety reasons. Emergency stop buttons for both the user and the operator was also considered a safety priority. To accurately measure the position of the cart, an accelerometer and gyroscope were needed to feedback the cart's position when it moves.

3.6 Control design

3.6.1 Communication protocol

The selection of the communication protocol mainly considered the latency. In the TCP protocol, all network packets arrive in the exact order in which they were sent. If a packet is lost, the latter packets will hold until the lost one is found, called and re-sent properly. Also, applications using TCP can quickly perceive the existence of congestion and automatically slow down the sending. However, in this project, the order of packets is of far less concern given the size of data and the packet loss rate on Ethernet with wire connection is very low. Thus, UDP is chosen to directly receive packets.

3.6.2 Motor Control

To control the BLDC motors, an ODrive was used. The ODrive consists of a cascading controller and a BLDC three phase converter. The cascading controller, shown in figure 3.28, takes the position as the reference input and controls the current that goes into the motor. The BLDC three phase converter, includes a control circuit and three pairs of MOSFET, that converts the one-phase DC current into three phase and therefore controls the whole motion platform. The BLDC motor control circuit is shown in figure 3.29.

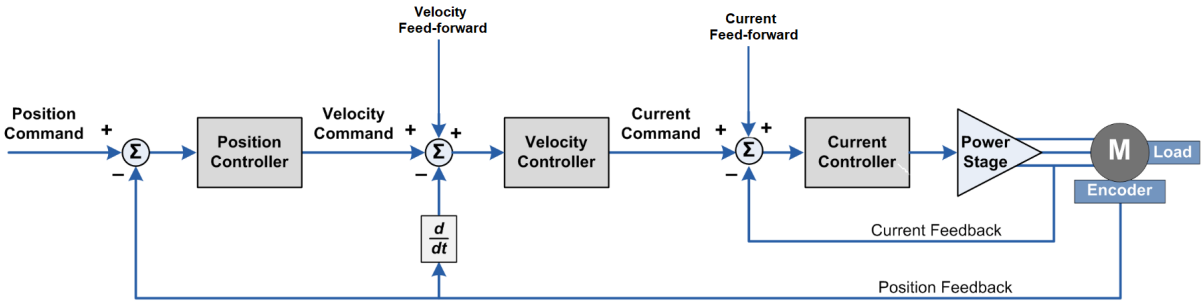

Figure 3.28: Cascade Control in ODrive[**ODrive**]

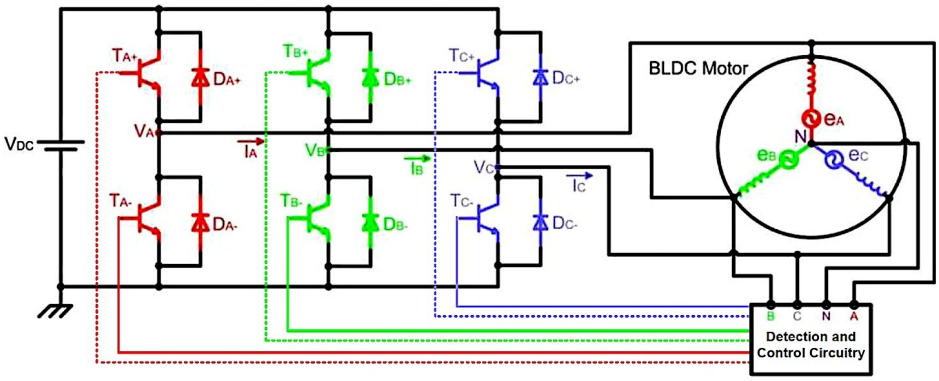

Figure 3.29: BLDC motor control circuit[39]

3.6.3 Cart Control

The motor position reference to the ODrive can be generated using the feedback position of the cart, using an Inertial Measurement Unit (IMU). A potential problem with the feedback approach is the dependency on the IMU sensor working reliably and the communication between the sensor and the personal computer (PC). It was therefore considered appropriate to use the derived model in section 3.4.2, to check if it would be viable to just map the motor position without using the sensor in the intended motion range. This was done by sending a ramp reference to the Simulink model, and then studying how the active length of the belt on the pulling motor side changed as θ changed, see z in figure 3.24, the result can be seen in figure 3.30.

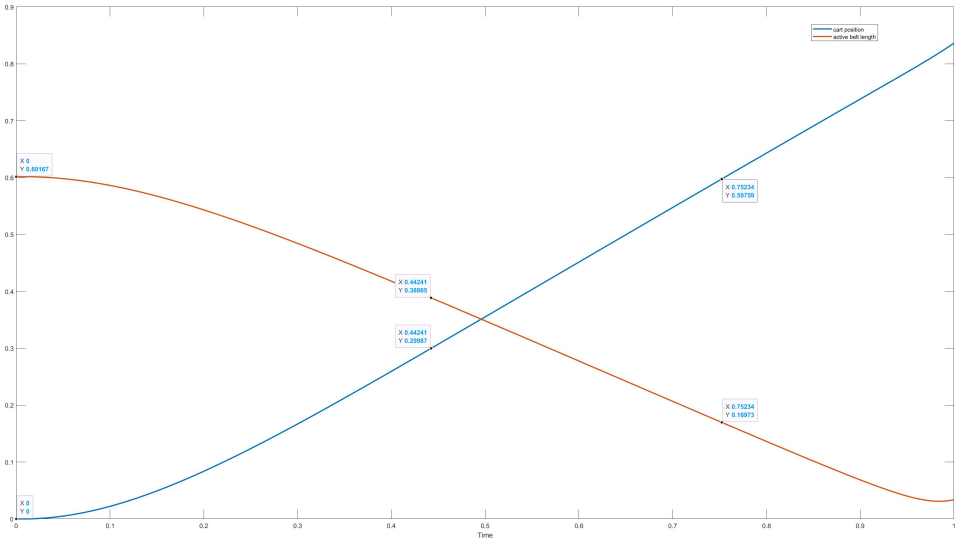

Figure 3.30: Visualisation of how the active belt length changes as the cart position (θ) changes according to the derived model in section 3.4.2. The data cursors in the figure are set to specific positions of the cart, at 0, 0.3 and 0.6 rad. The starting length of the belt is 0.6017 m when $\theta = 0$ rad and 0.1680 m when $\theta = 0.6$ rad.

The result in figure 3.30 shows that the relationship between the active belt length and the cart position is fairly linear. Therefore the motor position should be able to be mapped from the cart position reference, as in feedforward control. According to figure 3.30, the active belt length is 0.6017 m when $\theta = 0$ rad and 0.1680 m when $\theta = 0.6$ rad. Knowing this, it can be calculated how much of the original active belt length is used in order to actuate the cart 0.6 rad:

$$\Delta z = 0.6017 - 0.1680 = 0.4337m \tag{3.18}$$

The circumference of the pulley is 0.3676 m (O_{pulley}), which can be used to calculate how many turns the pulley needs to turn (n_{pulley}) for the cart to move 0.6 rad:

$$n_{pulley} = \frac{\Delta z}{O_{pulley}} = \frac{0.4337}{0.3676} = 1.1798 \tag{3.19}$$

Finally the mapping constant ($n_{mapping}$)from the cart position reference to the motor position can be derived:

$$n_{mapping} = \frac{1.1798}{0.6} 2\pi n = 308.88 \tag{3.20}$$

This means the motor needs to rotate 308.88 rad in order for the cart to move 1 rad.

3.7 Dimensioning

To realise the MP design, a number of parts were chosen, made and bought. This section is a description of the reasoning behind the decisions of some key components.

3.7.1 Motor components

The motor used for the pitch motion were BLDC motors and was purchased comparing the price with the power that satisfied the required power calculated in 3.5.1. The chosen motor, shown in figure 3.31, had a maximum power of 3500 W and four 12V car batteries were connected in series to provide the required 48 V for the motors.

Figure 3.31: Turnigy SK8 6372-139KV Sensored Brushless Motor (14P). [40]

However the torque was not enough to drive the whole construction. Thus, a gearbox was required in order to increase the output torque of the motor.

The output torque needed to be at least 70Nm according to the model. The motor in turn had a maximal speed of 6500 rpm and an output torque of around 5Nm. Therefore a gearing ratio between 1:25-1:35 was considered. A difficulty was to find a gearbox that had the right gear ratio as well as being able to handle the output torque and at the same time not breaking down due to radial forces or high input speeds from the motor. In the end, a gearbox called GPLE80-2S-25-F87 from the company Nanotech, with a ratio of 1:25 was chosen since it was able to both handle a large output torque as well as high input speeds. The downsides of chosing this gearbox was that it had to be supported radially with bearings to withstand the radial forces as well as a gearing ratio of 1:25 would allow a much higher speed then required.

A motor driver for BLDC motors called ODrive V3.6 from the company ODrive Robotics was chosen for this application. ODrive can control two motors at the same time and provide them with the right voltage and current for the chosen motor in the project. The encoder feedback is internal and maintains precise movements. For the microcontroller, an Arduino Uno was chosen

to control the motor drive. The ODrive has a built in library for Arduino, which facilitated the control.

The hall-effect sensors built in with the BLDC motors makes it possible for the controller to know the angle of the motor and thus knows what coil to power, but has a very low resolution so therefore does not provide and accurate positioning of the motor. To solve this problem, separate encoders with much higher resolution were bought and replaced the hall-effect sensors entirely. ODrive's associated encoder, the CUI AMT102 capacitive encoder, was chosen as it satisfied the specifications for the motor and provides the exact position of the motor required. [**ODrive˙spec**]

The linear actuator, shown in figure 3.32 was chosen in regard to the calculated values of the force and speed needed. The piston length was also considered in order to fit well mechanically as well as the choice of feedback from the motor. A built in potentiometer was choosen here since this was considered easy to use as a feedback for the actuation.

Figure 3.32: Linear motor, 12 VDC, 250 N and 2.4 A. [41]

This linear actuator, being able to carry out a dynamical load of 250 N, was able to fulfil the requirement of at least 195 N. However it was not as fast as desired, with a speed of 23.5 mm/s compared to the desired value of 50 mm/s. The alternative however would have been to get a less strong actuator and the decision was to prioritize that the motor was able to carry the dynamical load.

3.7.2 Other electronic components

For safety reasons, fuses were necessary to be connected before the motor driver and relay. As the current varies, three different fuses, 50 A, 100 A and 200 A from the company Littelfuse Inc. were used. After the fuses, a relay switch to turn on and off the relay was added to make it user friendly and to be able to add an external emergency stop for increased safety. Appendix B.1 shows the schematic of the relay controller that controls the relay switch. When the relay switch is turned off, the relay becomes inactive and everything else is turned off. This leads to the chair going back to it's initial position.

To keep the motors, ODrive and relay cool, fans were placed around these components. Three smaller fans (48 V, 16.8 W, airflow of 1.82 m^3/min) for the two motors and one for the ODrive and the relay. The schematic for the fan controller can be seen in appendix B.2.

To further increase the safety of the construction, another emergency stop function was desirable to implement. This emergency stop function is activated if the chair is at a maximum position before it hits the frame, if the user on the chair presses an emergency stop button or if a software failure occurs. Limit switches are triggered when the chair is at it's limit. The logic for this

emergency stop function can be seen in the circuit diagram in appendix B.3. The emergency stop button for the user and the software emergency stop is connected in the same schematic. The circuit works as a latch, when one of these buttons is pressed, the signal is kept high instead of going low when the button is released. Limit switches will send a high signal when it is pressed, but as the chair moves past the limit switch, the switch is released and it is turned back to low. Therefore, this circuit was invented as it was crucial to implement a logic to keep the signal at high once one of the buttons were to be pressed. As long as the signal is high, the relay is turned off. A reset button is connected to the limit switch controller that resets the signal to low.

Arduino has a sensor called Grove, which is a 6-axis accelerometer and gyroscope. This measures the positions and accelerations accurately and was therefore chosen. [42]

3.7.3 VR set-up components

The most important thing for the VR set-up was to be able to easily implement VR motion cancellation. VR motion cancellation means that certain movements in the virtual reality is removed or *cancelled*. In this application, the motion that needed to be cancelled is the motion from the motion platform, as it was desired to keep the user in the same position in the virtual reality but not in the room.

This is achieved by a HTC Vive tracker in figure 3.33. HTC Vive tracker comes with 18 sensors that senses the axis position for X, Y and Z-axis. It is used to bring physical objects into virtual reality. When used on a motion rig it can be used for motion cancellation to keep the driver stationary in their seat whilst still being able to look around in the virtual world.

Figure 3.33: HTC Vive tracker. [43]

Base stations are placed in the room and is used for tracing the exact position of the VR headset, VR controllers and VR tracker. It was important that the VR set-up came with base stations as these were crucial for the tracker to work. Hence, the best choice for the VR set-up was HTC Vive Cosmos Elite, since it was required that the VR headset needed to be compatible with the tracker and the VR headset needed to come with base stations. [43] Figure 3.34 shows the HTC Vive Cosmos Elite VR headset, the base stations and the controllers.

Figure 3.34: HTC Vive Cosmos Elite. [44]

3.7.4 Mechanical components

The frame holding the curved rails is essential for the stability and robustness of the MP. It serves as the structure, and therefore needs to be rigid and strong. To maximise strength, and facilitate welding, steel was chosen as the material. While the frame was being designed, it was run through a number of FEM analyses. In simulation, the frame was subjected to 2000 N of force straight down, and fared well in terms of stress and displacement. With this result as backup, 40x40 mm square steel profile with 2 mm wall thickness was chosen as the building material for the frame. Parts of the structure, later welded together, can be seen in figure 3.35.

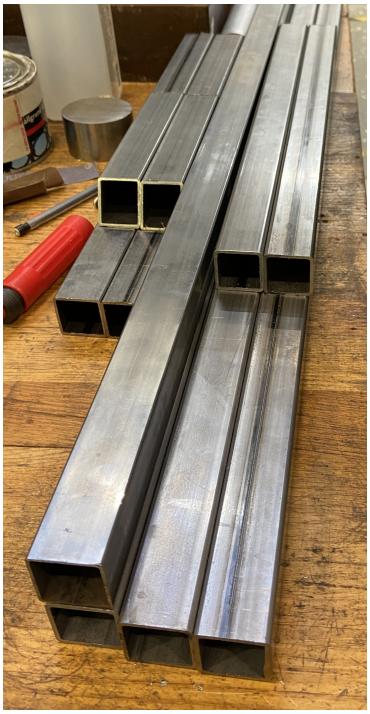

Figure 3.35: Square steel profile

One challenge with the pulley frame was that it needed to be very narrow, in order for it to fit between the user's legs while travelling along the rails. At the same time it needed to be strong enough to support the pulleys when the belt is transmitting the pulling force from the motor to pull the cart. To mitigate this problem, long beams were designed to be as close to parallel to the pulling force as possible in order to prevent bending of the pulley frame. The pulley frame is constructed out of 40x40 mm steel profiles with a wall thickness of 2 mm.

The cart has stringent requirements of size and weight. It needs to fit between the rails, and cannot be too heavy to for the motors to lift. Both aluminium and steel were considered for the cart. Again, using FEM analysis, two chassis proposals were made, and checked for stress and displacement. If aluminium was to be used the profile needed to be thick, to reach the same performance as the steel chassis. As a result, there was little space to fit the chair, wheel holders and belt guide. The steel version was chosen as it is simpler to produce and is smaller in size. The profile used for the construction of the cart chassis was 30x30 mm square profile, with 2 mm wall thickness.

The foot rest beams were designed to use the same material as the cart chassis. They were tested using FEM to ensure their robustness, and performed well.

Since the cart has no suspension, the wheels need to be soft in order to achieve a smooth actuation. Large wheels also provide a smoother roll. The wheel also needs to be small enough to fit around the curved rail. Some group members are skateboarders and therefore have experience in dealing with skateboard wheels. Skateboard wheels come in a variety of sizes and hardness. For this application longboard wheels were chosen as they are soft and small enough. The wheels chosen were 70 mm longboard wheels which Jonas Xu had in stock at home. Longboard wheels are designed to fit an 8 mm axle, and have a 22 mm inner diameter. The bearings were 8x22x7 mm to fit the longboard wheels, and bought from Kahalani and SKF. In figure 3.36 the longboard wheels can be seen.

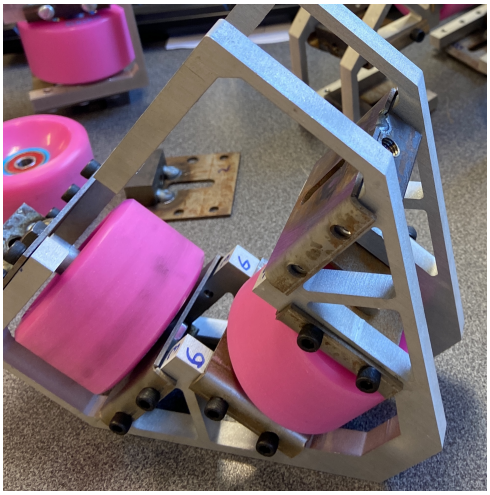

Figure 3.36: The longboard wheels

When choosing belt and pulleys, only one belt and four pulleys were needed at first. The requirement at that moment, was that the belt needs to support forces up to 2000 N. Pulleys and belts are categorised according to the size and number of teeth. A high AT number, a larger tooth. After speaking to a sales representative at NK Technics, they suggested to buy one AT20 belt with steel cords and with the width of 32 mm. Therefore they were ordered, together with four AT20 pulleys. Later, there was a need for additional belt and pulleys. It was found out that AT10 is enough, therefore, two AT10 belts with the length of 1900 mm and the width of 32 mm were bought. Together with the belts, four AT10 pulleys were bought, all this from Aratron who could provide fast delivery.

To withstand both the radial and twisting forces the axles in the powertrain need to be sturdy. The gearbox has an output diameter shaft of 20 mm, so the axle connected the gearbox to the driving pulley was chosen the same diameter. 20 mm was also chosen for the pulleys pulling the cart. This axle is shown in figure 4.5. The pulleys pulling the cart did not come with bearings, so bearings had to be found for them. Since the axle was 20 mm the bearings were chosen according to this. The bearings chosen were 20x42x12 mm from Biltema. There was also a need to transfer the torque from the gearbox to the axle, while adsorbing slight inaccuracies in alignment. A prop shaft called Rotex stål, model 4012-8459, with inner diameter of 20 mm was used together with a gear ring of model 3002-4401, both from the company Momentum Industrial.

For the pulleys responsible for tensioning the cart belt loop, smaller axles and bearings were chosen. When the motors pull the cart along, all the tension will be on the upper side of the belt loop, therefore the stress on the lower pulleys will be small. For simplicity, the axles and bearings were chosen to be same as the cart wheels. I.E 8 mm axle provided by KTH, and

bearings from Kahalani and SKF.

3.7.5 Controller

To control the system, a control board was needed. An Arduino Uno and ODrive were chosen to be used for the system, see figure 3.37 and 3.38. The Arduino Uno was chosen to deal with the communication, including Ethernet and serial communication. Compared to other control boards, the Arduino Uno is a lightweight real time control system that can also handle several communications and lightweight computational tasks at the same time.

An ODrive was chosen to control the BLDC motors. It was chosen because it is able to control the BLDC motors with a cascading controller, that is already built into it. Other BLDC motor controllers mostly only include the 3-phase converter, shown in figure 3.29. Therefore ODrive has a significant advantage compared to other BLDC control boards.

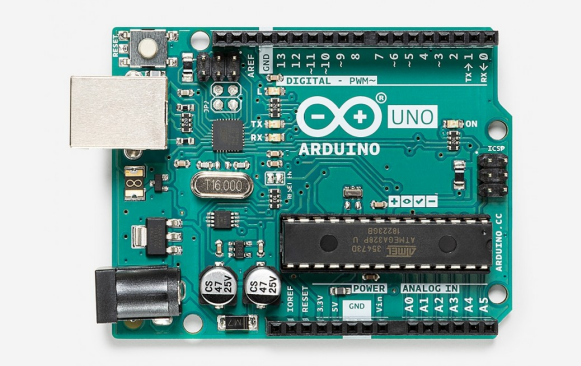

Figure 3.37: Arduino Uno [45]

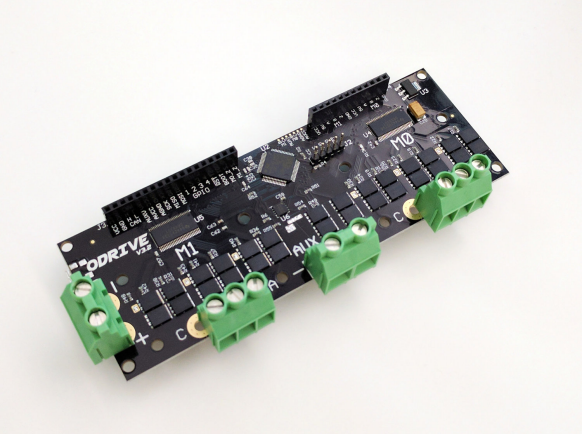

Figure 3.38: ODrive [46]

3.7.6 Control System

In this project, a lot of effort has been put into reducing the latency of the system, especially in the Arduino controllers, for a more realistic response on the platform to avoid motion sickness. To reduce the computational load on, two controllers are implemented. The first one is used to control all the motors from the DCS output, while the second one is attached to the chair and used to feedback the chair's position. For the same reason, the data in DCS is transformed to the cart reference position in the PC by Lua. This reference is then directly sent to the Arduino through Ethernet.

Using data from the PC and the position of the the cart from the IMU sensor, the controller sends the reference position of the motor to the ODrive. The ODrive controls the BLDC motors through a cascaded controller. The system overview is shown in figure 3.39.

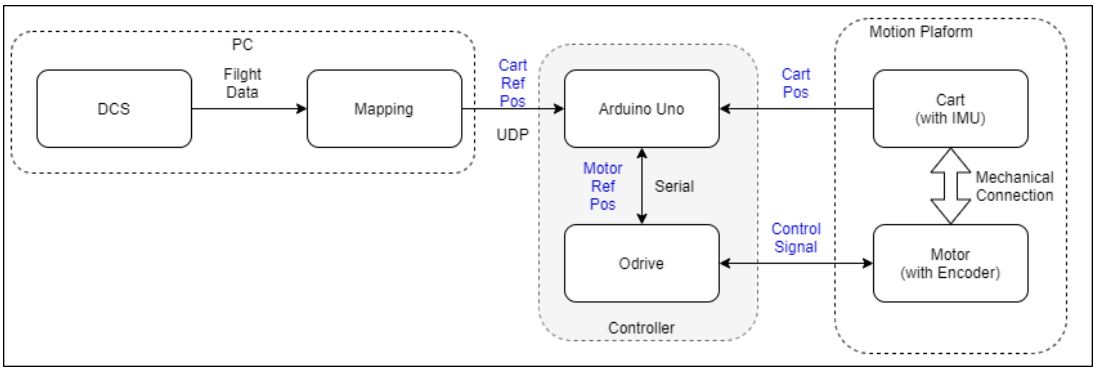

Figure 3.39: Control System Overview

3.8 Budgeting

The supplies for this project were provided as a joint collaboration between Meta Simulations Immersive Synthetics (Meta Aerospace Group) and KTH. The table below presents the items and their respective acquirement costs for the project.

KTH keeps stock of commonly used construction materials, such as square steel profiles and sheet metal as well as smaller electrical components. These are not included in the budget. Further, the list of purchases has been divided in mechanical components and electrical components. The mechanical components represents most of the total cost and this is also excluding mechanical work from staff employed at KTH. The price for the pulleys and belt ordered from NK Technics are estimated to around 10000 SEK. This is because the exact numbers for this order was unknown due to lack of communication between the person who made the order and this project group.

Lastly, all purchases can be seen in table 3.2 and 3.3 below. The total cost combined was roughly 53000 SEK.

Table 3.2: List of purchases for mechanical components.

List of purchases			
Mechanical components	**Quantity**	**Unit price**	**Total cost**
Sportchair	1	1709	1858
Curved rails	2	1934	4768
Bearings 8x22x7 mm	3	194	632
Seat belt	1	439	488
Belt AT10	2	1635	3270
Pulleys AT10	4	709	4836
Belt and pulleys AT20	1	10000	10000
Hinges	2	260	520
Bearings 20x42x12 mm	4	50	200
Velcro straps	1	60	60
Bolts M8x5	1	80	80
Shims	1	33	33
Bearing housings	4	275	275
Gearbox	2	3416	6832
Total cost			**33852 SEK**

Table 3.3: List of purchases for electrical components.

List of purchases			
Electrical components	**Quantity**	**Unit price**	**Total cost**
Ethernet Shield	2	228	456
Grove	2	105	210
Arduino Uno	2	249	498
Odrive	1	1264	1264
Encoder	2	414	828
Brushless DC motor	2	923	1846
Temperature sensor	2	60	120
Fuse 200 A	2	135	270
Fuse 100 A	3	30	90
Fuse 50 A	3	30	90
Fan 48 V	3	124	372
Fan Orion	1	174	174
Banana adapter (red)	2	21	42
Banana adapter (black)	4	21	84
6 AWG cable (14 ft)	1	722	722
8 AWG cable (30 ft)	1	981	981
Battery SMF 12 V 105 Ah	4	1299	5196
Main Switch, 250 A	1	319	319
Round cable shoes	1	70	70
Terminal blocks	1	65	65
Ring cable shoes	1	25	25
Battery connector	4	43	172
Limit switch	4	31	124
Solidstate relay	1	1164	1164
Powerbank	1	149	149
USB hub	1	63	63
USB cable	2	27	54
Sensor cable	2	150	300
USB DC cable	1	29	29
USB serial adapter	1	39	39
Motor driver	1	129	129
Micro switch (roller)	2	19	38
Micro switch (long arm)	2	18	36
Fan 12 V	1	29	29
Red switch	1	89	89
Linear actuator	1	2555	2555
Installation cable	1	199	199
Total cost			**18891 SEK**

Chapter 4

Implementation

This chapter goes through implementation and the construction of the MP.

4.1 Mechanical implementation

In this section an overview of the production, construction and implementation of the mechanical part of the MP is presented.

4.1.1 Curved rails and the main frame

The curved rails constitute the core of the design concept and the construction. Their shape - a half circle with a radius of 600 mm - make up the path at which the user moves in the MP to simulate linear acceleration from the fighter jet in DCS. Figure 4.1 shows the curved rails.

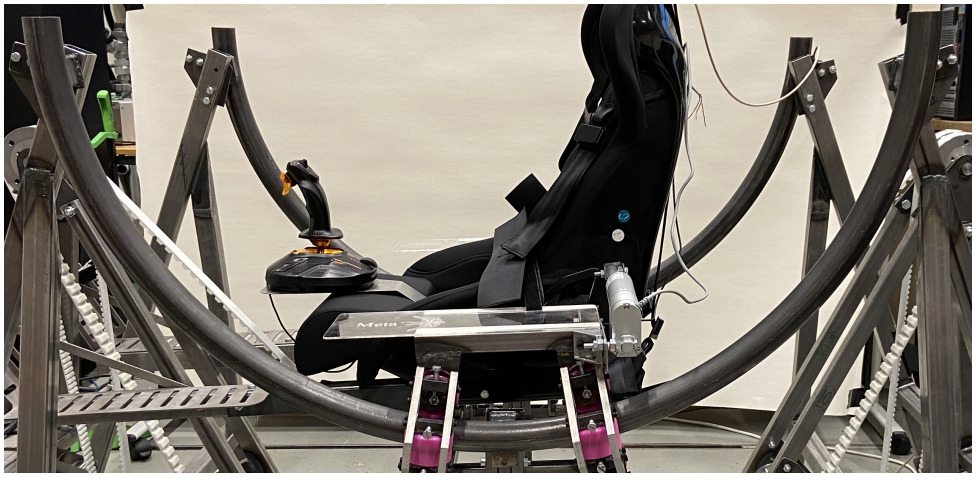

Figure 4.1: The curved rails.

It was crucial that the curved rails would be able to withstand the mass and inertia from the cart with the user in it without deforming or displacing. Another important aspect of the rails was that they should be smooth enough to ensure a smooth ride for the wheels. First, a circular pipe with 60 mm diameter was considered to ensure a great safety factor against displacement and deformation. Unfortunately, the supplier of the bent pipe was not able to achieve good results

when bending such a big pipe, after which the dimension was decreased to 48 mm in diameter, which was the next largest diameter the supplier was able to bend with satisfying results.

The parts included in the main frame are highlighted in figure 4.2. The purpose of the main frame is to support the curved rails and the pulley frame.

Figure 4.2: The parts that make up the main frame are encircled in red.

The parts were cut out to the correct lengths and with the designed angles at the ends. They were welded together to ensure rigid and stiff characteristics of the frame. Ideally, the frame should be infinitely stiff so that the curved rails do not move at all while the cart is in motion.

To mount the curved rails to the frame, several parts had to be manufactured and assembled. First, small parts of a 40x40 mm steel profile were cut out and holes with the same diameter as the curved rails were drilled in the pieces as shown to the left in figure 4.3. These parts were then welded both to a water cut steel plate and to the curved rail. The plates were then fastened with bolts and nuts to another plate that was attached to the frame. This can be seen to the right in figure 4.3. In this way, the curved rails are detachable from the frame by unscrewing the bolts and nuts holding the plates together. This fact also means that the front and rear frame are detachable from each other because the curved rails are the only parts holding them together.

Figure 4.3: The mounts where the curved rails are attached to the frame.

4.1.2 Pulley frame and belt tensioner

The parts included in the pulley frame are highlighted in figure 4.4. The pulley frame is a sub frame to the main frame and its main purpose is to hold and support the belt pulleys.

Figure 4.4: The parts that made up the pulley frame are encircled in red.

At the top of the pulley frame there are two pulleys connected on the same axle. In figure 4.5, the left pulley is driven by one of the motors via a belt. This pulley is then firmly connected to the other pulley, to the right in the figure, that in turn pulls the cart. The pulleys were machined in the lathe to accept the bearings. They where also drilled and threaded in a mill, and screws were used to bolt them together, in order for them to transfer torque between each other.

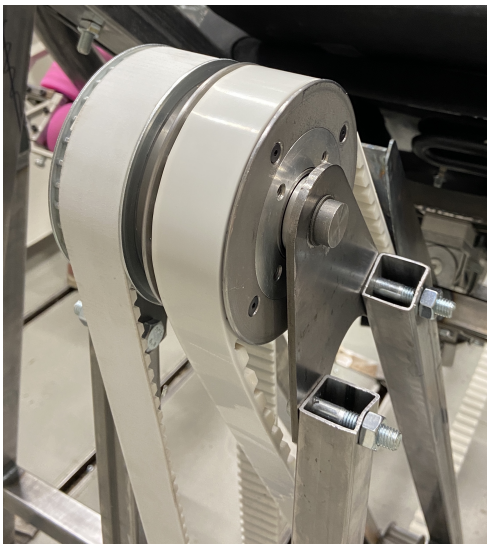

Figure 4.5: The two pulleys that are connected on the same axle.

4.1.3 Cart

Figure 4.6 shows the implementation of the cart. The cart is the unit which travels along the rails and holds the chair which the user sits in. The pulling belt is attached to the underside of the cart along the curved belt guide. The curved belt guide is welded together with the cart.

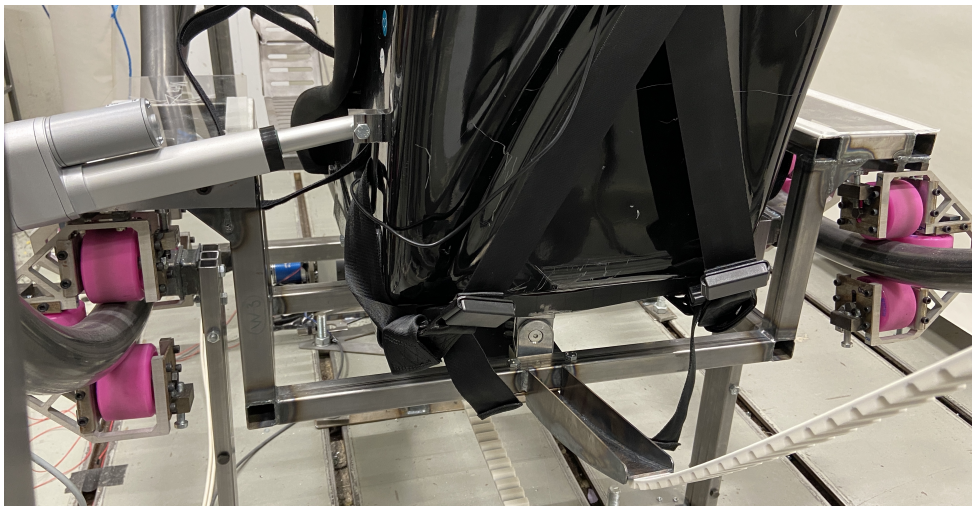

Figure 4.6: The cart mounted in the MP.

The cart was made by cutting out pieces of a steel square profile in the correct lengths, that were then welded together to ensure a rigid and durable construction.

The cart holds the wheel holder units, the belt mounting assembly including the belt guide, the chair and the roll mechanism. All of these will be described in a more detail below. Also, there are plexiglass plates above the wheel holder units to prevent the user from getting their fingers pinched between the wheels and the rail. Figure 4.7 shows these plates, that were manufactured through a laser cutter machine.

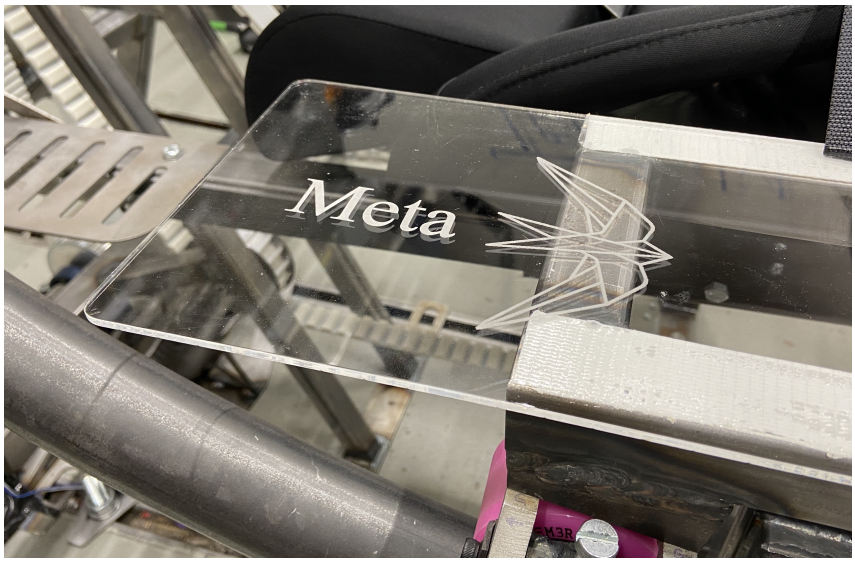

Figure 4.7: The plexiglass plates.

4.1.4 Wheel holder units

There are four wheel holder units in the design, two on each side of the cart. Figure 4.8 shows one of these units mounted on the rail in the MP.

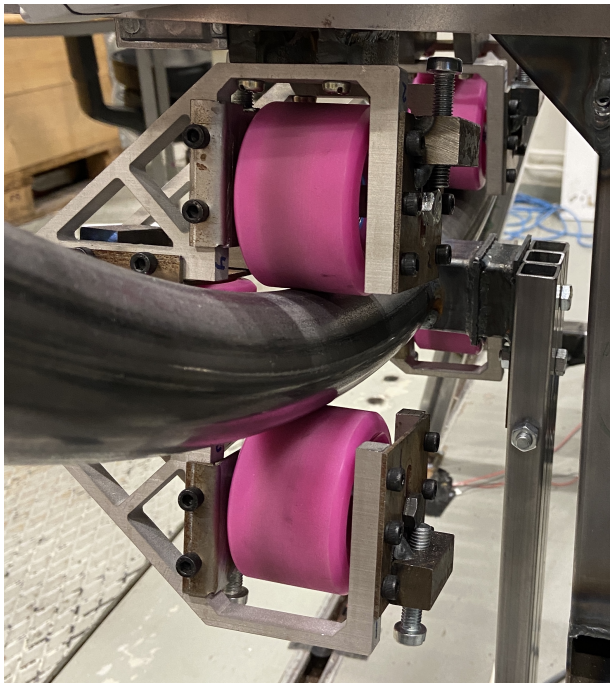

Figure 4.8: A wheel holder unit mounted on the cart on the rail.

The wheel holder units were constructed out of water cut aluminium profiles that are assembled together with 2 mm thick steel plates that are screwed to the aluminium profiles. The aluminium profiles were chosen because of their lightweight characteristics, and the water cutting manufacturing method was chosen for its large flexibility in designing the profile. The steel plates serve as axle supports as well as the elements holding the aluminium profiles together.

They were water cut and bent into shape. Adjustment screw holes were made from solid steel square profile, with an M8 hole drilled and threaded to hold the adjustment bolt. They were welded to the steel axle holders. Some adjustment was needed to the holes in the axle supports, as the bending process is not exact. For the wheels to stay in the middle of the holder, spacers were needed. They were cut from aluminum tubing. Due to the unique shape of each wheel holder due to variances in manufacturing, the spacers were custom made to fit their wheel.

Because there were no exact dimensioning work done when designing the wheel holder units, the manufacturing process started with just building one complete unit that went through some simple stress tests. These tests were passed, and the three other units could then be built in the same way and with the same dimensions. Figure 4.9 shows the simple stress tests performed on the first wheel holder unit. One test was a person hanging on the wheel holder unit that were hooked on to a table. The other test was a person putting all his weight on a metal bar resting on top of the wheel holder unit.

Figure 4.9: The stress tests performed on the first wheel holder unit.

4.1.5 Belt guide and belt mounting assembly

The belt guide, that is a part of the belt mounting assembly, is simply a bent piece of sheet metal. The sheet metal strip was cut out using an industrial scale metal sheet cutter and then a manual sheet metal slip rolling machine was used to curve the metal strip into the desired radius. The purpose is to give the belt a shape of a circle sector below the chair, and to keep the belt from intersecting the cart or chair at large angles. In figure 4.10 the circle sector that the belt guide follows is shown.

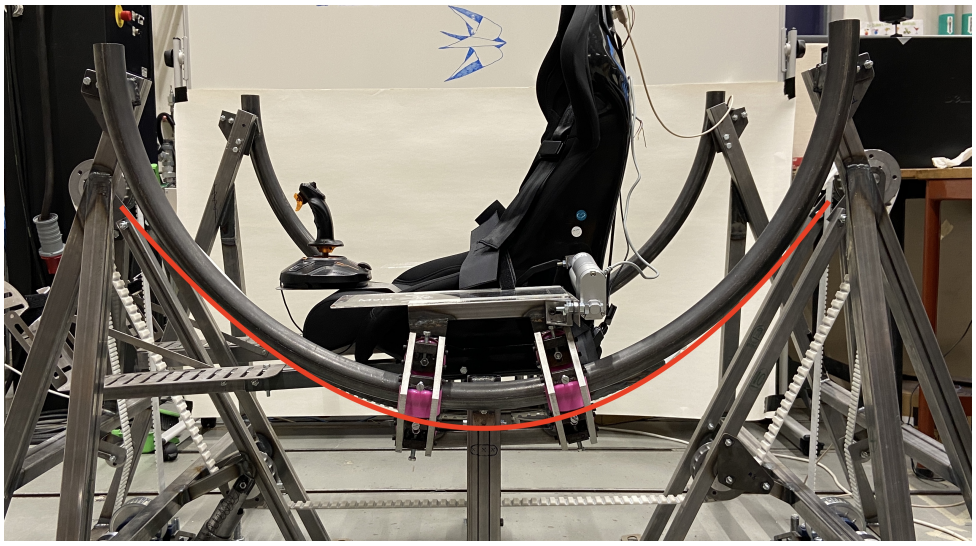

Figure 4.10: The circle sector that the belt guide resembles.

In figure 4.11 the belt mounting assembly is visible at the center of the belt guide. One problem with implementing the belt mounting assembly was the drilling of the holes in the belt. Since the belt is made out of a quite elastic material, the holes contracted when the drill was removed from the newly drilled hole. Because of this, the drill size had to be increased by approximately 25 % in order to get an acceptable hole size. Moreover, the belt was reinforced with steel wires that also made the drilling process harder since the wires did not break, but instead twirled around the drill. All of this resulted in difficulties, assembling the belt mount and getting the bolts through the holes in the belt. Although, it was possible and worked as expected in the end.

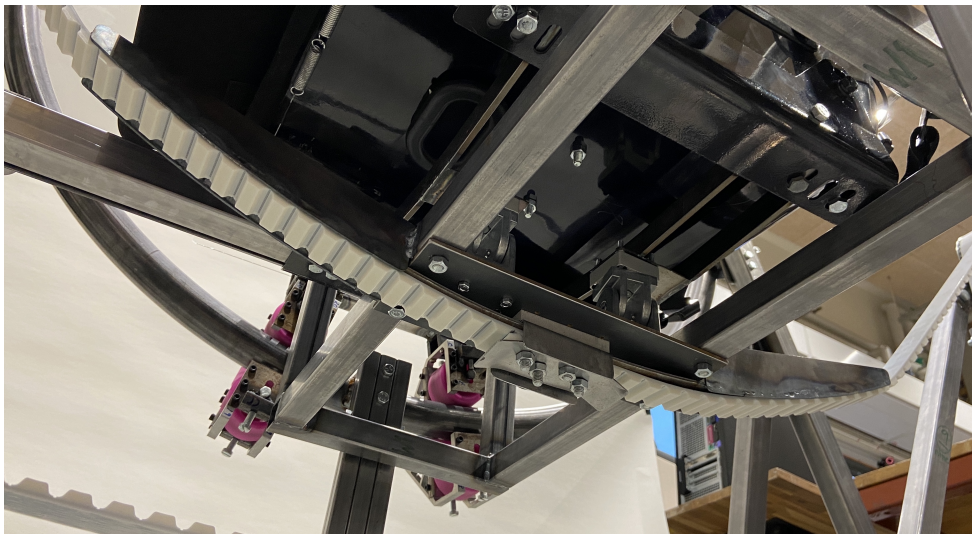

Figure 4.11: The belt guide and the belt mounting assembly.

4.1.6 Chair mount and roll mechanism

The chair is mounted on two concentric axles which enables the chair to do a small roll motion, as can be seen in figure 4.12. The roll axles chosen are simple, they do not even have any

bearings. Each axle consists of two screws that are tightened into the threads of the inner part of the joint. The screw heads then work as axles on which the outer part of the joint rotates on.

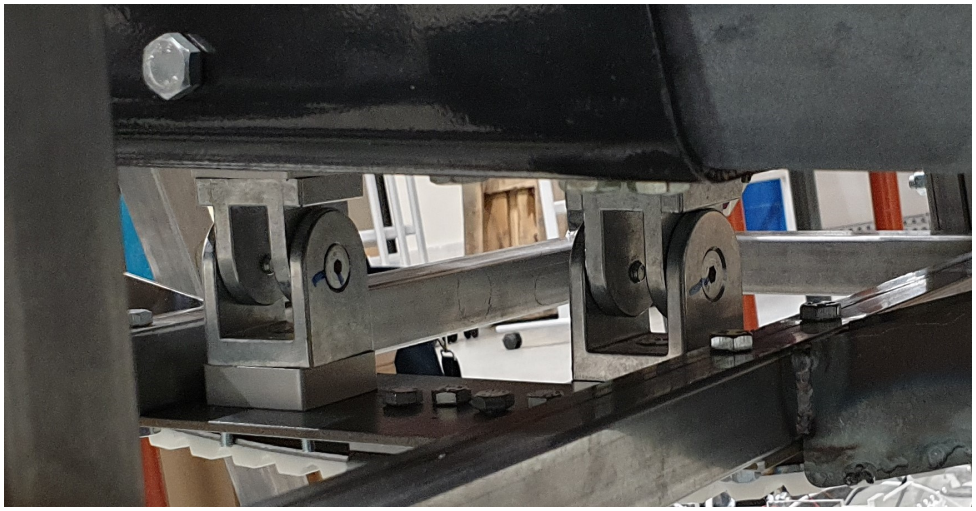

Figure 4.12: The roll axles below the chair.

There are four steel profiles that connect the roll axles with the mounting rails on the chair, as shown in figure 4.13. These profiles were manufactured using a water jet machine that cut out the profiles from a thick steel plate. There were also smaller steel plates that were cut out with a water jet machine that were used to connect the support beams to each other. These smaller steel plates were welded to the support beams and then mounted with screws to the chair mounts. The bolts that were used to fasten the steel plates can also be seen in figure 4.13.

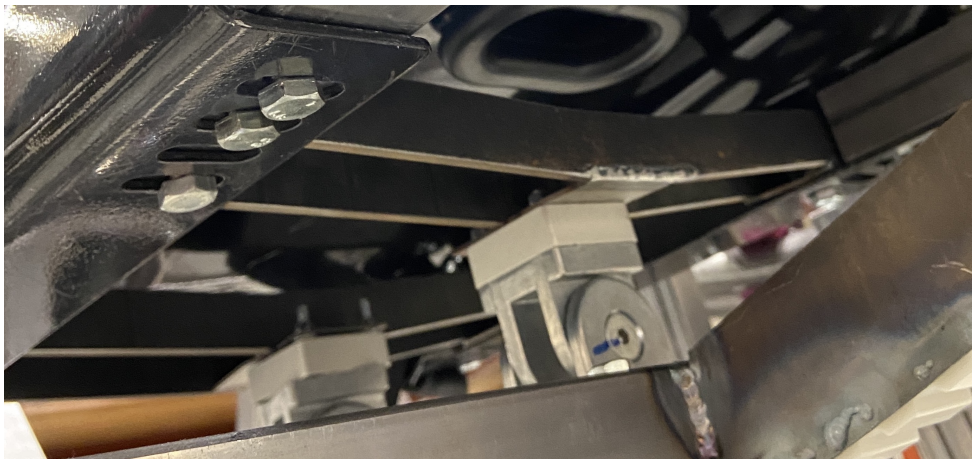

Figure 4.13: The support beams that connect the chair to the roll axles.

On one side of the cart there is a linear actuator that pushes and pulls the chair from side to side, around the aforementioned roll axles. The actuator is mounted on a bolt working as an axle on the cart. Also, the end of the piston is mounted with an axle to the chair to enable the actuator to move and adjust to the position while working. Figure 4.14 shows a close-up of the roll actuator, near its two end positions.

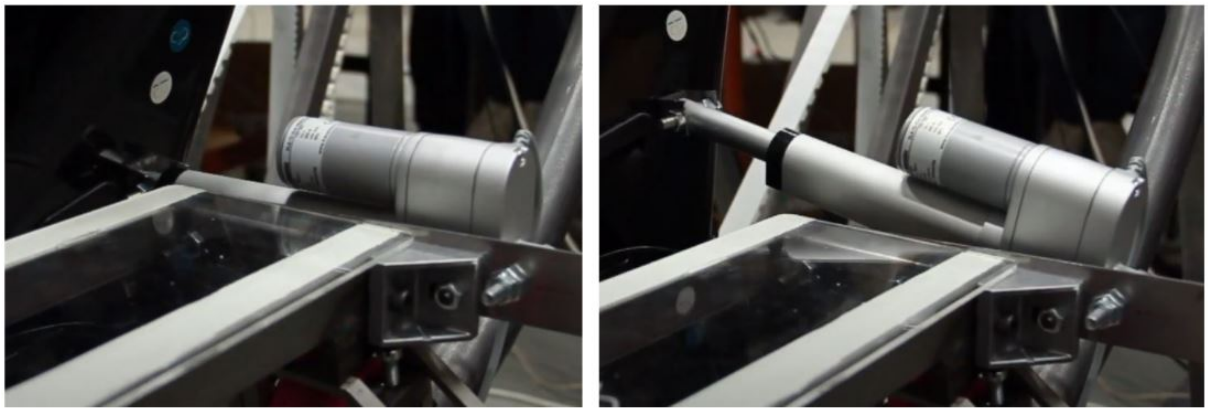

Figure 4.14: Close-up of the roll actuator, near its two end positions.

One problem that was discovered during the implementation of the roll actuator was that the mounts were not as rigid as desired. The mount in the chair flexed due to the chair casing flexing. Also, the mount on the cart flexed even more due to the sheet metal piece that was holding the axle was bending. Because of this, an extra 90 degree angled support piece was attached between the sheet metal part and the cart to prevent some of the bending in the sheet metal.

4.1.7 Motor and gearbox assemblies

In essence, all of the parts in the power train support are manufactured using a water jet machine on steel plates with various thickness. The parts are then welded together and mounted to the mounting rails in the floor with M20 bolts. The adapter axle between the motor axle and the gearbox input shaft was made using a lathe. Also, the axle that holds the pulley in the two bearing housings was made with a lathe.

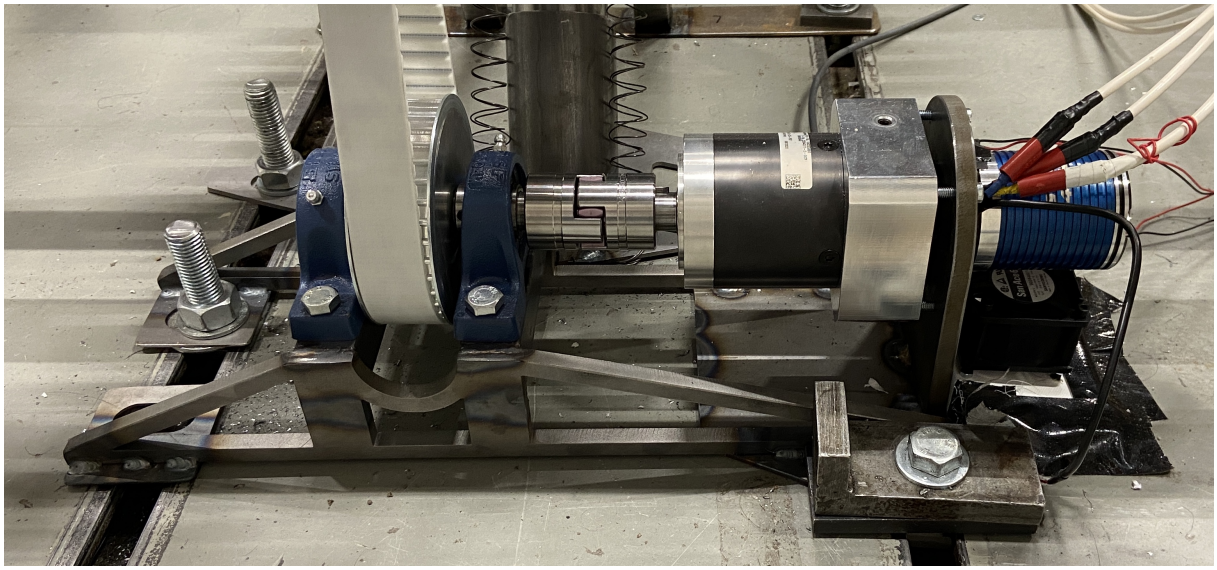

Figure 4.15: The final motor-gearbox-pulley assembly.

The power train support had a design flaw that prevented the gearbox from being fitted on the

motor axle. The two upright supports were placed too close. Since they are so thick, and the axle is securely mounted using the bearings, the front upright gearbox mount was cut off using an angle grinder. The power train now fit, and when tested produce little to no flex. Figure 4.15 displays the final built motor-gearbox-pulley assembly.

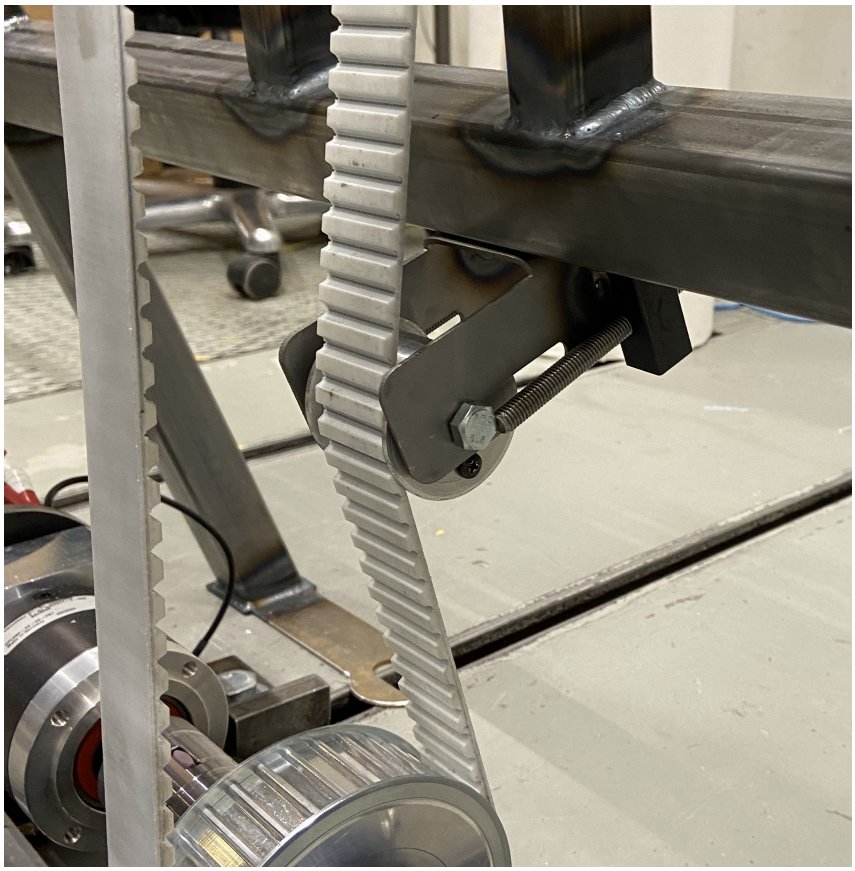

Figure 4.16: One of two tension wheels on the frame.

No standard part that could be ordered quickly fitted the role of power train tension wheel. Therefore they were designed to be custom made by the group members. Both tension wheels were made using a lathe. Due to a shortage of material, one tension wheel was made from aluminium, and the other made from steel. The same type of bearing used for the wheels were pressed into the tension wheels using a hydraulic press. The support holding the tension wheel was water cut steel, and bent to the proper shape. Adjustment screw holes where welded and an M8 bolt was used as an axle. The completed tension wheel holder can be seen in figure 4.16.

4.1.8 Chair accessories

On the chair, there are some accessories fitted to enhance the feeling of flying a fighter jet. Two footrests, a four-point belt and a joystick mount are attached to the chair. The four-point belt was chosen for its capability of holding the user firmly in place during all possible movements of the chair. Figure 4.17 gives an overview of the chair with its accessories.

Figure 4.17: The chair with the accessories.

The foot rests seen in figure 4.17 were manufactured in different steps. First, the load carrying foot beams were made by cutting pieces of a 40 x 40 mm steel profile. These were meant to be robust and be able to hold the foot rest, and support both feet while a person is sitting in the chair. The foot rest was cut out of 3 mm sheet metal, using a water cutter. These were then bent manually into the right shape, in a bending tool. With this design, there was some flex in the footrests when the user has his or her feet on them. Ideally, they should have been stiffer.

Figure 4.18: The joystick mount.

Figure 4.18 shows the joystick mount that is attached under the chair's seat. The joystick mount is one part made out of 2 mm sheet metal. This has also been water cut and then bent into the right shape, manually, using a bending tool. Under the pad the user sits on, the joystick mount is attached with two M8 bolt. Then the joystick is mounted using M6 screws.

4.2 Electronic Implementation

In this section, the implementation of the electronic design and the chosen components in 3.7.1 and 3.7.2 is described.

4.2.1 Electronics design implementation

The electronic design was divided into three parts: the electronic box, the frame and the cart. These three parts, their components and how they are connected is shown in figure 4.19.

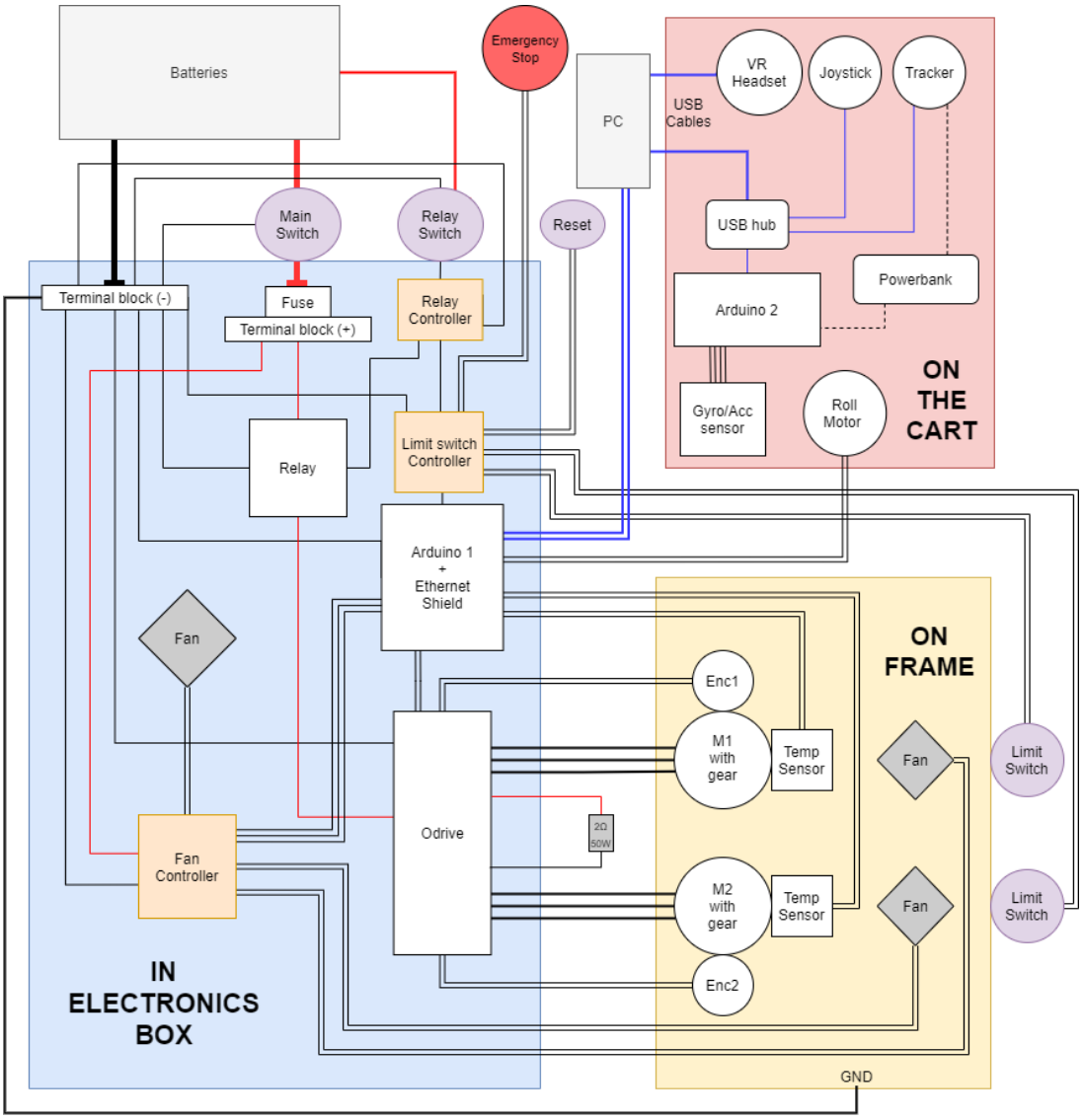

Figure 4.19: Overview of the electronics and the connections.

The electronics on the cart (highlighted with the red box in figure 4.19) is placed on a plate mounted on the backside of the seat and the main function is to feedback the cart's position. The electronics on the cart mounted on the chair is shown in figure 4.20. As aforementioned, the cart's position is measured using an accelerometor and gyroscope sensor connected to the Arduino. The Arduino then sends this value to the computer through the USB hub. The USB hub also works as a power supply to the Arduino and the tracker. The power bank placed on the plate can be used as a power supply as well. The roll motor is a linear actuator that is placed besides the seat, however it is controlled by the Arduino in the electronic box and not by the Arduino on the cart.

Figure 4.20: The electronic plate mounted on the chair with all the components.

The electronics on the frame (highlighted with the yellow box in figure 4.19) are placed on the floor, on either side of the cart besides the gearbox for the driving belt.

The electronic box (highlighted with the blue box in figure 4.19) is placed on the floor between the motion platform, the batteries and the computer and is the core part of the electronic design. The main power from the batteries goes through the electronic box that then supplies the motor with power. Figure 4.21 shows the end product of the electronic box with the components inside.

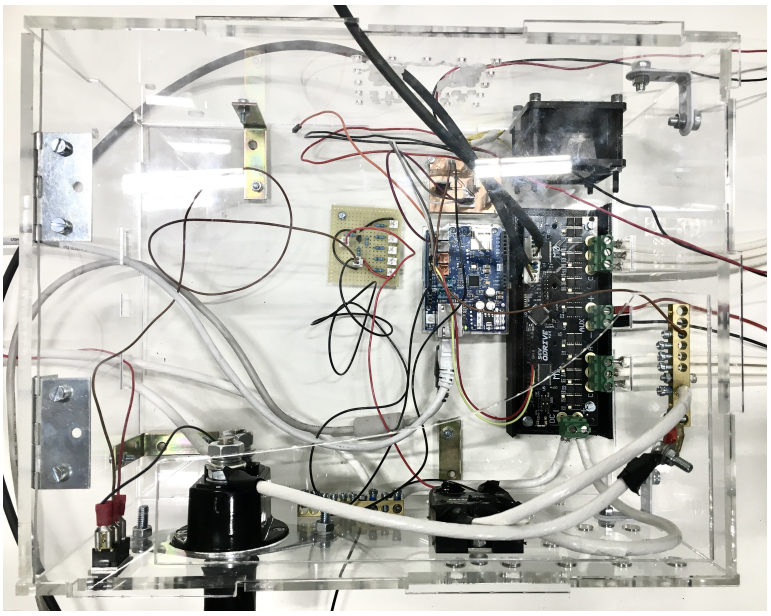

Figure 4.21: The electronic box with all the components inside.

The original idea of the electrical design is shown in this figure 4.19, however a few things were changed from that idea to the implementation and the end product. The differences were that the roll motor, the temperature sensors and the limit switches controller along with the limit switches, emergency stop button and the reset button were not implemented, the reason being mainly lack of time. The relay switch has the same function as the emergency stop button and it was therefore not considered unsafe to remove it. This is further discussed in chapter 7.1.2.

4.2.2 MCU and logic PCB for switches

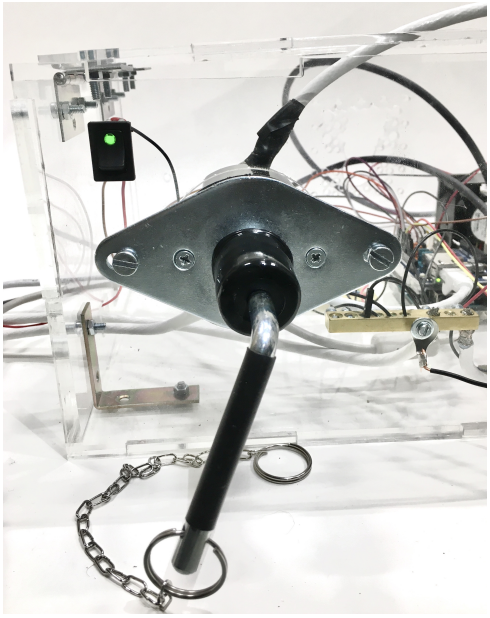

Figure 4.22: The main switch (right) and the relay switch (left).

The smaller switch with the green LED in figure 4.22 is the relay switch. The main switch to the right is turned off when the handle is pointing down and turned on when it is turned 90 degrees up. There is no current when the main switch is off, so when the main switch is turned off everything will be turned off as well.

Figure 4.23 shows the Arduino, fan controller and relay controller in the electronic box. The fan controller is a PCB that controls the three fans with the logic shown in the circuit diagram in appendix B.2. The relay controller controls turns the relay on when the relay switch is turned on, and turns the relay off when the relay switch is turned off. The logic is shown in the circuit diagram in appendix B.1.

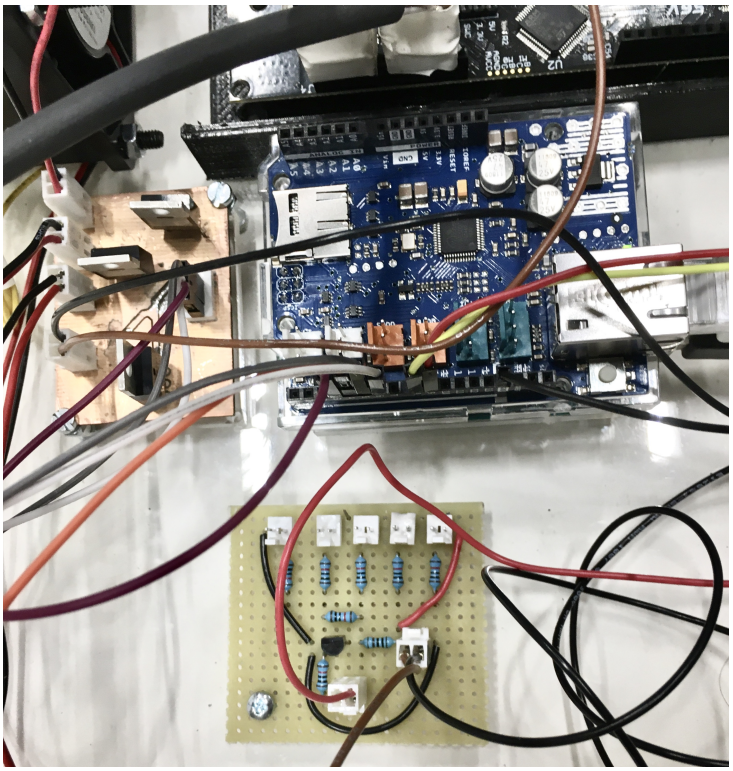

Figure 4.23: Arduino (upper right), fan controller (upper left) and relay controller (below).

4.2.3 Cables

Due to the high current the motors can draw during high loads (80A max), the cables for the motors and from the batteries needed to be large enough to be able to deliver the current needed without the risk of damaging. The cables chosen from the batteries were 6 American wire gauge (AWG) and for the motors 8 AWG. Because the BLDC motors, as well as all other electronics used produce noise, shielded sensor-cables were used for the encoders so they would perform as reliably as possible.

4.2.4 Sensors and fans

The fans for the motors were placed under the motors and the temperature sensor above the motor as seen in figure 4.24. The temperature sensor was placed on the opposite side of the fan so that the fan would not interfere with the measured temperature by cooling the sensor. Although

the temperature sensors were placed and connected to the motor, they were not implemented and the fans were therefore on full power the whole time the MP was turned on.

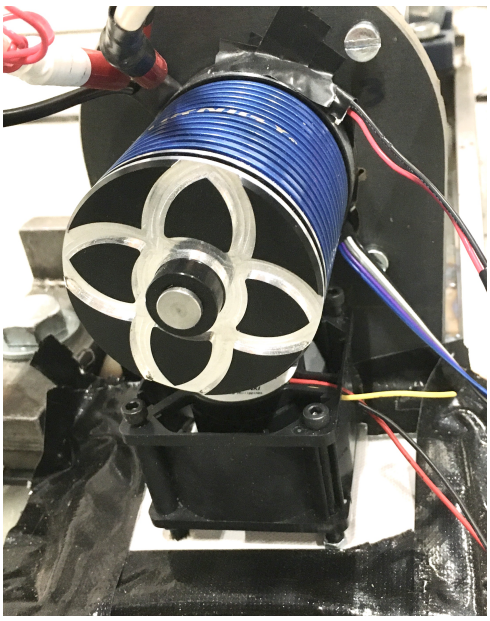

Figure 4.24: Motor with temperature sensor and fan.

4.3 Control implementation

4.3.1 Control Loop

The control loop of the system includes four main parts. DCS generates the flight data and sends it to a python server. The python server does the mapping by adding gains to both the pitch and acceleration from the game and then adding them together. The signal passes a saturation to make sure the cart does not exceed the motion limit, for safety reasons. A low pass filter is also required to avoid extreme vibration which might damage the system. After the lowpass filter, the signal is applied to a controller which turns the cart position reference into a motor position reference. The python server sends the signal to the Arduino via UDP. The Arduino calculates a differential position for the two motor. The differential is to ensure the belt stays tight during actuation. After that, the Arduino sends the reference position of both the motors to the ODrive and finally the ODrive controls both of the motors by an cascading feedback control. The control loop is shown in figure 4.25.

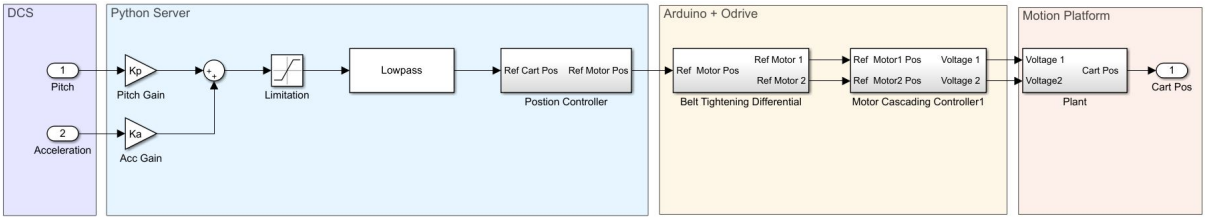

Figure 4.25: The Control Loop

4.3.2 Position Controller

For the position controller on the python server, feedforward or feedback control are two ways to implement it. The feedforward control is simple and stable but requires an accurate model. The feedback control does not require as good of a physical model as the feedforward control but it relies on the accuracy of the sensor. During the implementation, the IMU sensor proved to not be very reliable, and therefore the feedforward control that was derived in section 3.6.3 was used instead as the position controller.

4.4 Software

The software consisted of implementing the control system into a code structure that made it possible to move the platform. The software also included code for different sensors and exports from DCS, which is described below. The final codes can be found in this project's Github repository [47].

4.4.1 Structure and latency

The heart of the software system is the acceleration values that are being received to the motion platform via DCS. This is done via interfacing with the DCS application programming interface (API) in a Lua script placed in a folder within the DCS system in order to extract the desired values for the system. From the API of DCS, it is possible to get acceleration values for the plane that the player is currently using, similarly to what an acceleorometer in a real plane would produce. For each frame of the game, an acceleration value is exported from DCS via the exports produced from the API. So if an assumption is made that it is constantly possible to run DCS at 60 frames per second, the base latency for the exports is 16.6 ms.

4.4.2 Communication

An ethernet cable connected the PC with Arduino 1, in the electronic box. The PC sends the data from DCS through UDP. Arduino 1 receives this information and forwards it through UART communication to the motor driver which then actuates the motors. The fans are controlled by PWM signals, though this was not integrated in the final product. Arduino 2 is located on the moving platform and consists of a accelerometor and gyroscope sensor. This sensor sends data through I2C to Arduino 2, which then sends this to the PC using an USB cable. The value received is compared to the real actuation with the input from DCS.

Chapter 5

Verification and Validation

To verify and validate the requirements from chapter 1.6, different tests were executed and explained in this chapter.

5.1 Verification

This section focuses on the verification, by confirming through review and testing that each component meets their specifications and fulfills their functions.

5.1.1 Actuation verification

Motor and ODrive

To verify that the motor, encoders and ODrive worked as expected together with an Arduino, a smaller test setup was made. The test setup included a holder for the motor, a temporary encoder mount, a bench power supply to power the Odrive and motors and the odrivetool that was used form a PC. Even though only one motor was used for this test, it allowed for confirmation on how to interact with the ODrive through the Arduino. The errors received during the tests also proved useful, as it gave an understanding of how noisy BLDC motors can be, and thus the need for shielded encoder-cables was discovered.

After the verification of the BLDC motor and the ODrive, it was integrated with the hardware construction and tested again using the same procedure to verify the system.

Linear actuator and motor controller

To verify the functionality of the actuator, the actuator and the controller was connect together with an Arduino. A test code was used to run the actuator and showed that it worked as intended. However, there was not enough time to integrate the linear actuator, the motor controller and the corresponding software with the hardware and therefore no further tests were made to verify it's functionality.

5.1.2 Electronics verification

Fan function

To confirm that the circuit for the fan controller worked as intended, the circuit was connected to an Arduino, a bench power supply and one fan. By sending a PWM signal from the Arduino to the corresponding fan output pins, the output effect of the fan could be controlled. Hence, all inputs and outputs of the circuit proved to be working correctly. It also verified the fans working properly. This was however not implemented with the temperature sensor and did therefore not need further testing.

Relay function

The relay controller was verified similar to the fan controller. It was connected to an Arduino, a flip switch, a bench power supply and an oscilloscope on the output. The flip switch was used to simulate an emergency stop button. When the circuit was powered on, if the flip switch was turned on, the output signal shown on the oscilloscope was low and thus the relay was turned off. The same applied to the Arduino, if a high signal was sent from the Arduino, the output signal was low and the relay was off. When all input ports received a low signal, that is the flip switch and the Arduino being low, the output signal was high and the relay was turned on. This concluded that the circuit worked as intended.

After the circuit was proved to be functional, the relay needed to be verified. To confirm that the relay worked together with the circuit, it was connected to the circuit as well as ground. When the relay was supposed to be turned on, a multimeter was used to the verify the continuity of the relays output. When the relay was supposed to be turned off, the same test was done with the multimeter and as supposed to. Both tests verified the functionality of the relay.

The relay switch went through the same verification testing. The relay switch has the opposite function as the flip switch. When the relay switch is turned on, the relay is turned on and when the relay switch is turned off, the relay is turned off as well. The same procedure was continuously tested during the integration phase to verify the relay working properly as it is one of the most important components.

Temperature sensor

Despite the temperature sensor not being implemented in the final product, a smaller test was made to verify it's function. By reading the temperature sensors data-sheet [48], the connection between the sensor and an Arduino was made as proposed. By reading the voltage output value from sensor, mapping it to the corresponding temperature value found in the data-sheet table [48] and printing it to Arduinos serial monitor, it was evident that the sensor worked accurately for it's purpose.

Acceleration and gyroscope sensor

From the data-sheet of the sensor [42], the wire-diagram between the sensor and an Arduino can be found. By using a test code made specifically for use of the sensor with the Arduino, the

output from the sensor is mapped to G-forces. As 1 G equals 9.82 m/s^2 at earths surface, it was easy to see that the sensor worked as intended. Tilting the sensor 90 degrees showed that the axis of the sensor, that was parallel to the earth was 0 G, while the axis pointing towards earth was 1 G.

Ethernet connection

To verify that the Ethernet connection worked between the PC and an Arduino, an Ethernet shield was connected to the Arduino and then connected with an Ethernet cable to the Ethernet port. Then a UDP server was setup in python, sending UDP packages to the IP-address assigned to the Arduino. By printing the received packages in Arduinos serial monitor, it was possible to see and compare the received packages with the ones that were sent.

5.1.3 Control verification

Belt separation

The belt starts to separate from the belt guide at roughly 25° and at 35° the separation is obvious. This means the model and the feedfowrad controller derived in section 3.4.2 and 3.6.3 is the most valid until 25°, and then the accuracy decays as θ of the cart increases.

Belt tension

The belt tension is somewhat maintained with the help of the belt tensioner in figure 3.14. The belt tightening is further improved with the help of the belt tightening differential mentioned in section 4.3.1. But even with these two tensioning features the belt still loses tension as θ of the cart increases. This means the actuation performance is worse when θ increases, since the pulling motor first has to overcome the slack part of the belt before the actual actuation can happen. This problem could probably be solved with a more optimized belt tightening differential, this is further elaborated in section **??**.

Model simulation

The feedforward control that was derived in section 3.6.3 was verified by inputting the game reference to the model derived in section 3.4.2. And then comparing the model response to the reference, see figure 5.1. It should be noted that the model in section 3.4.2 is not very accurate above 25° as mentioned previously. The model also did not include any filters or limiters except for the voltage saturation. The real performance of the feedforward control can be seen in figure 6.1 in the result chapter. The same game reference is used in both cases for easier comparison.

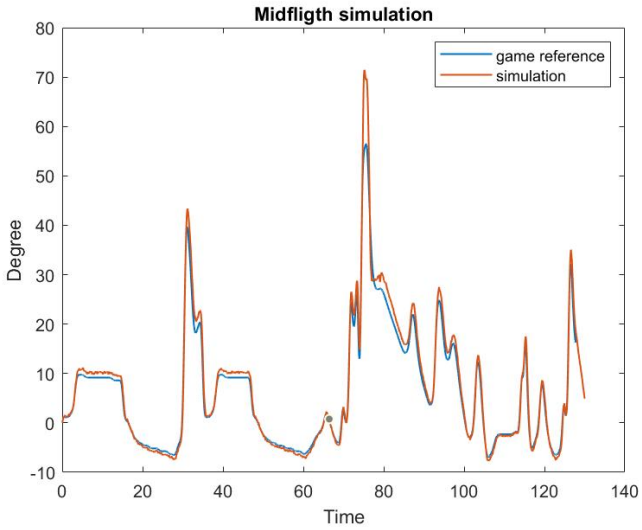

Figure 5.1: Simulation of the feedforward control in mid flight, using the model that was derived in section 3.4.2.

5.2 Validation

Test cases were performed corresponding to the requirements, both stakeholder and technical ones. More information about how the tests performed and the results of requirements fulfilled can be seen in C.1 and C.2 in appendix C. As can be derived, the MP was proven to fulfill most requirements, though there is room for improvements.

Chapter 6

Results

The test results and factual findings are presented in this chapter.

6.1 Mechanical design

Overall, the mechanical design and build was robust. The main frame together with the curved rails were stiff and stable. The curved rails was also smooth and provided a smooth path for the cart to travel on. When using the MP, there were no feelings of the frame being too weak or feelings of the frame moving or deforming. This was true for the pulley frame as well. The structure was stiff enough to support the pulleys and the forces they had to transfer through the frame. Moreover, the cart did also show satisfying characteristics when in use. It was also stiff and did not deform noticeable. It was well dimensioned to support the weight of the chair and user.

However, there were some minor deformation and unwanted movements in the chair during use, coming from the chair mount and the roll axles. Also, the flexibility in the chair itself contributed to these problems. The roll axles had too much play in them, and the supporting beams connecting the roll axles to the chair were too weak. Another factor that impacted the unwanted movements of the chair was the roll actuator. The roll actuator was the only element holding the chair upright in regards to the roll angle, which in itself was not a problem since the actuator was strong enough to hold the chair in place, even with no voltage supplied to it. The problem was the mounts of the actuator. Both the mount on the chair and on the cart holding the actuator flexed, making the chair move from side to side when used by a person sitting in the chair. It was also noticeable that the heavier the person in the chair, the more unwanted movements were present. Another part related to the chair was the footrests that flexed too much when loaded.

The wheel holder design worked satisfactorily. in the end the adjustment features of all the wheels were invaluable for the design. One advantage of this feature was that the wheels could be perfectly adjusted to the actual size of the curved rails. The wheel adjustments could also rise and lower the cart, which could help to increase the clearance to other parts that otherwise could collide with the wheel holder units. This was also true for adjusting the cart sideways. For example, if the driving belt was not perfectly centered in the belt guide mounted under the chair, some adjustments to the side wheels could help center the belt. The wheel holder units felt very stiff, but maybe they could have been made with bigger dimensions for a greater safety factor against failure.

All the tension wheel designs for the belt drives also worked satisfactorily. There were two types of tension wheels in the design, a spring loaded one mounted to the floor and two wheels that were adjustable with screws mounted on the main frame. They did what they were expected to do. The spring loaded tension wheel needed quite stiff springs to work properly though. This was because the belt itself was stiff and therefore needed bigger force than expected to be tensioned.

The drive train construction also worked out fine. All mounts were robust and stable, and the adapters and axles too. There were no noticeable play in any sections of the drive train.

The design proposed in this report has one big disadvantage though: the weight. As it is constructed mainly from steel, the weight is high. Some sections of the frame are welded together and the bent pipes can not be disassembled into smaller parts which makes the construction bulky to store or to transport. Generally, the frame is probably over-dimensioned for the loads it is built for.

Another general disadvantage of the mechanical design is the need to mount it to the floor. The frame could maybe stand on its own weight, but the drive train as it was designed has to be mounted to the floor to function correctly.

6.2 Actuation

There were two actuation systems in this project; the roll actuation and the pitch actuation on the MP. The roll actuation was never implemented in software and control due to lack of time and can therefore not be completely evaluated here. It was however implemented physically, in terms of being mounted on the cart and chair. Hence, making it possible to try the actuator itself by supplying it with power from a battery. The actuation was adequate, being able to push and pull the chair to its left and right end positions with a person seated in the chair.

The only problem detected by doing this was the speed of the actuation, which was rather slow. It was calculated that 7 deg/s for roll would be enough, however linear actuators cannot output high torque and actuate fast at the same time. Evidently, a stronger actuator was more important than speed, as it was considered more crucial that it was able to withstand the torque from the weight of both the chair and the user sitting on the chair. This slowed down the desired 7 deg/s to roughly 3.68 deg/s.

The other actuation, the pitch actuation along the curved rails, worked as intended. The motors in combination with the gearboxes was well suited for the task of pulling the cart along the rails. The actuation was smooth and yet distinct. As expected, the belt drive was quite non-elastic and was well-suited for the application.

However, one problem that sometimes were present with the belt drive was that one of the sides lost tension and contact with the upper pulley on the pulley frame. It was crucial that the motors worked together in a synchronised way. For instance, if the cart is being pulled forward by the motor at the front, the motor at the back has to keep the belt tense at the back of the chair. Otherwise the belt becomes loose at the pulley at the top of the pulley frame behind the chair, resulting in the belt skipping cogs on the pulley and making the cart and chair rumble in an undesirable way. Later, when everything was better tuned in the software, this issue was solved.

6.3 Control

The control part of the project mainly focused on the pitch motion of the platform. Based on the simulation model in Simulink, the controller was developed considering the overall behavior of the MP.

The control implementation prioritized the reduction of latency. This was achieved through both system design and selection of communications protocol. The platform was fully capable to respond to the real-time data from DCS with relatively low latency, which significantly reduced the motion sickness for a more realistic experience.

The performance of the control can be seen in seen in figure 6.1 and 6.2 below, where the reference angle from the game is compared with the actual position of the user. Figure 6.1 shows scenario when the plane is already up in the sky, while figure 6.2 illustrates when the plane is taking off from the runway. It should be noted that the sensor signal has been smoothed out in Matlab for easier reading. The result is better is better during mid flight as compared to take off. This is because the low pass filter has a bigger effect on the motor position reference during take off. The low pass filter is also the reason why the MP ignores the large peaks in figure 6.1.

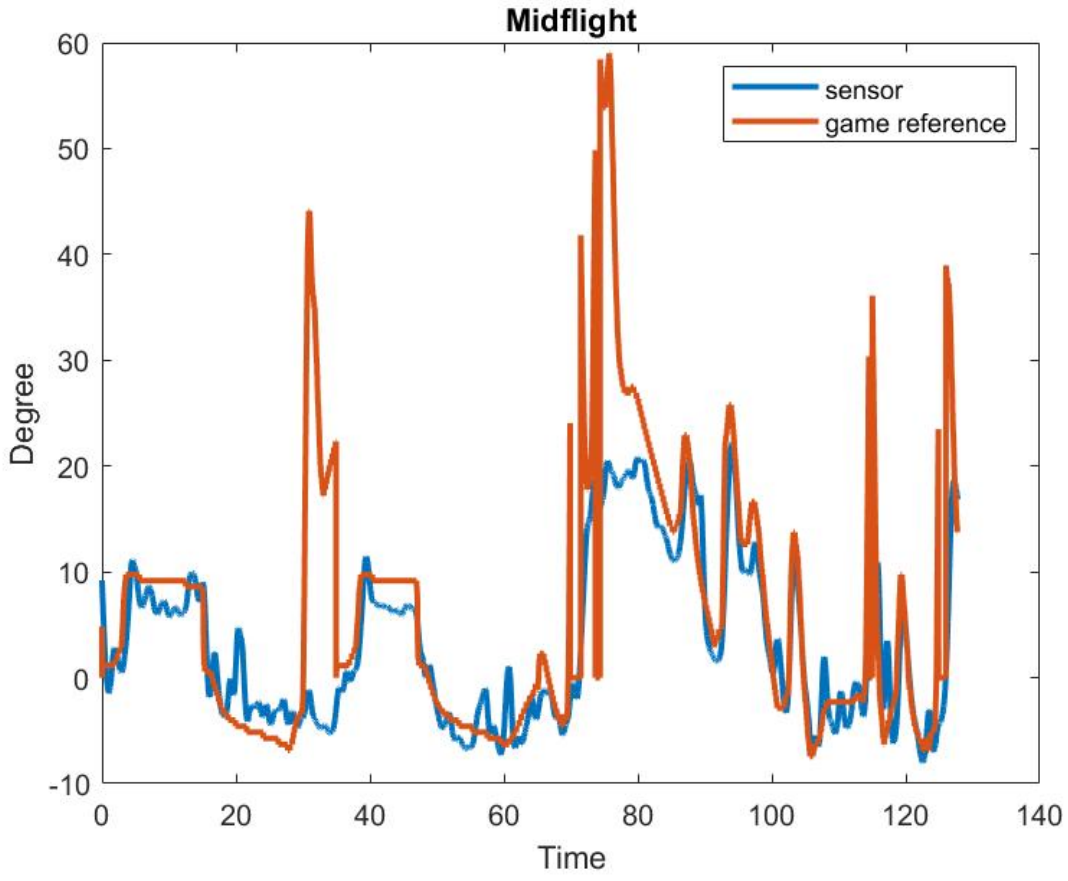

Figure 6.1: The MP tracking the reference generated after the mapping from the game, during midflight. The sensor data has been smoothed out in Matlab using the smoothdata command, for easier reading. The large peaks form the game reference are ignored due to the low pass filter.

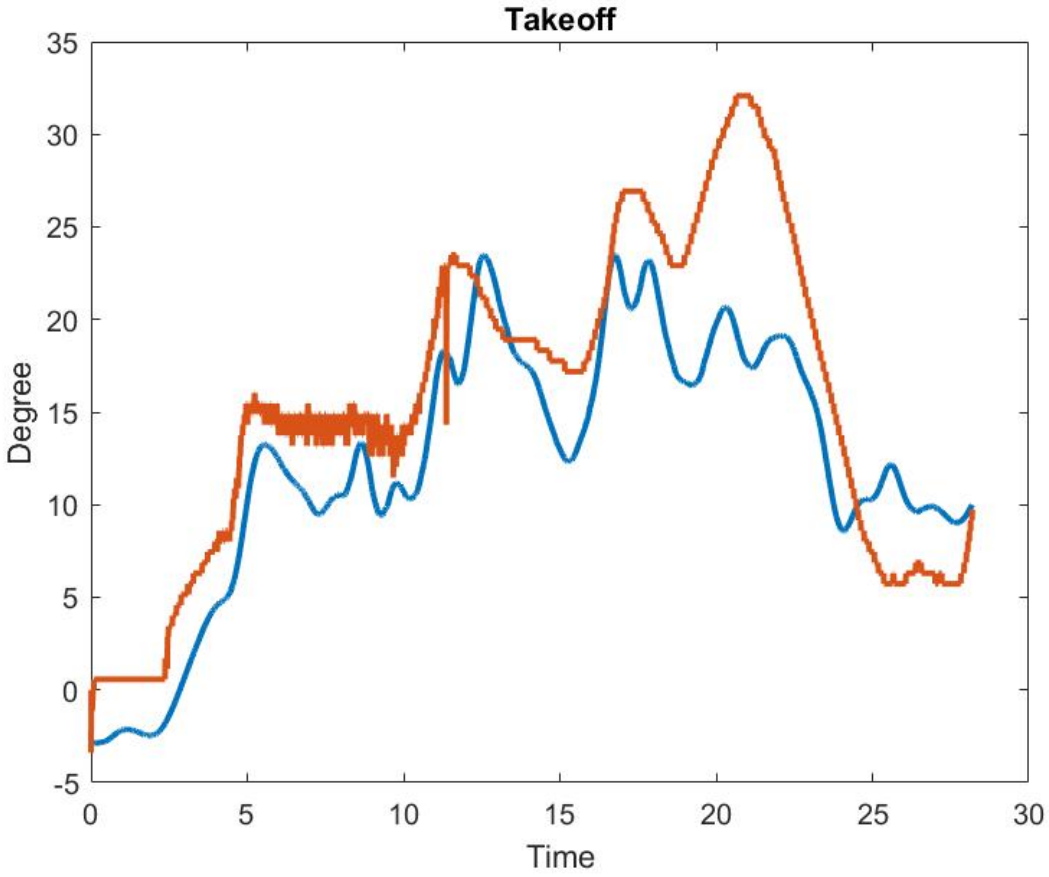

Figure 6.2: The MP tracking the reference generated after the mapping from the game, during take off. The sensor data has been smoothed out in Matlab using the smoothdata command, for easier reading.

6.4 Virtual Reality and immersion

The MP worked well together with VR. The motion cancellation that was paramount for the whole concept to work did work well. The motion of the MP did not transfer in the VR headset, indicating that the VR motion cancellation was successful. The placement of the center of rotation also helped with cancelling the motion of the platform. Since the VR headset was placed close to the centre of rotation, it did not require much of the system in order to cancel the motion.

The immersion factor was also good. One thing that the MP did well was to give the sensation of flying the plane towards the ground or straight up in the sky. The user could feel the gravitational force, in real life, acting on the body in the right direction depending on where you were heading.

However, the main idea of the motion platform was to give the user sensations of longitudinal acceleration of the aircraft when thrusting with the jet engines of the aircraft. This feeling was good, but could have been better. The MP acted as expected; when the user thrusted the engines, the MP tilted the chair backwards and gave the user a feeling of force acting on their body. The main problem with this was that the user could also feel their head being tilted, because of the head not being at the COR. Of course, the height of the user has an influence

over this phenomenon. A taller user will have their head further away from the COR making the sensation of the head tilting even worse. A shorter person will have their head closer to the COR and will not feel these unwanted forces in the same way.

Moreover, it is worth noting that different people have different perceptions of feelings such as acceleration, resulting in that some people felt the sensation of acceleration to be more real than others.

6.5 Electronics

With a person sitting in the cart, the higest current measured was around 21 A during motion from initial position to the MP's highest position, and about 10 A when static at its highest position. This is by far the highest current draw of all the electronics, where the second highest are from the fans with a current draw of 0.3 A each, drawing a total of 0.9 A for all fans. This means that with the current battery setup of 105 AH, and a maximum current draw of about 22 A, the batteries would last for 4.7 hours. In reality this would never be the case unless the the cart is going back and forth continuously, which rarely is the case.

Chapter 7

Discussion and conclusions

In this chapter, reflection upon the results are discussed and concluded.

7.1 Discussion

7.1.1 Mechanical design

The design concept itself demands a stable and rigid frame to hold the curved rails steady in place at a certain distance from the floor, therefore the weight problem is hard to solve or work around. One way to make the design smaller and lighter is to move the COR further down below the user's chest area. Then, a smaller radius can be used on the curved rails and a more compact design can be achieved. The drawback from this approach though is that there may be larger unwanted ghost forces acting on the user which will decrease the immersion factor of the use of the MP. Maybe, a completely different design concept has to be used to solve the weight problem.

Another problem was that the frame and powertrains had to be mounted to the floor. This could be solved by letting the powertrains be connected to the frame, and the frame be held in place by its own weight.

7.1.2 Electrical design

The power supply that was supposed to be used in this project was defective and could not be repaired. Car batteries were therefore used instead. The main disadvantages of using car batteries instead of a power supply were the need to recharge, the recharge time and the limited power range. However, there were no better alternatives that were cheap and easily accessible as car batteries.

The motors worked 20-30% of their maximum power during the tests and only two of the four batteries were used in the end, supplying the motors with 24 V instead of 48 V. The motors were never over-heated because of this. All of this implies that the motors that were chosen were excessive to this application. Though, this is not necessarily bad as it increases the safety factor. On the contrary, having a motor that was too weak could easily over-heat and causing fire hazard or other safety issues.

The reason for not using all four batteries was because of the relay. For some unidentified reason, the relay could not handle voltages above around 30 V although according to the data sheet [49], it should be able to handle up to 100 V. This issue could not be solved as the main source of the problem was unknown and there were nothing that could be done if it was a manufacturing fault.

Due to the time constraints and other external factors, some functions were not implemented. This includes the whole limit switch function, the linear actuation for the roll motion and the temperature sensors.

The reason for not implementing the limit switch function was not only time related. In the testing of the MP, it was clear that the motors would not be able to handle the torque if the chair was in the maximum position for long enough to become a safety issue and the motors would then shut down. When the motor shuts down, the MP will evidently go back to it's initial position which is the function that the limit switch would provide making the limit switch function redundant. Another issue was the placement of the limit switches and the cables that would most likely get entangled with the cart moving, causing more issues.

The linear motion was proven to work as intended but due to lack of time, was not able to implement. However, as both the motor and the driver was working during testing, the implementation from here is reasonably straightforward.

The fans were kept on full speed during the whole time when the MP was active, instead of controlling the fans with the temperature sensor. This worked well as the motors were kept cool all the time. Nonetheless, implementing the temperature sensors would have saved power from the batteries, although the amount of power saved would most likely be negligible in this project.

Since only the pitch movement was implemented, the tracker was not necessary. As the testing showed, the VR headset did not move as long as the COR was kept close to the head. Nevertheless, if time allowed and the roll movement was implemented, it would have been needed.

The cables lying around the platform were a safety risk and could have been avoided if wireless communication was implemented between the microcontroller and the computer.

In the end, there were functions considered in this project that were not implemented or necessary in the end product.

7.1.3 Control design

The derived model in section 3.4.2 is accurate enough for a feedforward controller to be implemented to give the sensation of flying an airplane on the MP. The belts starts to separate from the belt guide at roughly $\theta = 25°$. It is not enough with just mechanical belt tensioners to maintain the tension of the belt during actuation. To maintain the tension the motors need to rotate differently, only then can the belt stay tensioned during actuation. The current MP can not handle high frequency signals since the system starts to vibrate.

The mapping of the MP is crucial for a realistic immersion. In this project, the reference position of the MP is calculated through combining longitudinal acceleration with the angle of the plane. These two sensations are scaled in mapping to adapt the limitations of actual motion span. From the result, the mapping was proven to be feasible for an indication and effective in giving the user the sensation of flight.

On the other hand, the proper combination of sensations is of similar importance to the immersion, that a better balance between two sensations would bring more realistic feelings. Given the limited time and the inconvenience of the current pandemic, it was not feasible to carry out massive tests of different users. Since it was not really a mechatronic's issue, more professional input is also required. However, the approach to apply this improvement is to change parameters for mapping, thus can be achieved without any technical difficulties.

7.1.4 Ethical considerations

Due to the nature of this project, there are no need for any extensive ethics discussions. The main purpose of the MP designed in this project is to educate pilots and to be used when playing computer games as a leisure activity. It is hard to argue for that this design could be used in an unethical manner. However, if the MP is used for educating fighter jet pilots that will ultimately join a war, you could maybe argue for that the MP makes it easier and cheaper to educate people that will contribute to war actions. This argument is a bit far-fetched though as there already exist many ways to educate fighter jet pilots, including other MPs and simulators.

Moreover, if a proper safety system to prevent the MP from harming users by getting squeezed and pinched is not implemented, the design is quite dangerous and could therefore be seen as unethical in that sense.

7.1.5 Sustainability

As with many topics, there are different views depending on who you ask. Two people that are asked the same question can give you two completely different answers depending on their values and views on the question. In the case of sustainability for this kind of project, there is no exception.

You could easily argue for that a project like this is unnecessary and will just consume energy, material and other resources that will eventually end up in a dump, like most physical products do. Why produce such a machine just for the sake of increasing the immersion factor while playing a computer game? These resources could have been used in a more meaningful way.

The polar opposite view of this, is that this kind of project, if done well, could actually save natural resources and energy in the long run. Imagine that a well designed MP together with VR would result in a really realistic flying experience, so real that it could substitute real life flying in real aircrafts. Ideally, aspiring fighter jet pilots could make their whole careers in a setup like that, except for real war situations. That would save a lot of energy and resources from not flying the real aircrafts as often.

Also, to increase the sustainability of the MP designed in this project, other materials could be used to minimize the environmental footprint.

Chapter 8

Future work

This chapter suggests potential areas in the project that can be further developed.

8.1 Overall design

In future work with this project, it would be needed to spend time to investigate feasible material options instead of steel for the frame and cart. Early in this project, different types of plastic were considered to build the frame. However, because of the tensile strength being lower than steel, plastic was rejected as a viable material choice to ensure the structure would have a high safety factor against failure. If another material with lower density than steel would be a viable option, a lower overall weight could have been easily achieved.

Also, the chair mount is not as rigid as preferred. When a person is moving in the chair, the chair also moves along. Future work for the chair mount could either be to manufacture more rigid parts, or to redesign the mount into a more robust structure. Also, the chair itself could be a part of the chair mount assembly not being rigid. The chair mount design would also be better if the seat height was adjustable. In that case, it would better fit persons of various heights and also the COR would be at least variable.

The wheel holders units were one of the first parts manufactured and during the project ideas about improving the wheel holders occurred. First, the dimensions of the wheel holders could be weak. No FEM has been done on them, the material is aluminium and the structure is thin. Both looking into how robust the wheel holders are, if the structure needs to be improved to increase their life cycle, or if the design needs to be improved, is relevant for further work. Also, the dimensions around the wheel holders, travelling on the curved rails could be improved. At the moment, the clearance to the frame, both under and over the wheel holders are less then half a centimeter. The clearance on the inside is also small towards the frame.

One big problem with this design is also the COR placement. A COR at the user's head gives a better immersion but at the same time a larger design and increased weight as it is now. In future work with this project, this issue should be given a good amount of consideration. Maybe, a totally different design, such as a swing, could turn out to be a better option to increase immersion and decrease the weight of the MP.

At the last meeting with the stakeholders, an interesting topic was brought up; the level of immersion is not only dependant on the mechanical design and factors such as the COR placement. Immersion and sensations of acceleration depends on many factors and is a neuroscientific

topic. Also, people's past experiences with flying and exposure to accelerations in vehicles could maybe also play a part here. Therefore, in future work, there should be some research on how you could increase the immersion and sensations of acceleration in other ways than described in this report.

8.2 Power supply

Another problem with the design is the motors large demand for current. Either an expensive power supply or car batteries that were connected in series were therefore needed. Both alternatives are big and heavy and not flexible. In future work, it would be beneficial to look at alternative options and how to work around this problem to get a cheaper, smaller and more flexible design.

8.3 Electronics

As some of the components and functions were not implemented due to lack of time, the first improvement would be to implement these. Mainly, the roll motion using the linear actuator, as well as the temperature sensors and the limit switches as well as the emergency stop button for the user. Additionally, making the communication wireless would immensely improve the over all electrical design.

Furthermore, the motor for the pitch motion was never used with it's full capacity due to the power limit that was caused by the relay and the software limit. This could be a development for future work. Fine tuning and finding the optimal preference for the best experience for the user, while considering all the different factors, such as voltage, current and capacity.

8.4 Control

The belt tightening differential can be further improved, by making it more aggressive without disturbing the overall motion of the MP. With the finished hardware available, different belt tightening strategies can be experimented with.

Currently the high frequency signals are filtered out with a low pass filter since the overall system can not handle it and thus not simulated. One way to simulate the high frequency signals would be to implement a rumble seat, that would vibrate the user.

By deriving a more accurate model, especially for the belt behavior a more accurate controller could be developed. It has been concluded that the MP is fairly linear for the first 25° of the pitch. After that the belt starts to really separate from the belt guide. To compensate for that a controller better suited for non-linear behaviour could be developed, which would allow for a larger and more accurate motion range.

8.5 Software improvements

In future work, some improvement in the over all software structure can be considered. By changing the Arduino code to pure C code would make the program run faster resulting in a faster system. By implementing the controller directly in Lua, instead of python, the need for a python script to read the data from Lua first, to do the control calculations, could be skipped. Thus, resulting in fewer steps and less delay.

Bibliography

[1] Trello. *Trello helps teams work more collaboratively and get more done.* URL: https://www.trello.com/. (accessed: 13.12.2020).

[2] Slack. *Welcome to your new HQ, a better way to communicate.* URL: http://www.slack.com/. (accessed: 13.12.2020).

[3] Zoom. *One Consistent Enterprise Experience.* URL: https://www.zoom.us/. (accessed: 13.12.2020).

[4] Swesim. *Swesim homepage.* URL: https://www.swesim.se/. (accessed: 08.05.2020).

[5] Shelley Canright. *Human Vestibular System in Space.* URL: https://www.nasa.gov/audience/forstudents/9-12/features/F_Human_Vestibular_System_in_Space.html. (accessed: 25.03.2020).

[6] Richard C. Fitzpatrick Brian L. Day. *The vestibularsystem.* URL: https://www.cell.com/current-biology/pdf/S0960-9822(05)00837-7.pdf. (accessed: 25.05.2020).

[7] William H. Ittelson. *Size as a Cue to Distance: Radial Motion.* URL: https://www.jstor.org/stable/1418666?origin=crossref&seq=1#metadata_info_tab_contents. (accessed: 25.05.2020).

[8] Ricampelo. *Playing at salar.* URL: https://commons.wikimedia.org/wiki/File:Playing_at_salar.JPG. (accessed: 24.05.2020).

[9] Franz van Duns. *Two Passiflora caerulea flowers arranged as a stereo image pair, Dortmund, June 2019.* URL: https://commons.wikimedia.org/wiki/User:Franz_van_Duns#/media/File:Passiflora_caerulea_STEREO_(R-L)_2019-06-27.jpg. (accessed: 24.05.2020).

[10] Markus A. Hietanen; Nathan A. Crowder; Michael R. Ibbotson. *Differential changes in human perception of speed due to motion adaptation.* URL: https://jov.arvojournals.org/article.aspx?articleid=2122159. (accessed: 25.05.2020).

[11] Steve Aukstakalnis. *Practical Augmented Reality. A Guide to the Technologies, Applications, and Human Factors for AR and VR.* Addison-Wesley, 2017.

[12] Polona Caserman, Michelle Martinussen, and Stefan Goebel. "Effects of End-to-end Latency on User Experience and Performance in Immersive Virtual Reality Applications". In: *ENTERTAINMENT COMPUTING AND SERIOUS GAMES, ICEC-JCSG 2019.* Ed. by VanDerSpek, E and Gobel, S and Do, EYL and Hauge, JB and Clua, E. Vol. 11863. Lecture Notes in Computer Science. IFIP TC 14; Peruvian Govt; ICEC; JCSG Steering Grp. 2019, 57–69. ISBN: 978-3-030-34644-7. DOI: {10.1007/978-3-030-34644-7_5}.

[13] Tom Benson. *NASA: Aircraft Pitch Motion, Glenn Research Center.* URL: https://www.grc.nasa.gov/www/k-12/VirtualAero/BottleRocket/airplane/pitch.html. (accessed: 24.03.2020).

[14] Glenn Research Center. *NASA: Stabilators, Glenn Research Center.* URL: https://www.grc.nasa.gov/WWW/k-12/airplane/stablator.html. (accessed: 25.03.2020).

[15] Tom Benson. *NASA: Aircraft Roll Motion, Glenn Research Center*. URL: https://www.grc.nasa.gov/www/k-12/VirtualAero/BottleRocket/airplane/roll.html. (accessed: 25.03.2020).

[16] Force Dynamics. *Center of rotation, center of rotation, center of rotation!* URL: https://www.force-dynamics.com/cor. (accessed: 27.03.2020).

[17] Nicolas A Pouliot et al. "Motion Simulation Capabilities of Three-Degree-of-Freedom Flight Simulators". eng. In: *Journal of Aircraft* 35.1 (1998), pp. 9–17. ISSN: 0021-8669.

[18] Chang-Chun Zhou and Yue-Fa Fang. "Design and Analysis for a Three-Rotational-DOF Flight Simulator of Fighter-Aircraft". eng. In: *Chinese Journal of Mechanical Engineering* 31.1 (2018), pp. 1–12. ISSN: 1000-9345.

[19] SuperJet International. URL: https://www.flickr.com/people/48440363@N06. (accessed: 25.05.2020).

[20] Maurizio Pesce. URL: https://www.flickr.com/photos/pestoverde/. (accessed: 25.05.2020).

[21] BEC Motion Simulators. URL: https://www.https://www.motion-simulators.com/. (accessed: 25.05.2020).

[22] Olsen Actuation. URL: https://www.olsenactuation.com/case.html?id=129. (accessed: 25.05.2020).

[23] Firgelli Automations Team. *Linear Actuators 101 - Everything you need to know about a linear Actuator*. URL: https://www.firgelliauto.com/blogs/news/linear-actuators-101. (accessed: 24.05.2020).

[24] MotionControlGuide. URL: http://www.motioncontrolguide.com/learn/tech-tips/actuators/what-are-actuators/. (accessed: 25.05.2020).

[25] LISA EITEL. *How to select a pneumatic actuator: An engineer's guide*. URL: https://www.motioncontroltips.com/selecting-a-pneumatic-actuator/. (accessed: 24.05.2020).

[26] Carlos Gonzalez. *What's the Difference Between Pneumatic, Hydraulic, and Electrical Actuators?* URL: https://www.machinedesign.com/mechanical-motion-systems/linear-motion/article/21832047/whats-the-difference-between-pneumatic-hydraulic-and-electrical-actuators. (accessed: 24.05.2020).

[27] DOF reality. URL: https://dofreality.com/. (accessed: 25.05.2020).

[28] Steve Haigh. URL: https://www.youtube.com/watch?v=my-YMms4hIE&t=98s. (accessed: 25.05.2020).

[29] Rotacaster Wheel Pty Ltd. URL: https://en.wikipedia.org/wiki/Omni_wheel#/media/File:Triple_Rotacaster_commercial_industrial_omni_wheel.jpg. (accessed: 25.05.2020).

[30] Bsim Racing. URL: https://www.bsimracing.com/a-look-at-the-feel-three-virtual-reality-motion-simulator/. (accessed: 25.05.2020).

[31] Aviation Simulator Technology. *Simulator Levels Explained*. URL: https://www.ast-simulators.com.au/resources/simulator-levels-explained. (accessed: 23.05.2020).

[32] Aircraft Compare. *The Differences Between Types of Flight Simulators Explained*. URL: https://www.aircraftcompare.com/blog/types-of-flight-simulators/. (accessed: 23.05.2020).

[33] D. Allerton. *Principles of Flight Simulation (Aerospace Series)*. Hoboken: Wiley. p453, 2009.

[34] VRXsim Virtual Reality eXperience. URL: https://www.vrxsim.com/simulators/flight-simulator/. (accessed: 25.05.2020).

[35] *Digital Combat Simulator World*. URL: https://www.digitalcombatsimulator.com/. (accessed: 25.05.2020).

[36] Hoggit fighter wing. *DCS export*. URL: https://wiki.hoggitworld.com/view/DCS_export. (accessed: 24.05.2020).

[37] *TCP (Transmission Control Protocol)*. URL: https://searchnetworking.techtarget.com/definition/TCP. (accessed: 25.05.2020).

[38] *UDP (User Datagram Protocol)*. URL: https://searchnetworking.techtarget.com/definition/UDP-User-Datagram-Protocol. (accessed: 25.05.2020).

[39] Electrical4Us. *Brushless DC Motors (BLDC): What Are They How Do They Work?* URL: https://www.electrical4u.com/brushless-dc-motors/. (accessed: 09.12.2020).

[40] Hobby King. *Turnigy SK8 6374-149KV Sensored Brushless Motor (14P)*. URL: https://hobbyking.com/en_us/turnigy-sk8-6374-149kv-sensored-brushless-motor-14p.html?queryID=1e7736feeb91e0c90f72be982aeb9d2a&objectID=74469&indexName=hbk_live_magento_en_us_products&___store=en_us. (accessed: 10.12.2020).

[41] Transmotec. *Linjärt ställdon 12VDC 250N 2,4A*. URL: https://www.transmotec.se/product/DLA-12-10-A-50-IP65/. (accessed: 12.12.2020).

[42] Arduino. *Grove - 6-axis Accelerometer & Gyroscope*. URL: https://store.arduino.cc/grove-6-axis-accelerometer-gyroscope. (accessed: 10.12.2020).

[43] VIVE. *VIVE Tracker - Go Beyond VR Controllers*. URL: https://www.vive.com/us/accessory/vive-tracker/. (accessed: 10.12.2020).

[44] VIVE. *HTC VIVE Cosmos Elite*. URL: https://www.vive.com/us/product/vive-cosmos-elite/features/. (accessed: 12.12.2020).

[45] Arduino Store. *ARDUINO UNO REV3*. URL: https://store.arduino.cc/arduino-uno-rev3. (accessed: 12.12.2020).

[46] Odrive. *Odrive Documentation*. URL: https://docs.odriverobotics.com/control. (accessed: 29.10.2020).

[47] Björklund Conradi Landin Lindström Liu Lyu Nore Strand Xu. *Github repository for the project*. URL: https://github.com/FilipBd/HK-Meta. (accessed: 24.05.2020).

[48] RS PRO. *Datasheet - Platinum Resistance Pt100 Pt1000 Thin Film Detectors*. URL: https://docs.rs-online.com/b049/0900766b815bb28b.pdf. (accessed: 13.12.2020).

[49] crydom. *Datasheet Panel Mount - 1-DC Series*. URL: http://www.crydom.com/en/products/catalog/d1d-series-dc-panel-mount.pdf. (accessed: 13.12.2020).

Appendix A

GANTT charts

A.1 GANTT chart for spring term

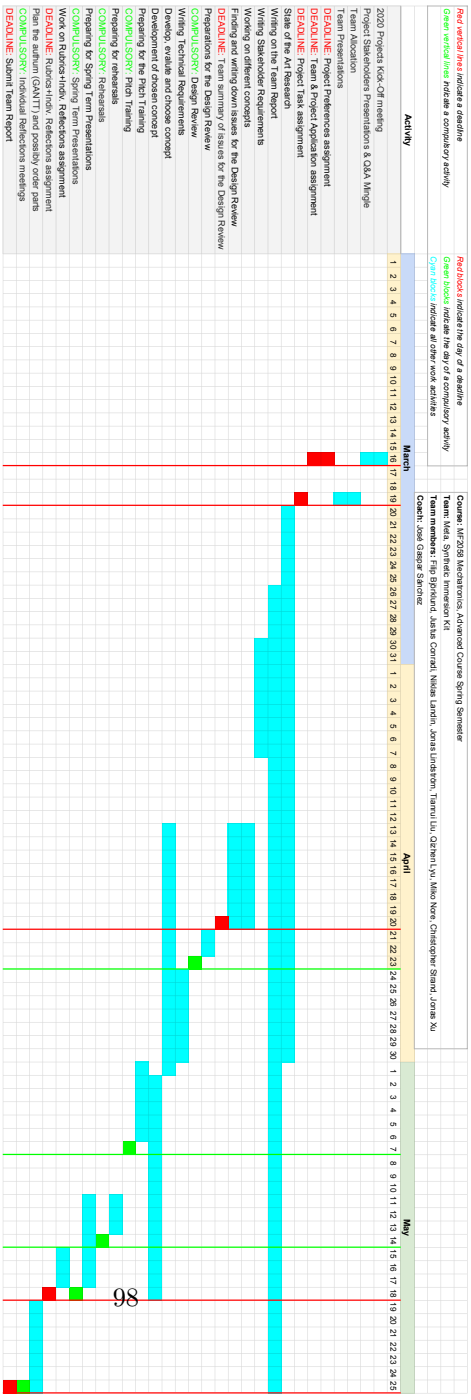

A.2 GANTT chart for fall term

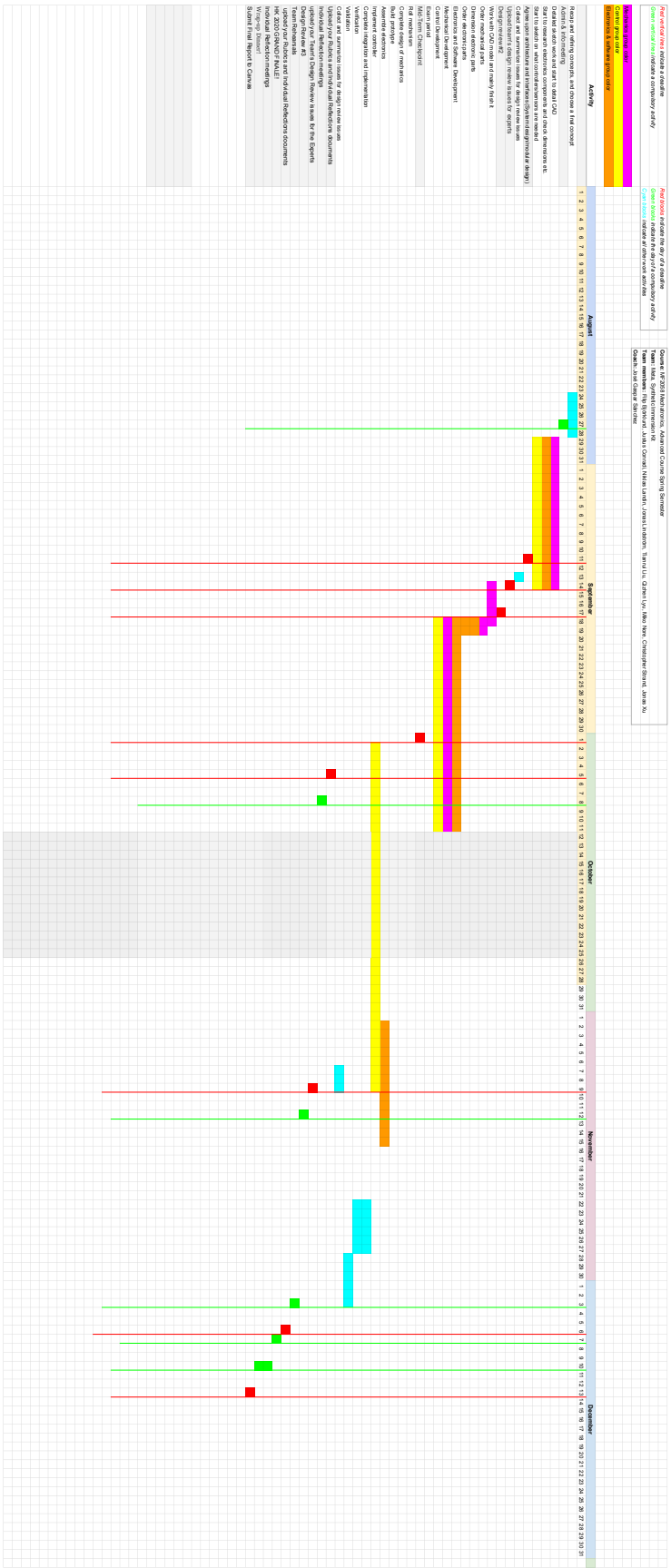

Appendix B

Circuit diagrams

B.1 Relay controller

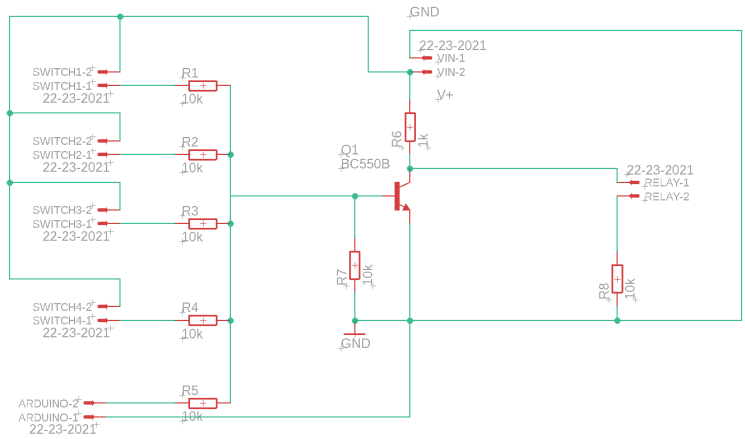

B.2 Fan controller

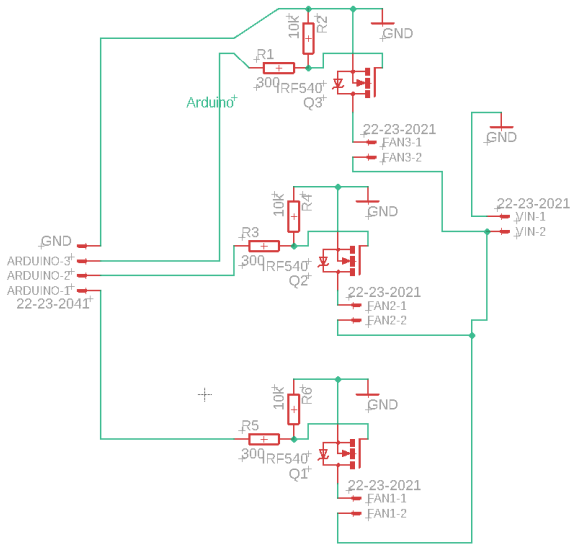

B.3 Limit switch controller

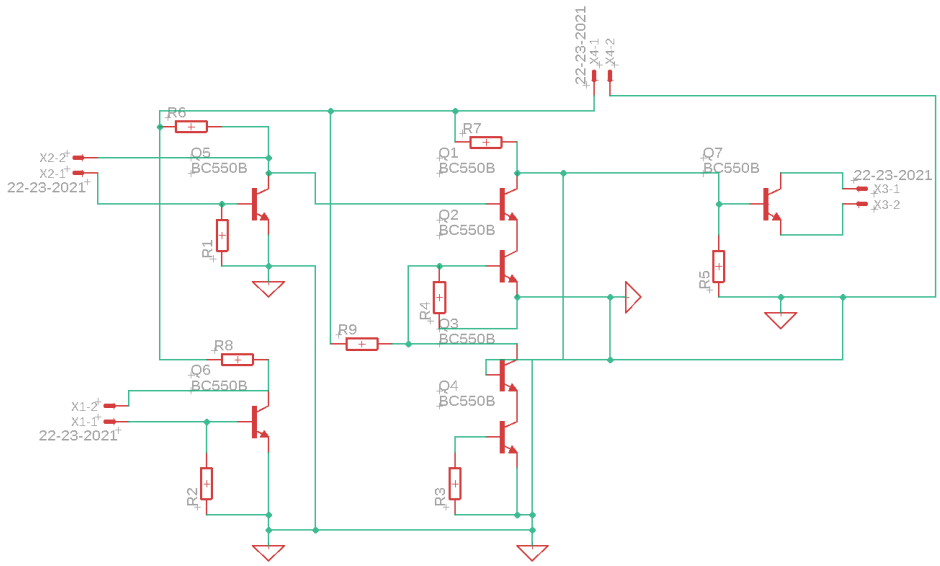

Appendix C

Test cases and results

Table C.1: Test for stakeholder requirements.

Requirements	Descriptions	Test Steps	Expected Results	Test Results
Immersive and good experience	Immersive and good training experience for pilots in training	Let different user's test the MP and rate their experience playing DCS	Good rating from users	Good rates for regular people (not pilots)
Small and Compact	MP is small and compact so it is possible to have several in a room	Make decision based on the finished MP	MP is small enough	relately small (big compared to yaw VR for example)
Safe	MP is safe to use	Look at possible safety issues, in mechanical, electrical and control design e.g. risk of getting stuck in the MP, test emergency/fan functions, test motor movements.	No risk of getting crushed. Emergency stop, fans and motors works as it should.	Some safety issues, risk of getting crushed and one part that broke, emergency stop works
Feeling of acceleration	Feelings of acceleration in different directions that are important for maneuvering the aircraft	Test MP while running DCS	User feels acceleration	Regular user's felt acceleration
Robust	MP is robust	Make decision based on the finished MP	MP is robust enough	Reasonably robust, but some screws needs maintenance and the foot rests are not robust, electronics are not robust (cables lying around)
High Quality	MP is of high quality design	Make decision based on the finished MP	MP is high quality	Good quality, if there are issues it would be because of the design not the quality of the construction
Reproducible	MP is able to be produced in large quantities	Make decision based on time and cost	MP is reproducible	Most things are reproducible (CAD drawings and electronic design are documented)
Shipping	MP is able to be shipped worldwide	Make decision based on the finished MP	MP is shippable	Not easily shippable
Compatible with different aircrafts	MP is compatible to use with several different aircraft models	Test different aircrafts	Works as it should	Yes
Low cost	MP is low-cost in terms of production and thereby in purchase for the customer	Make decision based on the cost	MP is relatively low-cost	Lower than 100,000SEK so low-cost in comparison
VR sickness	Risk of VR sickness is minimized ensuring that longer priods of usage is possible	Test flying in multiple time intervals (5 min, 10 min, 15 min etc)	No VR sickness	VR sickness due to person using VR, not due to any system design fault
Easy to install	MP is fast and easy to install and implement together with the software	Look at installation steps	Few and easy steps	Construction is not easily installed (if all hardware is in place, then electronics are easy to install)

Table C.2: Tests for technical requirements.

Requirements	**Descriptions**	**Test Steps**	**Expected Results**	**Test Results**
Dimensions	MP have maximum dimensions of 180x180x180	Measure MP	180 x 180 x 180 m	200 x 125 x 145
Weight	MP does not weigh more than 150 kg	Weight MP	150 kg	Not feasible to test
Joystick features	The joystick does not prevent the user from accessing the seat and is mounted on the seat	Make decision based on different user's experience of getting in and out of the seat	Joystick is stable and user can easily get in and out	Joystick is stable and is not in the way for the user (getting inside is harder than getting out)
Throttle features	The throttle does not prevent the user from accessing the seat and is mounted on the seat	Make decision based on different user's experience of getting in and out of the seat	Throttle is stable and user can easily get in and out	Throttle is stable and not in the way of the user
Foot pedals	Foot pedals are mounted on the seat	Make decision based on the finished MP	Foot pedals are stable	Foot pedals not implemented, foot rest are not very stable
Seat features (back rest angle)	The seat has adjustabe back rest angle from 90 °to 130 °	1. Adjust back rest 2. Measure min angle 3. Measure max angle	min 90 °, max 130 °	Not implemented
Seat features (back rest to pedals)	The seat has adjustable distance from the back rest to the pedals, from 60 cm to 90 cm	1. Adjust distance on backrest to pedals 2. Measure min distance 3. Measure max distance	min 60 cm, max 90 cm	Not implemented
Seat features (height)	The seat has adjustable height to fit a person that is between 160 cm to 195 cm, COR for pitch adjusts accordingly	1. Adjust height 2. Measure min height 3. Measure max height	min 160 cm, max 195 cm	Not adjustable but works for different heights
Visual feedback	Visual feedback from the simulator is a VR headset	Make decsion based on the finished MP	Visual feedback is VR	Yes
Force simulation	Forces and accelerations up to 1G can be simulated	1. Simulate 1G in DCS 2. Check output from acc/gyro	1G	Approximately 0.76 G (sin(50°))
Input from DCS	Accepts input in real-time from the exports of DCS for controlling the simulation	1. Open DCS game 2. Position output are read real-time	No delay	Negligible delay
DCS simulation	The simulation is based upon the calculations of the real-time exports of DCS	1. Position output from DCS 2. MP position input calculated from output	No delay	No delay
Actuators	The actuators of the system are electronic	Make decision based on finished MP	Actuators are electronic	Yes
Control actuators	Embedded system to control the actuators	Make decision based on finished MP	Motors are controlled by an embedded system	Yes
Max pitch velocity	30 deg/s	1. Measure angle from A to B 2. Take timer from A to B 3. Calculate angular velocity	30 deg/s	40 deg/s, it can handle more depending on the how much capacity of the motor is used (this was measured with 30%)
Max roll velocity	30 deg/s	1. Measure angle from A to B 2. Take timer from A to B 3. Calculate angular velocity	30 deg/s	2.3 cm /s, approximately 3.68 deg/s
Max pitch motion range	45 °	Measure angle at maximum position	45 °	50 °
Max roll motion range	15 °	Measure angle at maximum position	15 °	8 °
Motion delay	The delay from user input to motion output shall not exceed 50 ms	Time delay	<50 ms	The communication delay of the system is less than 10 ms. For the end-to-end delay, it is hard to measure.
Visual delay	The delay from user input to visual output shall not exceed 20 ms	Time delay	<20 ms	11 ms (90 Hz refresh rate)
Unessecary movements	MP does not do any moevemnts that is not needed for the simulation within an error span of 1 °	Measure unnecessary movements	<1 °	Relatively ok, but hard to measure
Calculated movements	MP provides the same movements as the calculated reference values provide within an error span of 1 °	1. Get calculated position 2. Compare to real position	<1 °	It is fulfilled in most cases. See Fig 6.1 and Fig 6.2
DOF	MP has 2 DOF	Make decision based on finished MP	MP has 2 DOP	Roll not implemented, but has the possibility
COR pitch	COR for pitch is maximum 5 cm above/below the center of the user's ear	Measure COR for pitch	<5 cm	Approximately 15 cm
COR roll	COR for roll is maximum 5 cm under the seat	Measure COR for roll	<5 cm	9 cm
User weight	MP can support a user weighing under 100 kg in all possible working positions	Test with 100kg user	works as it should	100 kg ok
Emergency stop	Two emergency stop buttons, one for the user and one for the technician that stops the MP movement completely within 10 ms	1. Test emergency stop 2. Take timer to measure delay	<10 ms	Yes, it is purely electrical
MP cost	MP costs no more than 10 000 EUR	Calculate total cost	<10 000 EUR	Yes